Theoretical Studies of Some Transition-Metal-Mediated Reactions of Industrial and Synthetic Importance

Maricel Torrent,† Miquel Solà,*,‡ and Gernot Frenking*,§

Cherry L. Emerson Center for Scientific Computation and Department of Chemistry, Emory University, Atlanta, Georgia 30322, Institute of Computational Chemistry and Department of Chemistry, University of Girona, 17071 Girona, Catalonia, Spain, and Fachbereich Chemie, Philipps-Universität Marburg, Hans-Meerwein-Strasse, D-35032 Marburg, Germany

Received May 17, 1999

Contents

I. Introduction

Looking backward at the beginning of the new millennium, dramatic progress in the scope and the accuracy of quantum chemistry can be seen, particulary when current applications of modern quantum chemistry are compared with the kind of chemical problems that used to be solved in the 1960s and 1970s. At that time, quantum chemistry was mainly limited to provide purely mathematical or physical interpretations, with not much interest for the experimental chemist. Only a few theorists could believe at that early stage in the promise of employing computation to probe, e.g., catalysis and catalytic reactions. This notwithstanding, what was a dream 40 years ago is today a reality.

One of the main factors that has made quantum chemistry a much more accessible and attractive field for the chemist in the lab is the development of its application-oriented side. Nowadays, quantum chemistry has reached a level that allows it to be easily integrated into a multidisciplinary environment. Interactions between synthetic chemists from both academia and industry and quantum chemists are currently feasible mainly because the latter have grown to the point of being complementary to the former in a practical way. Such an achievement would not have been possible without the availability of sophisticated computational routines and modern computers. Again, the best example probably comes from the enormously important catalytic activity of TMs and their compounds, which now can be studied by means of computational methods with the same accuracy as small organic molecules used to be tackled some decades ago. The extremely fruitful synergic relationship between experiment and theory is exactly what the experimental organometallic chemist needs to understand (and predict) structural

† Emory University. Permanent address: Institute of Computational Chemistry and Department of Chemistry, University of Girona.
‡ University of Girona.
§ Philipps-Universität Marburg.

10.1021/cr980452i CCC: $35.00
Published on Web 01/25/2000

Maricel Torrent, born in Girona, Spain, in 1970, studied chemistry at the University Autonomous of Barcelona. She graduated in 1993 and then began Ph.D. work on mechanisms of transition-metal-assisted reactions at the University of Girona under the direction of Prof. M. Duran and Dr. M. Solà. During her Ph.D. study, she visited the group of Prof. T. Ziegler (University of Calgary, 1996), who is credited with outstanding applications of density functional theory on transition metal systems. Upon completion of her Ph.D. thesis in 1998, Maricel Torrent spent three months at Marburg University (Germany) with Prof. G. Frenking, where she continued working in the field of organometallics. Presently, she is a Postdoctoral Fellow in the group of Prof. K. Morokuma at the Cherry L. Emerson Center for Scientific Computation, Emory University, Atlanta. Her current research interests include both organometallic and bioinorganic systems with particular emphasis on mechanistic aspects of reactions catalyzed by metalloenzymes. She has earned several academic honors and, very recently, also the Catalan Saint Albert Prize.

Miquel Solà was born in Fonteta, Catalonia, Spain, in 1964. He received his Diploma of Chemistry at the University Autonomous of Barcelona in 1986 and his Ph.D. at the same University in 1991, both with academic honors. His doctoral research on carbonic anhydrase enzymatic catalysis under the direction of Juan Bertrán and Agustí Lledós earned him the Catalan Saint Albert Prize. After several months at a private consulting company, in 1993 he moved to the University of Girona as an assistant researcher. In 1994 he did postdoctoral research in Amsterdam with Evert Jan Baerends and in 1995 in Calgary with Tom Ziegler. Since 1997, he has held a permanent position as Assistant Professor at the University of Girona. His research interests have been mainly focused on theoretical studies of organic and organometallic reaction mechanisms and on the use of quantum molecular similarity measures in the analysis of different chemical aspects.

and reactivity trends with no limitations along the periodic table. This is why quantum chemistry is at its best when it becomes combined with experiment. Theory and experiment complement each other in a dual way, because the two sides of chemical research can nowadays be used not only to check the accuracy of the calculated and measured results but also to design new experiments and new calculations. Theory

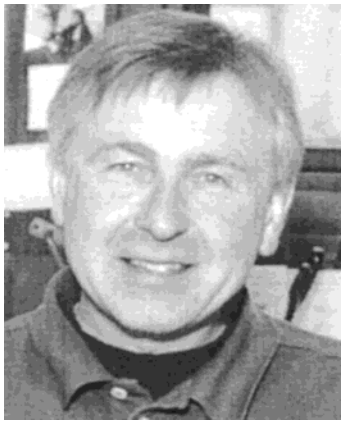

Gernot Frenking was born in Germany in 1946. He left school in 1960 and worked in the chemical industry before he went to school again and finally entered the university in 1969. He received his Diploma in Chemistry at the Rhenish-Westfalian Technical Highschool in Aachen in 1973. Following two years as a research student in the group of Professor Kenichi Fukui at Kyoto University (Japan), he returned to Germany and received in 1979 his doctoral degree from the Technical University Berlin under the guidance of Professor Horst Götz. After obtaining his Habilitation in Theoretical Organic Chemistry at the TU Berlin in 1984 he moved to the U.S. Following one year as a visiting scientist in the group of Professor Henry F. Schaefer III at the University of California (Berkeley), he became a staff scientist at the Stanford Resarch Institute (SRI International) in Menlo Park, CA. In 1989 he returned to Germany and became an Associate Professor for Computational Chemistry at the Philipps Universität Marburg. In 1998 he was appointed Full Professor for Theoretical Chemistry. His current research interests lie in the field of theoretical inorganic chemistry. Major topics are the nature of the chemical bond of heavy elements, particularly transition metals, reaction mechanisms of transition-metal-catalyzed reactions, and lately bioinorganic reactions.

and experiment also give information that can only be obtained from one of the two sides. Thus, complete information about a chemical problem needs the application of both experimental and theoretical methods.

The aim of the present review is to illustrate with some representative examples how quantum chemistry has been applied to solve real problems encountered in coordination chemistry for which the experimental chemist alone could not give an answer. Coverage is extensive, but not exhaustive. It is not our intention to review all the theoretical work done in the area of mechanistic elucidation of TM-mediated reactions for which a bulky literature exists. Rather, we confine our considerations to a selected number of organometallic reactions with a common denominator: All reactions herein examined are homogeneous metal-assisted or -catalyzed reactions that have an outstanding importance either *industrially* or *synthetically*.[1] Without exception, all mechanisms investigated in the present review yield products of special interest either in large-scale manufacturing or because of their properties as powerful drugs, antibiotics, or anticancer reagents. Since in these cases obtention of the desired product (or, on the contrary, of an undesired byproduct) can represent a gain (or a loss) of many millions of dollars every day, and since the final result is mainly governed by the path followed by the reaction, there is a great fiscal incentive to improve understanding of the operative mechanism of a given chemical process with the characteristics mentioned above. The coming years will certainly witness huge progress

in this particular area of increasing economic importance; however, we believe that there is no reason to delay revision of what has been done so far.

The format of our presentation is divided into two major topical sections: organometallic reactions involving CO or CO_2 (section II), and organometallic reactions involving unsaturated hydrocarbon compounds (section III). Within each section, whenever a name exists for a given type of reaction, this name has been used instead of a more general description. Thus, section II includes (A) hydroformylation of olefins, (B) the Dötz reaction, (C) the water−gas shift reaction, (D) hydrogenation of CO_2, and (E) hydrogenation of CO. Section III covers (A) olefin hydrogenation, (B) epoxidation and dihydroxylation, and (C) hydro-, di-, and thioboration reactions. Very active areas such as olefin polymerization or olefin metathesis reactions (which would constitute by themselves the subject of a separated review[2]) or others such as silastannation,[3] hydrozirconnation,[4] or alkane carbonylation[5] have been excluded to restrict the scope of information presented to a manageable size. Finally, in section IV a critical assessment of the performance and reliability of the methods most commonly used in theoretical TM studies is performed, and in section V the most outstanding findings are briefly summarized.

Throughout, it will be evident to the reader that quantum chemistry has become a powerful, must-have tool for penetrating the complexities of TM-mediated reactions of real synthetic and industrial importance, but as such, quantum chemistry is only the beginning, and not the end, of any inquiry into chemical reactivity. The full study is a combination of theoretical and experimental techniques, and the choice of the appropriate and best methods demands experience in both fields. Theoretical methods have become very complex because of the broad range of applications where they may be used. This is a warning against the belief that quantum chemical programs may be used as black-box methods. There are complicated mathematical methods behind the apparently simple computer programs, and it takes more than learning some abbreviations to become a skillful theoretical/computational chemist, but the efforts of learning quantum chemistry pay off. The combination of the results of theoretical calculations and experimental studies is often the only way to achieve true progress, indeed, a situation very close to the fruitful symbiosis desired in the 1960s, but still full of challenges for the new millennium. It is our wish that this review helps to define more clearly the present situation of the title area, and becomes a starting point for designing novel guidelines soon.

II. Organometallic Reactions Involving CO or CO_2

A. Hydroformylation of Olefins

The hydroformylation or oxo process converts alkenes and synthesis gas ($CO + H_2$) into predominantly aldehydes with alcohols[6] and alkanes[7] as minor products. Since its discovery by Roelen in 1938,[8] this homogeneous catalysis has developed into an extremely important industrial process with over 6 million tons per year of oxo products obtained via this method worldwide in 1993.[9] Hydroformylation allows the functionalization of C=C bonds, and consequently it can be seen as an efficient synthetic route for the preparation of fine chemicals. It involves low-valent cobalt[1,10] and rhodium[7,11] complexes as catalysts, although other metals such as platinum, ruthenium, iridium, and palladium have also been employed, especially in the field of asymmetric hydroformylation.[12] The overall equation for the formation of aldehydes from alkenes, dihydrogen, and carbon monoxide can be written as

$$RCH{=}CH_2 + CO + H_2 \xrightarrow[\text{cat.}]{} RCH_2CH_2CHO + RCH(CH_3)CHO \quad (1)$$

A mixture of linear and branched aldehydes is obtained.[13] Since the aldehyde products are mainly converted to detergent alcohols that have to be linear, the branched isomer is undesirable. Due to the importance of this process, the study of its mechanism has always given rise considerable interest from both experimental and theoretical points of view.[7,9,14] The most widely accepted mechanism for the hydroformylation reaction of eq 1 catalyzed by $HCo(CO)_4$ is due to Heck and Breslow[15] and involves five steps (see Scheme 1). The same basic steps, but with the

Scheme 1. Heck and Breslow Mechanistic Proposal for the Hydroformylation Process

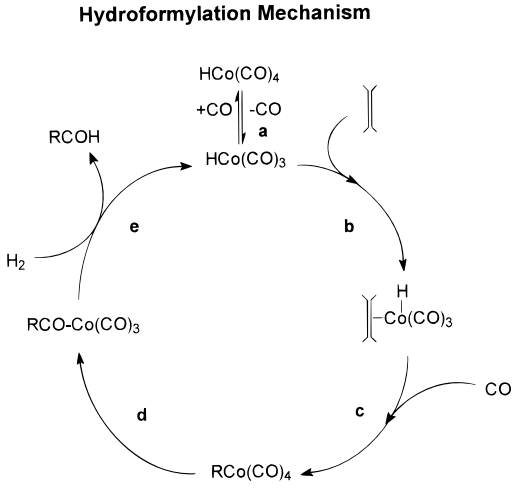

implication of a binuclear cobalt species in the last step of the mechanism, have been proposed by Orchin.[10a,c] Likewise, the mechanism proposed by Wilkinson et al.[16] for the catalytic cycle mediated by $HRh(CO)_2(PPh_3)_2$ consists of the same five steps: (i) ligand dissociation, (ii) olefin coordination, (iii) olefin insertion and PPh_3 addition, (iv) CO insertion, and (v) H_2 oxidative addition and aldehyde reductive elimination.

Despite this almost universally accepted general mechanism, the whole catalytic cycle with all possible intermediates, TSs, and reaction paths connecting reactants and products was not well established until the appearance of a series of theoretical works that have greatly contributed to the understanding of this reaction mechanism. Nowadays, hydroformylation is probably among the theoretically and mechanistically

Table 1. Selected Geometrical Parameters of the C_{3v} Structure of $HCo(CO)_4$ (2b) (Å and deg)

method	R(Co−H)	R(Co−C_{ax})	R(Co−C_{eq})	R(C−O_{ax})	R(C−O_{eq})	∠C_{ax}−Co−C_{eq}
RHF[a]	1.640	2.051	2.013	1.100	1.104	96.9
RHF[b]	1.71	2.02	1.96	1.12	1.13	118.8
RHF[c]	1.668	1.955	1.894	1.122	1.130	97.2
MP2[a]	1.323	1.673	1.707	1.164	1.154	99.0
LDA[c]	1.481	1.762	1.758	1.155	1.157	99.4
BP86[a]	1.482	1.803	1.793	1.150	1.153	99.0
BP86[d]	1.486	1.793	1.802	1.147	1.151	98.0
exptl[e]	1.556(18)	1.764(10)	1.818(3)	1.141(3)	1.141(3)	99.7(6)

[a] Using ECPs, ref 45. [b] Reference 39. [c] Reference 46. [d] References 31 and 44. [e] Reference 56.

best-understood homogeneous catalyses. Theoretical works on the hydroformylation process have already been covered in different reviews,[17−30] although in most cases either the authors have reviewed basically their own work or they have reviewed only some of the elementary reactions involved in the hydroformylation process. The following sections include both theoretical works analyzing the whole catalytic cycle and also studies on some of the elementary steps present in Scheme 1.

1. Generation of the Active Species

The first key step (**a** in Scheme 1) in the mechanism of Heck and Breslow is the formation of the catalytically active species $HCo(CO)_3$ by dissociation of a CO ligand from $HCo(CO)_4$. However, experimentally the reaction that initiates the hydroformylation reaction catalyzed by $HCo(CO)_4$ is the hydrogenation of $Co_2(CO)_8$ species to yield the precatalyst $HCo(CO)_4$:

$$Co_2(CO)_8 + H_2 \rightarrow 2HCo(CO)_4 \qquad (2)$$

Folga and Ziegler[31] have optimized two possible isomers of $Co_2(CO)_8$ (**1**) with C_{2v} and D_{3d} symmetries using the BP86 nonlocal DFT functional. The authors showed that the C_{2v} structure was more stable than the D_{3h} one by 22.3 kJ mol^{-1}, in agreement with experimental data[32] and preliminary EHT calculations.[33] The calculated enthalpy of hydrogenation for the C_{2v} species of 27.4 kJ mol^{-1} is close to the two available experimental values of 19.7[34] and 16.9[35] kJ mol^{-1} and agrees with the experimental observation that $Co_2(CO)_8$ is readily converted to $HCo(CO)_4$.[10a]

$HCo(CO)_4$ is one of the most well-studied organometallic compounds.[33,36−55] There are at least three possible structures for $HCo(CO)_4$: SPy (C_{4v}, **2a**), TBP (C_{3v}, **2b**), and distorted TBP with hydride in the equatorial position (C_{2v}, **2c**) (see Scheme 2). Gas-

Scheme 2

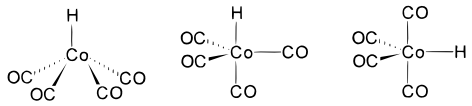

phase electron diffraction experiments showed that $HCo(CO)_4$ has C_{3v} symmetry.[56] Semiempirical EHT[33,37,38] and CNDO/2[36] calculations already yielded the C_{3v} structure as the most stable for $HCo(CO)_4$. The electronic factors favoring structure **2b** were put forward by Elian and Hoffmann,[38] who showed that, in **2a** and **2c**, unlike **2b**, there is a four-electron destabilizing interaction between the two 1s electrons of the hydride and a filled d orbital of the $Co(CO)_4^+$ fragment of a_1 symmetry.[38] HF calculations by Antolovic and Davidson[39,40] (AD) indicated that the C_{4v} structure is not stable, and that the C_{2v} structure is slightly more stable than the C_{3v} one by 5.5 kJ mol^{-1} in disagreement with experiment. A subsequent CI calculation[39] based on the HF geometries gave **2b** more stable than **2c** but by only 1.5 kJ mol^{-1}. Both, HF and CASSCF results by Veillard et al.[48] at the experimental geometry favor **2b** over **2c** by 29 and 64 kJ mol^{-1}, respectively, showing that the discrepancy between the experimental and theoretical structures found by AD at the HF level can be attributed to the poor HF geometries. Ziegler et al.[42,43] reported similar results, finding that structure **2b** was more stable than **2c** by 63 and 58 kJ mol^{-1} with the HFS and BP86 methods, respectively. Table 1 collects the most relevant parameters of $HCo(CO)_4$ computed at different levels of theory. In all cases, the equatorial CO ligands are bent toward the hydride to reduce the steric repulsion and to get a better 1s−a_1 overlap due to increased hybridization of the a_1 orbital.[38] As one can see, HF yields Co−C and Co−H distances up to 0.2 Å longer than those observed experimentally, because of the inability of HF to describe π back-donation correctly,[41,57−60] in particular for the first-row transition metal complexes. MP2 overcorrects this effect, yielding Co−C and Co−H distances 0.1−0.2 Å too short. LDA metal−ligand bond lengths are also shorter than experimental distances but by less than 0.1 Å. As expected, inclusion of nonlocal corrections at the BP86 level[19,20,61] tends to elongate these bonds and improves the agreement between theory and experiment.

Evidence not entirely conclusive for the existence of $HCo(CO)_3$ has been provided by matrix isolation techniques.[62] A kinetic study by Ungváry and Markó indicated further that $HCo(CO)_4$ is about 0.3% dissociated to $HCo(CO)_3$ at room temperature.[63] Similar results were reported by Orchin and co-workers.[62,64] The coordinately unsaturated $HCo(CO)_3$ species has the three possible structures shown in Scheme 3.

Scheme 3

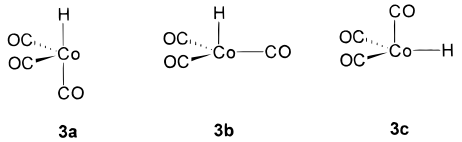

Experimentally its structure is unknown. Preliminary EHT calculations[33] of structures **3a** and **3b** at

Table 2. CO Dissociation Energies from 2b To Give 3a (kJ mol^{-1})

method	ΔE	ref	method	ΔE	ref
HF[a]	188	36	CI	140.4	39
HFS	186	43	exptl[c]	53.1	65
BP86	169.3	44	exptl[d]	54	63
CASSCF	115[b]	47, 48			

[a] At CNDO/2 geometries. [b] 73 kJ mol^{-1} for the **2b** → **3b** + CO process. [c] Enthalpy at 200 °C and 1 atm. [d] Enthalpy at 20 °C and 1 atm.

a fixed geometry indicated that **3a** is more stable than **3b** by 12 kJ mol^{-1}. CI calculations[52] on partially optimized C_{3v} and C_s forms pointed out that the ground state of $HCo(CO)_3$ is a triplet of C_{3v} symmetry. The first comprehensive theoretical investigation on $HCo(CO)_3$ was performed by AD[39] with the HF method. AD concluded that the $^3A_2$ state of C_{3v} symmetry is the ground state of $HCo(CO)_3$, and that the most stable singlet state $^1A_1$ corresponds to structure **3c** of C_s symmetry. In a subsequent work[41] by the same authors, limited CI calculations confirmed that the $^3A_2$ state of C_{3v} symmetry was the ground state of $HCo(CO)_3$. However, the difference in energy between the triplet ground state and the lowest-lying singlet state was too small to ascertain which form represents the most stable species. AD concluded that a quantitatively correct picture would require full MCSCF optimizations. CCI calculations[48] on partially optimized CASSCF structures gave a $^1A_1$ state of C_{3v} symmetry as the ground state, with the $^3A_2$ state of the C_{3v} structure and a closed-shell $^1A_1$ state of structure **3a** 29 and 42 kJ mol^{-1} higher in energy, respectively. The study of Versluis et al.[43] with the HFS method was confined to the singlet states of $HCo(CO)_3$. Geometry optimization yielded **3a** as the most stable one, the **3b** and **3c** forms being 38 and 69 kJ mol^{-1} higher in energy, respectively. A more recent study by Ziegler, Cavallo, and Bérces[44] based on a nonlocal DFT method indicated that $HCo(CO)_3$ adopts a singlet ground state of structure **3a**. The other singlet structure with a geometry of C_{3v} symmetry is 35 kJ mol^{-1} higher in energy, while triplet states of $HCo(CO)_3$ are about 100 kJ mol^{-1} higher in energy than the singlet species **3a**. In summary, there is no agreement about the molecular structure of $HCo(CO)_3$ in its ground state. As yet, the most sophisticated calculations[44,48] predict a closed singlet ground state of either structure **3a** or structure **3b**. Further assessment must await CCSD(T) or multireference CI calculations with full geometry optimization. Remarkably, the comparison between experimental[62] and calculated[44] infrared spectra suggests that both conformers **3a** and **3b** are observed in the experimental study.[62] However, one must bear in mind that **3a** and not **3b** has the suitable structure to insert the alkene in the next step.

Table 2 contains the dissociation energies computed at different levels of theory corresponding to the process **2b** → **3a** + CO on the singlet surface. Important discrepancies can be seen between the values computed at different levels of theory and also with experimental dissociation enthalpies. Only the CASSCF result of 73 kJ mol^{-1} by Veillard and Strich[47] for the **2b** → **3b** + CO dissociation is close to experimental enthalpies. Most of the methodologies give dissociation energies larger than 140 kJ mol^{-1}, in agreement with the fact that high temperatures are required to generate a sufficient concentration of $HCo(CO)_3$ from the precatalyst $HCo(CO)_4$. The difference between experimental[63,65] and computed dissociation energies of about 100 kJ mol^{-1} is probably too large to be attributed only to errors produced by the theoretical methods employed, and further experimental and theoretical studies are necessary to discern the origin of this difference. The mechanism for the photodissociation of CO from $HCo(CO)_4$ has also been discussed in different works,[47−55] but the results will not be examined here because photodissociation does not occur during the industrial process.

$HRh(CO)_4$ (**4**) has also been employed as a precatalyst by Ruhrchemie in a process that is more selective to aldehydes than its equivalent process catalyzed by $HCo(CO)_4$.[9c] The most comprehensive study on the molecular structure of $HRh(CO)_4$ has been performed recently by Pidun and Frenking (PF).[66] In their work MP2 geometry optimizations using ECPs were used to analyze the C_{2v}, C_{3v}, and C_{4v} forms of $HRh(CO)_4$. PF found that only the structure with C_{3v} symmetry (such as **2b** in Scheme 2) is a real minimum in the PES of $HRh(CO)_4$. The authors showed that the C_{4v} structure does not exist as a stationary point on the PES, while the structure with C_{2v} symmetry, which is 56 kJ mol^{-1} higher in energy than the C_{3v} structure, is a TS of the degenerate Berry pseudorotation (BPR)[67] connecting two C_{3v} minimum structures. In BPR processes, two equatorial ligands become axial, the two axial ligands become equatorial, and one ligand, called the pivot, is unaffected. Experimentally, Vidal and Walker[68] concluded that the geometry of $HRh(CO)_4$ has C_{3v} symmetry from a comparison between IR spectra of $HRh(CO)_4$ and $HCo(CO)_4$. The molecular structure of $HRh(CO)_4$ with C_{3v} symmetry has also been studied with the HF,[45] MP2,[45,66] HFS,[42] and BP86[45] methods. Unlike for $HCo(CO)_4$, all methods give similar metal−ligand bond lengths in the case of C_{3v} $HRh(CO)_4$, with the only exception of HF that yields Rh−C bond distances too large. This is not surprising taking into account that electron correlation effects to describe π back-bonding are less important for the second- and third-row than for the first-row TM complexes.[41,45,60,69]

In their study PF also investigated the structure of $HRh(CO)_3$ (**5**) using the MP2 method. The authors located two energy-minimum isomers: a quadratic planar form and the C_{3v} symmetry structure. The former was more stable by 38 kJ mol^{-1}. Previous LDA calculations by Schmid, Herrmann, and Frenking (SHF)[69] gave a slightly nonplanar structure for $HRh(CO)_3$. The minor differences found in the two structures obtained at the LDA and MP2 levels of theory have been attributed to the lack of nonlocal corrections and the neglect of relativistic effects in LDA calculations.[69]

Results by PF indicated that the reaction

$$HRh(CO)_4 + H_2 \rightarrow HRh(CO)_3 + CH_2O \quad (3)$$

is endothermic by 116.2 kJ mol^{-1} at the MP2 level.

Table 3. Calculated Ligand Dissociation Energies without ZPE (kJ mol^{-1})[a]

	$\Delta E_{6a\rightarrow 7}(PH_3)$	$\Delta E_{8b\rightarrow 7}(CO)$		$\Delta E_{6a\rightarrow 7}(PH_3)$	$\Delta E_{8b\rightarrow 7}(CO)$
HF//HF	−13.4	2.1	CCSD(T)//MP2	49.7	90.3
MP2//HF	81.1	118.7	LDA//LDA	113.3	165.5
MP2//MP2	94.9	137.5	NLDA//LDA	53.9	97.0
CCSD//MP2	43.1	78.6	NLDA//NLDA	56.0	100.3

[a] From reference 69.

From the experimental heats of formation at 0 K,[70] the process $H_2 + CO \rightarrow CH_2O$ is found to be slightly endothermic by 0.4 kJ mol^{-1}. These data provide an estimation for the dissociation energy of CO from $HRh(CO)_4$ of 115.8 kJ mol^{-1}, a value that is smaller than the dissociation energies computed for $HCo(CO)_4$, except for the CASSCF results.

In the so-called low-pressure oxo (LPO) process the precatalyst used is $HRh(CO)(PPh_3)_3$.[9b,11f−h,16a] This process has a high chemoselectivity (ratio of aldehydes to alcohols) for aldehydes and a high regioselectivity (ratio of linear to branched aldehydes) for *n*-aldehydes. The major disadvantage is that it is applicable only to lower olefins. Dissociation of a PPh_3 from $HRh(CO)(PPh_3)_3$ gives rise to the SPl 16-electron $HRh(CO)(PPh_3)_2$ catalytically active species. SHF[69]studied this process theoretically using HF, MP2, CCSD(T), and DFT methods with both local and gradient-corrected functionals. SHF used PH_3 as a model of PPh_3 in their calculations. For $HRh(CO)(PH_3)_3$ (**6**) the authors analyzed only TBP structures with an axial hydride ligand. They found that the TBP with axial CO (**6a**) was more stable than the TBP structure with equatorial CO (**6b**) by 5.5 kJ mol^{-1}. Dissociation of a phosphine ligand from the most stable $HRh(CO)(PH_3)_3$ TBP structure to yield $HRh(CO)(PH_3)_2$ (**7**) costs 49.7 kJ mol^{-1} at the CCSD(T)//MP2 level with a valence double-ζ plus polarization basis set. Dissociation energies for the **6a** → **7** + PH_3 process at other levels of calculation are listed in Table 3. Values in this table confirm that HF dissociation energies are very imprecise, while reliable bond energies can be obtained by DFT methods employing gradient-corrected functionals at a fraction of the computational effort necessary for CCSD(T) calculations. The MP2 method appears to overestimate correlation effects compared with other more precise methods such as CCSD(T) or QCISD.[71,72] The weaker π acceptor character of PH_3 compared to CO is responsible for the relatively small dissociation energy of PH_3. One can expect a large dissociation energy for the release of PPh_3 from $HRh(CO)(PPh_3)_3$, on the basis of the larger basicity of PPh_3 as compared to PH_3.[69,73] Analysis of the dissociation energy of PMe_3 from $HRh(CO)(PMe_3)_3$ by SHF[69] showed that PH_3 is not suitable as a model for PPh_3 and that at least PMe_3 must be employed when PPh_3 is modeled.

The same $HRh(CO)(PPh_3)_2$ catalytically active species can be obtained from $HRh(CO)_2(PPh_3)_2$ through CO dissociation. SHF[69] and also Matsubara, Koga, Ding, Musaev, and Morokuma (MKDMM)[74] studied this dissociation process. In both studies PPh_3 was replaced by PH_3. The TBP structure of $HRh(CO)_2(PH_3)_2$ (**8**) with two equatorial carbonyl ligands (**8a**) is slightly more stable than the TBP structure with two equatorial phosphine ligands (**8b**) by 1.7,[69] 10.5,[74] and 0.4[75] kJ mol^{-1} at the LDA, MP2, and BP86 levels, respectively. These small energy differences confirm the experimental observation that these isomers **8a** and **8b** are in equilibrium for $HRh(CO)_2(PPh_3)_2$.[75,76a] Table 3 contains calculated dissociation energies for the release of a CO from **8b** to yield $HRh(CO)(PH_3)_2$ (**7**). SHF chose **8b** instead of the more stable **8a** because the analogous PPh_3 complexes prefer the diequatorial arrangement for steric reasons. Dissociation of a carbonyl ligand in **8b** costs 90.3 kJ mol^{-1} at the CCSD(T)//MP2 level, whereas the dissociation energy of a phosphine ligand from **8b** is 53.1 kJ mol^{-1} at the same level of theory.[69] The authors concluded that CO is more firmly bonded to **8b** than PH_3 because of its higher π back-bonding interactions. Release of a PH_3 from **8b** was calculated by MKDMM[74] to be 78.2 kJ mol^{-1} at the MP2//HF level of theory, in good agreement with the experimental value of PPh_3 dissociation from $HRh(CO)_2(PPh_3)_2$ in solution (83 ± 4 kJ mol^{-1}).[76] However, as explained by SHF[69] the MP2//HF method gives dissociation energies close to the experimental and CCSD(T)//MP2 values because of error cancellation resulting from the fact that, on one hand, MP2 overestimates the dissociation energy and, on the other hand, HF predicts too long metal−ligand bond lengths.

2. Olefin Coordination

Once the unsaturated 16-electron $HCo(CO)_3$ species has been formed, the next step in the catalytic cycle is the coordination of the olefin to $HCo(CO)_3$, step **b** of Scheme 1. From the interaction of the olefin (ethylene in most theoretical studies) with complex **3a** two adducts can be formed, one with the ethylene molecule coplanar to the equatorial plane (**9a** in Scheme 4), and one with ethylene perpendicular to

Scheme 4

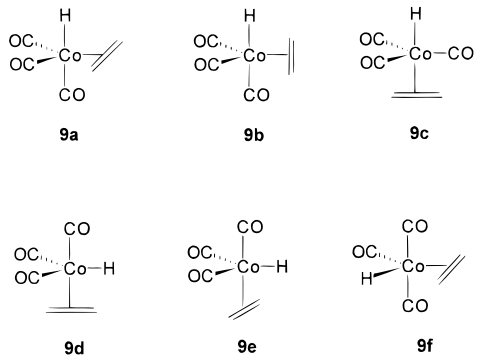

it (**9b**). The coordination of the olefin to species **3b** giving **9c** is also conceivable, but usually it has not been investigated because **9c**, having hydrogen and ethylene in trans positions, is unable to continue with

Table 4. Relative Energies for Different $HCo(\eta^2\text{-}C_2H_4)(Co)_3$ Complexes Studied (kJ mol^{-1})

	9a	9b	9d	9f	ref
CI//HF	0	94	42	−24	40
HFS	0	20	56		78

the next step of the catalytic cycle. From species **3c** two possible adducts can be obtained, one with ethylene parallel to the Co−H bond (**9d**), and another with ethylene perpendicular to it (**9e**). The latter has not been studied because the alkene molecule is not correctly positioned for olefin insertion. Finally, another possible structure for $HCo(CO)_3(\eta^2\text{-}C_2H_4)$ (**9**) is **9f**.

The first ab initio work on the coordination of ethylene to $HCo(CO)_3$ was carried out by AD.[40] In their work, the authors studied TBP complexes **9a**, **9b**, **9d**, and **9f** by means of a CI procedure using geometries optimized at the HF level. Results from the relative energies among these complexes have been gathered in Table 4. Conformation **9f** is predicted to be 24 kJ mol^{-1} more stable than **9a**, and this in turn 94 kJ mol^{-1} more stable than **9b**. The larger stability of **9a** as compared to **9b** was already predicted by Rossi and Hoffmann from EHT calculations,[77] and has been attributed to the more favorable π back-bonding interaction in this conformation.[77,78] Similar results based on the HFS model were reported by Versluis, Ziegler, and Fan (VZF).[78] VZF studied conformations **9a**, **9b**, and **9d**, and found that **9a** is the most stable, **9b** and **9d** being 20 and 56 kJ mol^{-1} higher in energy than **9a**, respectively. The ethylene dissociation energy from **9a** was calculated to be 70 kJ mol^{-1}.

In all $HCo(CO)_3(\eta^2\text{-}C_2H_4)$ complexes, the bonding between the olefin and the complex follows the well-known Dewar−Chatt−Duncanson scheme,[79] with σ donation from the ethylene π orbital to an unoccupied d orbital of the metal and back-donation from an occupied d orbital of the metal to the π^* orbital of ethylene. The latter interaction is responsible for the significant charge transfer from $HCo(CO)_3$ to ethylene.[36,78,80] The hydrogen atoms of the ethylene are tilted away from the metal, raising the energy level of the ethylene π orbital and lowering the energy of the ethylene antibonding π^* orbital,[40,78,80] thus favoring the main orbital interactions. The C=C bond length in ethylene is elongated as a result of the population of the π^* orbital of ethylene through back-donation.

Ethylene coordination to the $HRh(CO)_2(PH_3)$ complex was analyzed by Koga, Jin, and Morokuma (KJM)[22,81] and by MKDMM.[74] Scheme 5 shows the most relevant results obtained by KJM at the HF level for ethylene coordination to $HRh(CO)_2(PH_3)$. $HRh(CO)_2(PH_3)$ has two possible SPl isomers, **10a** and **10b**. The isomer with the two carbonyl ligands cis is 7.1 kJ mol^{-1} more stable than the isomer with the carbonyl ligands trans. Ethylene coordinates to $HRh(CO)_2(PH_3)$ in an equatorial position. $HRh(CO)_2(PH_3)(\eta^2\text{-}C_2H_4)$ complexes with axial hydride are more stable than those with equatorial hydride by about 40 kJ mol^{-1}. The preference for axial hydride and equatorial ethylene in this d^8 TBP complex can be

Scheme 5. Coordination and Insertion of Ethylene in the Hydroformylation Process Catalyzed by $HRh(CO)_2(PH_3)$[a]

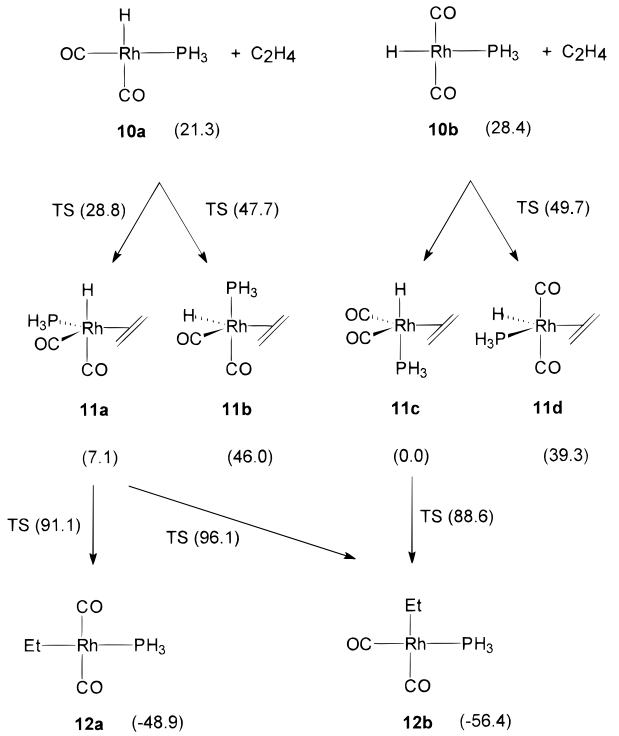

[a] HF energies in parentheses (kJ mol^{-1}).[22,81]

attributed to the presence of a formally vacant axial d orbital (d_{z^2}) suitable for σ bonding with the 1s orbital of the hydride, and occupied equatorial d orbitals ($d_{x^2-y^2}$,d_{xy}) appropriate for back-donation to the π^* orbital of ethylene. The formation of the most stable $HRh(CO)_2(PH_3)(\eta^2\text{-}C_2H_4)$ isomer **11c** with two equatorial CO ligands from **10b** is a barrierless process, while coordination of ethylene to **10a** to yield **11a** has a small barrier of 7.5 kJ mol^{-1}. As stated for $HCo(CO)_3(\eta^2\text{-}C_2H_4)$, KJM found that the energy difference between **11c** with ethylene parallel to the equatorial plane and the same structure with ethylene perpendicular to it is 84.4 kJ mol^{-1} at the HF level. MP2 calculations by MKDMM[74] confirm that **11c** is more stable than **11a** (by 10.0 kJ mol^{-1}). MP2 dissociation energies of ethylene from **11a** and **11c** are 103.7 and 134.6 kJ mol^{-1}, respectively, to be compared with the previous HF values[81] of 14.2 and 28.4 kJ mol^{-1}, respectively. As before, these differences between MP2 and HF dissociation energies of about 100 kJ mol^{-1} can be attributed to the HF erroneous description of π back-donation effects, reflected also in the longer metal−olefin and metal−CO distances in HF-optimized structures. Finally, KJM also studied nine possible SPy structures for $HRh(CO)_2(PH_3)(\eta^2\text{-}C_2H_4)$, concluding that all these SPy structures are TSs connecting TBP structures through BPR.

Rocha and De Almeida[82] (RDA) performed calculations at the MP4(SDQ)//MP2 level on the olefin coordination and insertion into the $HPtX(PH_3)_2$ complex ($X = Cl^-, SnCl_3^-$). This Pt(II) catalyst has special relevance in the field of asymmetric hydroformylation.[12] The authors studied the $HPtX(PH_3)_2(\eta^2\text{-}C_2H_4)$ complex, finding that the conformation with the two

phosphines and ethylene in equatorial positions of type **9a** is more stable than **9b** by 79.4 and 37.6 kJ mol^{-1} for X = Cl$^-$ and X = $SnCl_3^-$, respectively, in agreement with previous qualitative calculations with the EHT method by Thorn and Hoffmann.[83] Dissociation energies of ethylene from the most stable conformation of the $HPtX(PH_3)_2(\eta^2\text{-}C_2H_4)$ complex are 35.1 and 52.7 kJ mol^{-1} for X = Cl$^-$ and X = $SnCl_3^-$, respectively. The authors concluded that the major role of the $SnCl_3^-$ ligand as compared to Cl$^-$ is to stabilize the pentacoordinate intermediate, to favor the olefin internal rotation by 41.8 kJ mol^{-1}, and to weaken the Pt−H bond trans to it ($SnCl_3^-$ is a stronger trans director ligand than Cl$^-$), facilitating the subsequent ethylene insertion.

The coordination of an alkene different from ethylene to the metal 16-electron catalytically active species has been discussed in two works. In the first, Grima, Choplin, and Kaufmann (GCK)[36] carried out semiempirical CNDO/2 calculations to analyze the coordination of propylene to $HCo(CO)_3$. GCK studied structures **9a**, two conformers of **9b** (**13a** and **13b** in Scheme 6), and **9c**. The energies obtained for these

Scheme 6

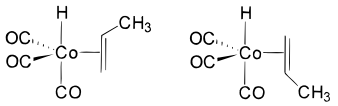

complexes were very similar, structure **9c** being the more stable. Interestingly, **13a** was slightly more stable than **13b** (by 18 kJ mol^{-1}). The difference between **13a** and **13b** is important because it governs the regioselectivity of the process: **13a** leads to linear aldehydes, while **13b** gives branched aldehydes. In agreement with experiment, CNDO/2 calculations favor the formation of linear products. In the second work, Trzeciak et al.[84] carried out calculations by the Fenske−Hall method on the interaction of hexadiene with $HRh(CO)(PPh_3)_2$ and $HRh(CO)_3$ at a frozen model geometry. The authors concluded that also for this system coordination of the olefin coplanar to the equatorial plane is more favorable and less reactive for insertion than the perpendicular coordination.

3. Olefin Insertion

The next step involves the insertion of the olefin into the Co−H bond of $HCo(CO)_3(\eta^2\text{-}C_2H_4)$. The main orbital interactions involved in this insertion process are well characterized:[23,25−28,30] first, donation from the π orbital of the olefin to the LUMO antibonding σ^*_{Co-H} orbital of $HCo(CO)_3$ and, second, back-donation from the HOMO bonding σ_{Co-H} orbital to the olefin π^* orbital.

The first crude estimation of the energy barrier for this ethylene insertion was provided by GCK[36] using the CNDO/2 method. The authors found a barrier smaller than 84 kJ mol^{-1} on the basis of partial optimizations on the linear transit from the $HCo(CO)_3(\eta^2\text{-}C_2H_4)$ **9b** structure to $Co(C_2H_5)(CO)_3$. Using the CI//HF methodology, AD[40] studied the insertion that transforms **9b** into **14a** (Scheme 7), the most stable $Co(C_2H_5)(CO)_3$ complex at this level of theory.

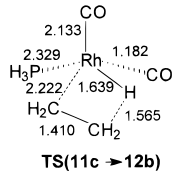

Figure 1. HF-optimized structure for the TS of the olefin insertion in species **11c**. Bond distances in angstroms.[81]

Scheme 7

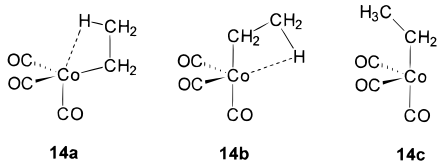

They found that the process is exothermic by 79 kJ mol^{-1} with an energy barrier of 73 kJ mol^{-1} in agreement with the value given by GCK[36] and not far from the experimental value of 25−33 kJ mol^{-1} determined for $Cp(P(OMe)_3)CoCH_2CH_2\text{-}\mu\text{-}H^+$.[85] Remarkably, the insertion from complex **9f**, which is the most stable $HCo(CO)_3(\eta^2\text{-}C_2H_4)$ complex found by AD, is quite endothermic (by 61 kJ mol^{-1}) and has a large energy barrier of 229 kJ mol^{-1}, and therefore it is unlikely to occur. HFS calculations by VZF[78] for the **9b** → **14a** insertion show that this reaction is exothermic by 8 kJ mol^{-1} and it has an approximate energy barrier obtained from a linear transit smaller than 6 kJ mol^{-1}. This is in accordance with experimental findings suggesting that the olefin insertion into an M−H bond is very facile. At the HFS level, the most stable $Co(C_2H_5)(CO)_3$ species is **14b**. With respect to **14b**, **14a** is found 28 kJ mol^{-1} higher in energy at the HFS level and 26.2 kJ mol^{-1} lower in energy at the CI//HF level. The difference has been attributed to the limitation of the HF method to describe the agostic interaction present in these two complexes.[78] For instance, in **14a** the Co−H bond is 1.62 Å in the HFS-optimized geometry and 2.78 Å at the HF level. The lower energy barrier for the **9b** → **14a** insertion found by the HFS method as compared to the HF level can also be related to the fact that the hydrogen atom is closer to cobalt throughout the insertion process. VZF found that the transit from **14a** to **14c** has a considerable activation barrier of 130 kJ mol^{-1}, and therefore, under catalytic conditions this conversion is probably superseded by the coordination of an incoming CO molecule in the axial site.

The intramolecular olefin insertion in the hydroformylation process catalyzed by Rh(I) complexes was studied by Morokuma et al.[26,74,81] in the $HRh(CO)_2(PH_3)(\eta^2\text{-}C_2H_4)$ complex. The authors carried out HF optimizations using ECPs and MP2 single-point energy calculations at the HF-optimized geometries for some species and analyzed different reaction paths for the olefin insertion process. The most favorable starts from structures **11a** and **11c** (Scheme 5) and proceeds through an SPy four-center TS (Figure 1) with basal olefin and basal hydride in which the Rh−H bond being broken is parallel to the C=C bond. The insertion process is exothermic by ca. 50 kJ mol^{-1}, and it has an energy barrier, insensitive

to electron correlation, of about 90 kJ mol^{-1}. The TS has reactant-like character, indicating that the most important origin of the activation energy is not the bond-breaking/forming process but the ethylene rotation coupled with the structural change from TBP to SPy.[26,74,81,83] This structural change occurs from **11** by bending the axial ligands toward the equatorial plane with a small rotation of ethylene. After the hydride migration, the apical ligand moves to the vacant site left by the hydride to generate **12** with SPl structure.

MP4(SDQ)//MP2 calculations by RDA[82] on the conversion of $HPtX(PH_3)_2(\eta^2\text{-}C_2H_4)$ from the most stable conformation to the SPl $PtX(PH_3)_2(C_2H_5)$ complex in its most stable arrangement having the two phosphine ligands in cis positions indicated that the insertion of ethylene is exothermic by 48.5 and 56.4 kJ mol^{-1} with an energy barrier of 141.7 and 49.3 kJ mol^{-1}, for X = Cl$^-$ and X = $SnCl_3^-$, respectively. For the reasons commented on before, the insertion of the olefin into $HPtX(PH_3)_2(\eta^2\text{-}C_2H_4)$ is easier for X = $SnCl_3^-$ than for X = Cl$^-$.

Other studies on olefin coordination to and insertion into other TM complexes apart from those relevant to the hydroformylation process have been summarized in previous reviews and will not be covered here.[22−28,30,86−88]

Following olefin insertion a 16-electron unsaturated complex is formed. Its vacant coordination site is filled by an incoming ligand. In the hydroformylation reaction catalyzed by $HCo(CO)_4$, the addition of a CO ligand in the final process of step **c** leads to the complex $RCo(CO)_4$ (R = alkyl). At the HFS level,[43] the C_{3v} structure of $RCo(CO)_4$ with R in the axial site is 63 and 42 kJ mol^{-1} lower in energy than the C_{2v} isomer with R in the equatorial position for R = H and R = CH_3, respectively, in agreement with Rossi and Hoffmann predictions based on an EHT analysis[77] of d^8 pentacoordinate systems.

Likewise, addition of a PH_3 ligand to complexes **12a** and **12b** yields species **15a** and **15b** (Scheme 8), **15b** being 8.4 kJ mol^{-1} lower in energy than **15a** at the HF level.[74] As found for $RCo(CO)_4$, conformations with ethyl in equatorial positions were found to be at least 40 kJ mol^{-1} higher in energy.[74] The exothermicity associated with the **12a** → **15b** process is 102.4 kJ mol^{-1} at the MP2//HF level.[74]

4. Carbonyl Insertion

Step **d** in the hydroformylation mechanism by Heck and Breslow corresponds to the CO insertion into the R−Co bond:

$$RCo(CO)_4 \rightarrow RC(O)-Co(CO)_3 \qquad (4)$$

This reaction has been investigated by ab initio MO[40] and HFS[43] methods for R = H and by the EHT[89] and HFS[43] methods for R = CH_3.

The carbonyl insertion in $HCo(CO)_4$ to give $HC(O)Co(CO)_3$ complex **16** (Scheme 9, R = H, M = Co) was studied by means of ab initio MO calculations starting from the most stable **2b** structure.[40] AD followed the migration of the hydrogen atom onto an equatorial carbonyl ligand using a linear transit

Scheme 8. Insertion of CO and Oxidative Addition of H_2 in the Hydroformylation Process Catalyzed by $HRh(CO)_2(PH_3)$[a]

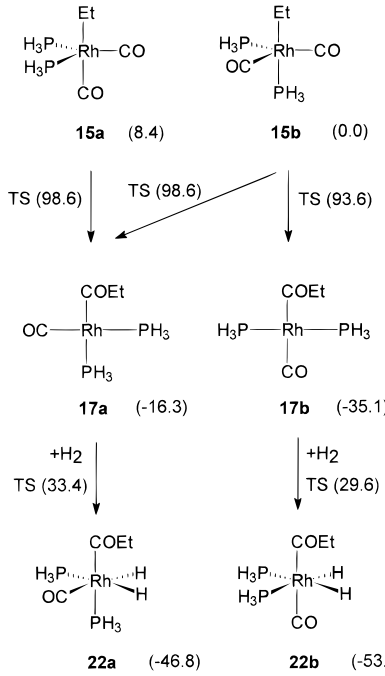

[a] HF energies in parentheses (kJ mol^{-1}).[74]

Scheme 9

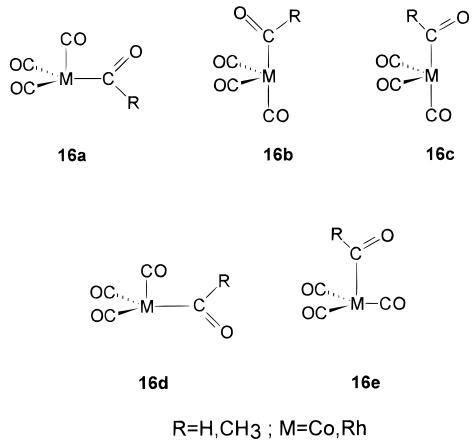

procedure at the HF level. According to their calculations, the insertion (**2b** → **16a**) proceeds with an endothermicity of 85.7 kJ mol^{-1} and an activation barrier of 212.5 kJ mol^{-1}. Two other insertion paths starting from structure **2c** were found to be even more energy demanding. These too large and unrealistic energy barriers for a catalytic process were probably the result of lack of electron correlation and the unoptimized TS structure.

HFS results by VZBR[43] were significantly different from those obtained with ab initio MO methods by AD. At the HFS level, the **16a** and **16b** $HC(O)Co(CO)_3$ species are unstable and revert to the parent hydrido complexes. Thus, the insertion in $HCo(CO)_4$ was found to be a thermodynamically and kinetically unfavorable process. These HFS results agree with the experimental finding that most neutral metal formyl complexes readily convert to the corresponding hydrido complexes.[90] On the other hand, species

16c and **16d** (R = H, M = Co) represent local minima, although as compared to $HCo(CO)_4$ these complexes are higher in energy by 151 and 116 kJ mol^{-1}, respectively. The higher stability of **16d** as compared to **16c** was attributed to the presence of an η^2 interaction in **16d**.[43]

Similar results were obtained by PF[66] studying the carbonyl insertion in the parent compound $HRh(CO)_4$ by means of the MP2 method. The authors carried out optimization processes starting from all possible arrangements of the ligands. Nevertheless, they found only two energy minima: **16c** and **16e** (Scheme 9, R = H, M = Rh), the **16e** species being only 5.4 kJ mol^{-1} lower in energy. The energy barrier for the interconversion between these two species was found to be only 24.2 kJ mol^{-1}. According to results by PF, the C_{3v} $HRh(CO)_4 \rightarrow$ **16e** carbonyl insertion is endothermic by 117.9 kJ mol^{-1} and has an energy barrier of 118.7 kJ mol^{-1}. Therefore, as found for M = Co and R = H,[43] complexes **16** with M = Rh and R = H can easily revert to $HRh(CO)_4$.

The carbonyl insertion of eq 4 with $R = CH_3$ was discussed by Berke and Hoffmann using the EHT method.[89] The authors concluded that the insertion from the most stable[89,91] $CH_3Co(CO)_4$ C_{3v} TBP complex with axial methyl proceeds with a small barrier of about 54 kJ mol^{-1} through a BPR that places the methyl in an equatorial site, and after that the migration of CO from the equatorial site faces only a very small kinetic barrier to form species **16c**. HFS calculations by VZBR[43] were also carried out for the CO insertion in the same $CH_3Co(CO)_4$ TBP complex. The two possible configurations of the $CH_3Co(CO)_4$ TBP complex with the methyl group in axial and equatorial sites were analyzed. In addition, VZBR discussed two possible pathways: the migration of the methyl group to a *cis*-carbonyl ligand and the insertion of the CO ligand into the $Co-CH_3$ bond. All four reaction paths were followed by a linear transit procedure in which an internal coordinate was chosen as the reaction coordinate. The energy profile obtained in this way sets an upper energy limit for the activation barrier of the process. The authors found that the energy profile for CO insertion has a high activation barrier of about 200 kJ mol^{-1}. The origin of such a barrier can be associated with the presence of a destabilizing four-electron interaction between the lone pair in the σ_{CO} orbital and an occupied nonbonding d orbital of Co that occurs along the transit. Migration of CH_3 takes place with a lower barrier. In particular, the conversion of $CH_3Co(CO)_4$ with axial methyl to species **16b** has an endothermicity of 21 kJ mol^{-1} and an activation barrier of 40 kJ mol^{-1}. Rearrangement of **16b** to **16c** is exothermic by 16 kJ mol^{-1} and has an energy barrier of 97 kJ mol^{-1}. Despite this rather high energy barrier (118 kJ mol^{-1} for the transit $CH_3Co(CO)_4 \rightarrow$ **16c**), the alkyl migration is thermodynamically and kinetically more feasible than hydride migration in $RCo(CO)_4$ complexes. The spherical H atom easily migrates to the M atom (M = Co, Rh) in $HC(O)M(CO)_3$ species, giving $HM(CO)_4$. This process is less favorable for the methyl group in $CH_3C(O)Co(CO)_3$ that has a much more directional singly occupied σ orbital. Further, M−H bonds are stronger than M−C bonds in neutral $RM(CO)_4$ (M = Co, Rh, and Ir) species.[31,42,60]

The intramolecular CO insertion process in species **15a** and **15b** that yields four-coordinate SPl complexes **17** (Scheme 8) was studied at the HF level by MKDMM.[74] The TS corresponding to the **15** → **17** transformation has a TBP-like structure. Along the reaction coordinate, there is, first, a bending of the axial ethyl and CO or PH_3 ligands toward the equatorial plane before the TBP-like transition structure is reached in which the ethyl group occupies an equatorial position. The process is slightly exothermic and the overall activation barrier is about 90 kJ mol^{-1} at both the HF and MP2 levels of theory. Therefore, in contrast to $HC(O)Rh(CO)_3$, $EtC(O)Rh(CO)(PH_3)_2$ is stable and does not revert easily to species **15**.

Other studies on carbonyl insertion not directly related to the hydroformylation process have been summarized in previous reviews and will not be discussed here.[22−24,29,30,60,88,89,92]

5. Oxidative Addition of H_2 and Aldehyde Reductive Elimination

The focus of this section is on the final elimination of aldehyde, step **e** of Scheme 1. In this step H_2 is assumed to add oxidatively to the unsaturated acyl complex, yielding a dihydro acyl species

$$RC(O)Co(CO)_3 + H_2 \rightarrow RC(O)Co(CO)_3(H)_2 \quad (5)$$

followed by an irreversible reductive elimination of the aldehyde molecule and the recovery of the initial catalyst $HCo(CO)_3$

$$RC(O)Co(CO)_3(H)_2 \rightarrow RCHO + HCo(CO)_3 \quad (6)$$

Experimental evidence of the existence of $RC(O)Co(CO)_3(H)_2$ species for R = H and CH_3 was provided by Sweany and Rusell in inert-gas matrixes.[93] Remarkably, inverse kinetic isotope effects when using deuterium gas instead of hydrogen support hydrogen atom transfer occurring before or during the rate-determining step.[94] This seems to point out that the rate-determining step could be the oxidative addition of H_2 or the reductive elimination of aldehyde. Further support for the rate-determining step being the oxidative addition of H_2 has been provided recently by Feng and Garland.[13a]

Theoretically, reactions 5 and 6 with $R = CH_3$ were studied at the HFS and BP86 levels by Ziegler and co-workers.[95,96] BP86-optimized structures of the reactants, intermediates, and products for this step are shown in Figure 2. Solà and Ziegler (SZ)[96] found that the addition of H_2 to complex **16c** (the most stable configuration for complex **16**) to yield $CH_3C(O)Co(CO)_3(\eta^2\text{-}H_2)$ species **18** (see Figure 2) was an exothermic process that releases 10.5 kJ mol^{-1}.[96] The main stabilizing orbital interaction in complex **18** is between the metal-base $3d_{xy}$ HOMO on $CH_3C(O)Co(CO)_3$ and the σ^* LUMO on H_2. As a consequence of this interaction, the H−H bond distance is somewhat elongated with respect to that of the free H_2 molecule. On the contrary, addition of H_2 to complex **16d** was calculated to be quite endothermic with a reaction enthalpy of 137 kJ mol^{-1} at the HFS level.[95] The

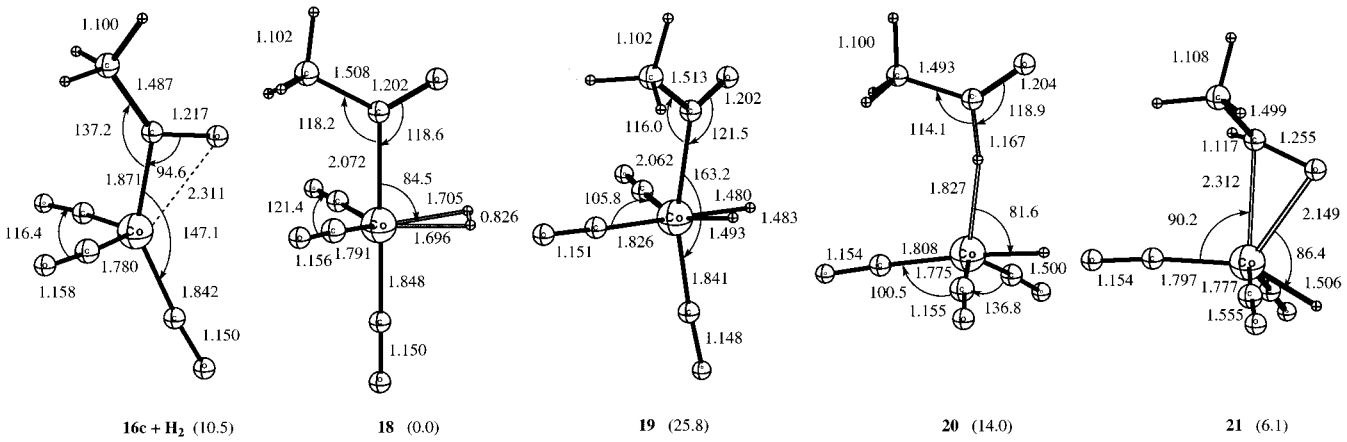

Figure 2. BP86-optimized structures for complexes **16** and **18**−**21**. Bond distances in angstroms and angles in degrees.[96] Energies referred to complex **18** (in parentheses) are given in kilojoules per mole. Reprinted from ref 96. Copyright 1996 American Chemical Society.

dihydride species **19** that results from an oxidative addition of H_2 was calculated to be less stable than the parent η^2 adduct **18** by 25.8 kJ mol^{-1} at the BP86 level.[96] The energy profiles of the different elementary processes were investigated by linear transit procedures.[95,96] Using this method, the activation energy for **18** → **19** is 30.5 kJ mol^{-1}. Reductive elimination of acetaldehyde from **19** to yield **20** is exothermic by 11.8 kJ mol^{-1} and has an energy barrier of 10.5 kJ mol^{-1}. As a whole, the postulated oxidative addition/reductive elimination process (**18** → **19** → **20**) is almost thermoneutral and has an activation energy of only 36.3 kJ mol^{-1}. The authors also analyzed an alternative σ bond metathesis pathway that connects **18** to **20** through a four-center TS. Previous HFS[95] calculations yielded similar activation barriers for these two processes. However, at the BP86 level,[96] the barrier for the σ-bond metathesis path is 70.4 kJ mol^{-1}, and therefore BP86 results indicated that the σ bond metathesis **18** → **20** process is less likely than the postulated oxidative addition/reductive elimination **18** → **19** → **20** pathway. The σ complex **20** can rearrange by a simple rotation of the acetaldehyde fragment to give the π complex **21**, which is more stable than **20** by only 7.9 kJ mol^{-1}. This small energy difference corresponds to the different stabilization provided by the agostic interaction in **20** and the π interaction in **21**. Release of acetaldehyde from **20** by breaking the agostic interaction between $CH_3C(O)H$ and $HCo(CO)_3$ is endothermic by 27.1 kJ mol^{-1}.

The addition of H_2 to the coordinately unsaturated complex **16c** (Scheme 9 with R = H and M = Rh) to yield $HC(O)Rh(CO)_3(\eta^2\text{-}H_2)$ was studied by PF at the MP2 level.[66] They found that this addition is slightly exothermic by 0.8 kJ mol^{-1}. Rotation by 180° around the Rh−C_{acyl} group in $HC(O)Rh(CO)_3(\eta^2\text{-}H_2)$ presents an energy barrier of only 7.9 kJ mol^{-1} and leads to a slightly more stable configuration (−0.4 kJ mol^{-1}). Oxidative addition to give the corresponding $HC(O)Rh(CO)_3(H)_2$ dihydro acyl complex is also exothermic by 13.4 kJ mol^{-1} with a small energy barrier of 11.3 kJ mol^{-1}. Finally, loss of H_2CO from the $HC(O)Rh(CO)_3(H)_2$ dihydro acyl complex has an activation barrier of 35.9 kJ mol^{-1}, and it is slightly endothermic by 20.5 kJ mol^{-1}.

Oxidative addition of H_2 to complex **17** has been investigated by MKDMM at the HF level.[74] In contrast to $HC(O)Rh(CO)_3(\eta^2\text{-}H_2)$, and as expected from the fact that the stability of the dihydride isomer increases in comparison to that of the dihydrogen species when CO is substituted by PR_3,[95] the $EtC(O)Rh(CO)(PH_3)_2(\eta^2\text{-}H_2)$ species are not stable and addition of H_2 to complex **17** produces directly the $EtC(O)Rh(CO)(PH_3)_2(H)_2$ dihydride isomer **22**. Addition of H_2 to $RhCl(CO)(PH_3)_2$ also gives the dihydride complex.[97] Experimentally, the cationic complex $[RhH_2(PP_3)]^+$ ($PP_3 = P(CH_2CH_2PPh_2)_3$) was found to be a highly dynamic dihydride complex.[98] Reaction energies and activation barriers for the oxidative addition of H_2 to complex **17** at the HF level are given in Scheme 8. In particular, the transformation **17b** + H_2 → **22b** is exothermic by 18.4 kJ mol^{-1} and has a modest barrier of 64.7 kJ mol^{-1}. Reductive elimination in **22b** to yield the π complex $HRh(CO)(PH_3)_2(\eta^2\text{-}EtCH(O))$ has an activation barrier of 105.8 kJ mol^{-1} (47.2 kJ mol^{-1} at the MP2//HF level) and a reaction energy of 7.1 kJ mol^{-1}. Finally, release of propanaldehyde and formation of $HRh(CO)(PH_3)_2$ from $HRh(CO)(PH_3)_2(\eta^2\text{-}EtCH(O))$ is endothermic by 29.7 kJ mol^{-1}, a value similar to those found by PF[66] and SZ[96] in their model systems. As a whole, all authors reported modest energy barriers for the gas-phase oxidative addition/reductive elimination step.

Aldehydes react with $HCo(CO)_4$ to yield alcohols.[7,99] This is a side reaction in industrial catalytic processes. In fact, at T = 183 °C alcohols are the main product of alkene hydroformylation in a process called hydroxymethylation.[10a] Alcohol formation is normally assumed[7,99] to result from further reaction of the aldehyde formed in step **e** with the catalyst $HCo(CO)_3$ to form a hydroxyalkyl complex

$$HCo(CO)_3 + RC(O)H \rightarrow HCo(CO)_3(\eta^2\text{-}RC(O)H) \rightarrow RC(OH)(H)Co(CO)_3 \quad (7)$$

which can react with H_2 to eliminate the alcohol and regenerate the catalyst $HCo(CO)_3$

$$RC(OH)(H)Co(CO)_3 + H_2 \rightarrow RCH_2OH + HCo(CO)_3 \quad (8)$$

Reactions 7 and 8 were studied by SZ at the BP86 level.[96] Starting from the $HCo(CO)_3(\eta^2\text{-}CH_3C(O)H)$ π complex **21**, migration of the hydrogen atom to the acetaldehyde oxygen results in the coordinately unsaturated hydroxyethyl complex $CH_3C(OH)(H)Co(CO)_3$. This hydrogen atom migration is slightly exothermic (11.1 kJ mol^{-1}) and has a modest activation barrier of 48.4 kJ mol^{-1} (55 kJ mol^{-1} at the HFS level[100]). The hydroxyethyl complex is equivalent to complex **16c**, the only difference being the substitution of the acyl fragment, CH_3CO, by a hydroxyethyl group, $CH_3C(H)(OH)$. Addition of dihydrogen to this hydroxyethyl complex yields ethanol and $HCo(CO)_3$. Again, two possible pathways are possible: the oxidative addition/reductive elimination and the four-center TS. The former has an energy barrier of 44.8 kJ mol^{-1}, whereas the barrier for the latter is 49.8 kJ mol^{-1}. The difference between the two routes is now smaller, although the oxidative addition/reductive elimination pathway is still preferred. It is worth noting that, from a thermodynamic point of view, alcohol formation is exothermic while acetaldehyde formation is slightly endothermic. However, from a kinetic point of view, while the barrier for the H_2-induced acetaldehyde elimination from complex **16c** process is 36.3 kJ mol^{-1}, the H_2-induced ethanol elimination from the same species has to surpass an energy barrier of 42.3 kJ mol^{-1}. Thus, kinetically, the acetaldehyde elimination is favored over the ethanol formation.

Some authors[101] have suggested an alternative mechanism for alcohol formation that involves a hydroxycarbene intermediate. It is suggested that hydroxycarbene is formed in step **e** of Scheme 1 by a hydride transfer to the acyl oxygen rather than the acyl carbon:

$$RC(O)Co(CO)_3(H)_2 \rightarrow RC(OH)Co(CO)_3H \quad (9)$$

Further isomerization of the hydroxycarbene complex will produce the hydroxyalkyl complex

$$RC(OH)Co(CO)_3H \rightarrow RC(OH)(H)Co(CO)_3 \quad (10)$$

which again can react with H_2 to eliminate $HCo(CO)_3$ and an alcohol according to eq 8. SZ found that the hydroxycarbene intermediate is thermodynamically accessible, although the energy barriers for the reaction pathways leading to its formation are larger than 95.5 kJ mol^{-1}.[96] They concluded that generation of alcohols do not proceed via the formation of this hydroxycarbene complex but rather through further hydrogenation of the aldehyde molecules.

Similar conclusions were reached by PF[66] with respect to the hydroxycarbene complex. The authors excluded for kinetic reasons the formation of the hydroxycarbene intermediate as a possible route to the synthesis of alcohol. On the other hand, PF found that the hydroxymethyl $H_2C(OH)Rh(CO)_3$ complex obtained from H migration to the formaldehyde oxygen in the $HRh(CO)_3(\eta^2\text{-}CH_2O)$ π complex was thermodynamically and kinetically slightly more favorable than the formation of the methoxy $CH_3ORh(CO)_3$ complex from H migration to the formaldehyde carbon. The H migration to form the hydroxymethyl species is slightly exothermic (14.2 kJ mol^{-1}) but has a rather large activation barrier of 73.6 kJ mol^{-1}. These values are similar to those reported by SZ[96] for the $HCo(CO)_3(\eta^2\text{-}CH_3C(O)H)$ π complex.

Finally, it is worth mentioning that reviews on oxidative additions to different TM complexes and reductive eliminations can be found in refs 22, 23, 26, 30, 86, and 87.

6. Final Remarks

The energetics of the hydroformylation reaction catalyzed by $HCo(CO)_4$ and by $HRh(CO)_2(PH_3)_2$ have been summarized in Figure 3. As one can see, in the reaction catalyzed by $HCo(CO)_4$, the first step of the catalysis is the rate-determining step of the whole reaction and thus responsible for the requirement of high temperature and pressure. Once the active species $HCo(CO)_3$ has been formed, a rather simple and smooth reaction profile is found, without thermodynamic traps or insurmountable barriers. In this case, the largest barrier corresponds to the CO insertion step, although if solvation effects were taken into account, probably the rate-determining step would be the final oxidative addition/reductive elimination step (vide infra).

Similar conclusions can be drawn from the free energy profile of the hydroformylation process catalyzed by $HRh(CO)_2(PH_3)_2$. Explicit inclusion of a C_2H_4 solvent molecule in the model of the catalyst changes the shape of the free energy profile dramatically (Figure 3b).[26,74] In solution, the H_2 oxidative addition step becomes one of the steps with a highest barrier in the catalytic cycle and could well be the rate-determining step, in agreement with experimental first-order dependency on hydrogen concentration[11f] and inverse kinetic effects.[94] The increase in the energy barrier, by about 60 kJ mol^{-1} at the MP2//HF level,[26] comes from the fact that, prior to H_2 addition, complex **17** has to be desolvated.

The hydroformylation process is one of the best-studied catalytic cycles. This notwithstanding, there are still unresolved questions that demand further work. Despite their importance,[26,74] an accurate quantum-mechanical description of solvation effects on hydroformylation catalysis has not yet been undertaken. It will also be interesting to analyze the possible implication of dinuclear species in the final steps of the reaction mechanism.[10c,99] Finally, further work is required to understand all steric and electronic factors that influence the regioselectivity of the hydroformylation process.[102] To our knowledge few works have discussed hydroformylation regioselectivities from a theoretical viewpoint.[36,84,103−105] Interestingly, since the olefin insertion is the crucial step that determines the regioselectivity of the process, the relative energies of the TSs corresponding to the olefin insertion have been successfully used to predict regioselectivities in a Rh-catalyzed hydroformylation process.[104]

B. Dötz Reaction

A decade after their discovery by E. O. Fischer,[106] carbonyl carbene complexes started to become valu-

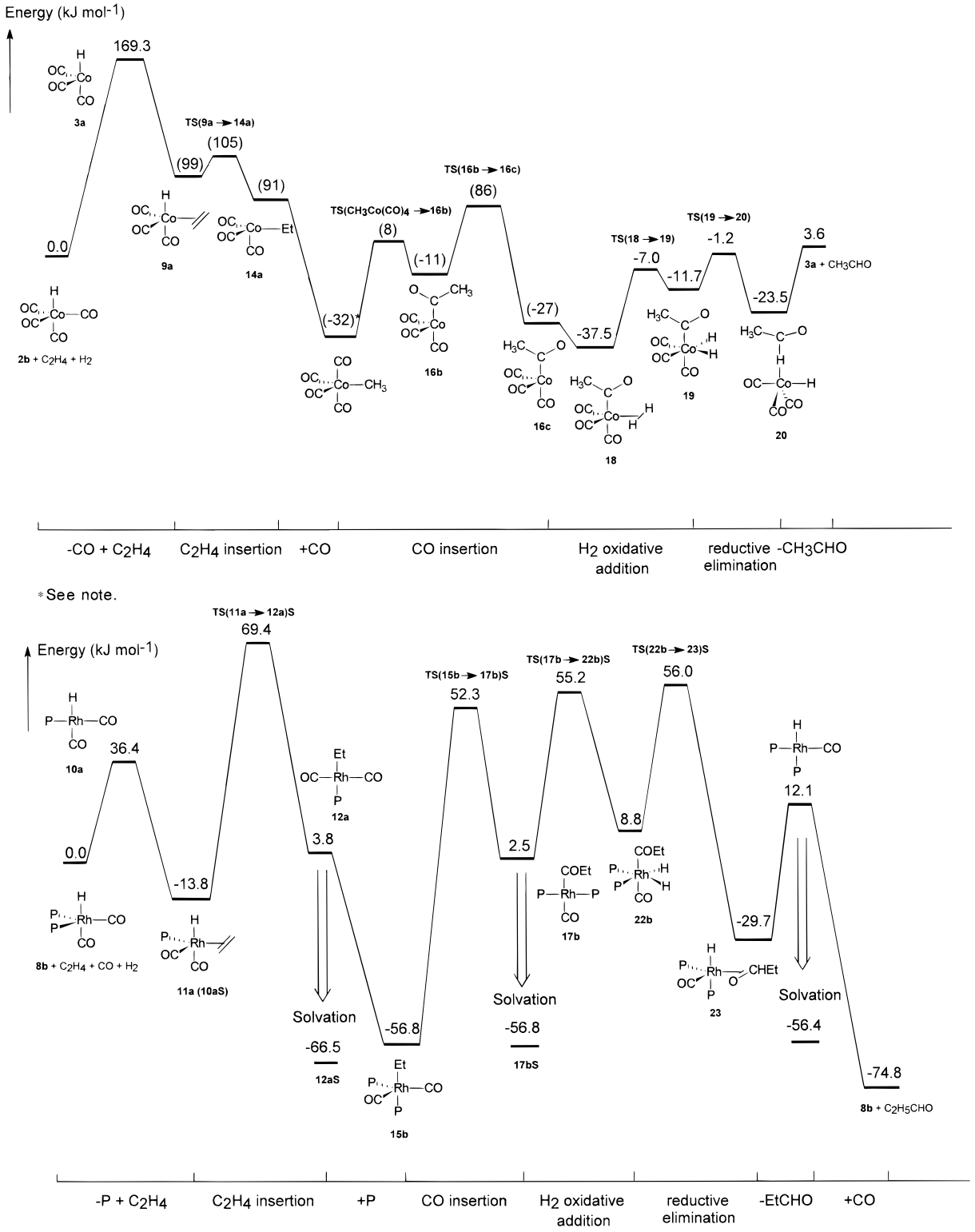

Figure 3. (a, top) BP86 (in parentheses HFS) energy profile (kJ mol^{-1}) for the entire catalytic cycle of the hydroformylation of ethylene catalyzed by $HCo(CO)_4$.[42−44,78,95,96] [Note: *The values for the CO dissociation from $CH_3Co(CO)_4$ or CH_3CH_2-$Co(CO)_4$ are not available. We have taken the CO dissociation from $HCo(CO)_4$ structure **1c** (123 kJ mol^{-1})[43] instead.] (b, bottom) MP2//HF free energy profile (kJ mol^{-1}) for the entire catalytic cycle of the hydroformylation of ethylene catalyzed by $HRh(CO)_2(PH_3)_2$, including solvation by an ethylene molecule (S). Reprinted with permission from ref 26. Copyright 1996 Academic Press.

able tools for stereoselective C−C bond formation in synthetic organic chemistry.[107] One of their most important synthetic applications is the so-called benzannulation or Dötz reaction,[108] i.e., the reaction of alkynes, **24**, with alkenyl- or aryl-substituted alkoxycarbene complexes of chromium, **25**, which results in the formation of densely functionalized phenols or naphthohydroquinones, **27**, respectively, by sequential coupling of the alkyne, the carbene, and one carbonyl ligand at a $Cr(CO)_3$ template, **26** (Scheme 10). This formal [3+2+1] cycloaddition proceeds with considerable regioselectivity in the case of alkyne

Scheme 10. Schematic Representation of the Benzannulation Reaction

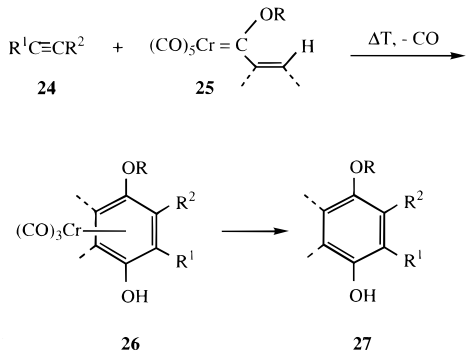

substituents R^1 and R^2 of distinctly different size.[109,110] Generally, the arene formation is the major reaction path; however, depending on both the substrates and the reaction conditions, other cycloaddition products have been observed as well.[111]

The synthetic potential of the benzannulation reaction has been demonstrated in the synthesis of various naturally occurring compounds,[112,113] and antibiotics.[114−117] Remarkable improvements have been reported experimentally regarding the optimization of the reaction yield, such as variations in the reaction temperature and solvent,[112d,118] and introduction of special techniques.[119−121] In contrast, mechanistic aspects of the Dötz reaction have just started to be explored by computational methods very recently.

Before the late 1980s, no theoretical studies on this reaction existed even though some mechanisms had already been proposed by experimental studies.[112d,122] The mechanistic complexity of the Dötz reaction partially explains why it was not until recent improvements in methodology and computer hardware[123] that the first theoretical works related to the Dötz reaction were reported.[124,125]

The mechanisms that have been proposed so far for the benzannulation reaction are depicted in Scheme 11. Reflecting the original mechanistic proposals of Dötz[108] (dissociative path and route A), it was suggested that metal-complexed derivatives **35** are obtained by the sequence (i) CO loss, (ii) alkyne coordination and rearrangement to complex **32**, (iii) migration of CO to yield coordinated ketene **33**, and (iv) collapse to the precursor of the phenolic substrate, **34**. A different alternative has been suggested by Casey[126] for the central part of the reaction (route B), where metalation of the arene ring would occur from complex **32** to form chromacyclohexadienone **36**; this species would then yield chromacycloheptadienone **37** upon carbonylation; reductive elimination from **37** would give intermediate **34**, and from that, **35**.

Validation of these two mechanistic suggestions has proven difficult since the rate-limiting step[127] usually involves ligand loss to open a coordination site for the alkyne to bind. Once bound, fast ring closure occurs to give the observed products.[128] No single reaction has been followed completely through the individual steps of routes A and B illustrated in Scheme 11. There are now several examples of the

Scheme 11. Mechanistic Pathways Postulated for the Benzannulation Reaction

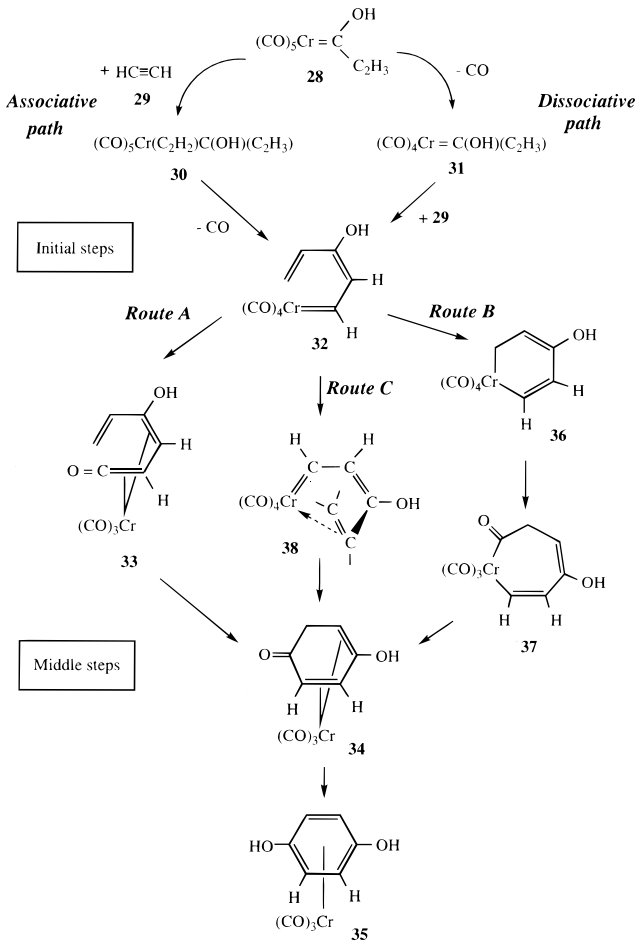

addition of alkynes to carbenes to form vinylcarbenes[129] (**32**), and the carbonylation of vinylcarbenes to yield vinylketenes[130] (**33**); however, the conversion of a well-characterized vinylcarbene (**32**) or vinylketene (**33**) chromium complex into a phenol product (**35**) has never been achieved.[131]

Experimental attempts to determine whether the reaction proceeds through one path or the other have been made by Garret et al.,[132] and also by Wulff and co-workers.[133] The approach followed by the former authors was to generate a coordinatively unsaturated carbene complex at a temperature sufficiently low to retard subsequent reactions so that they could be studied step by step.[132] Unfortunately, no mechanistic distinction was obtained. In the work of Wulff and co-workers,[133] the criterion taken for the mechanistic discussion was consistency with the observed product distribution, together with other experimental data. It was found that the vinylketene route seemed to explain more satisfactorily all of the data; however, at that time the authors concluded that there was not enough evidence to definitively rule out any of the studied mechanisms.[133]

With the appearance of the first computational studies,[124,125] some of the hypotheses that had been assumed from early experimental data were shown to be incorrect, and had to be reformulated. Thus, the EHT-MO calculation performed by Hofmann et al.[124,125] indicated that planar chromacyclobutenes

(usually thought to be initial products of the alkyne carbene coupling step at chromium[122a,127,134]) were indeed unrealistic intermediates. Moreover, as a result of very recent theoretical investigations,[135−138] alternative pathways have been formulated, namely, an associative path for the initial part of the reaction, and a third mechanism for the central part of the reaction which involves the formation of a chromahexatriene intermediate, **38**, bridging complexes **32** and **34** (route C in Scheme 11).

1. Initial Steps of the Reaction

Two different mechanistic proposals have been investigated theoretically for the initial steps of this reaction (Scheme 11): a dissociative mechanism,[136,139] and an associative mechanism.[136] Early studies have shown that reactions of chromium carbene complexes with alkynes are suppressed in the presence of external CO.[140] This makes it most probable that a carbon monoxide ligand will dissociate at the first step (dissociative route), which has later been verified by kinetic data.[127] An alternative mechanistic scenario is the insertion of an alkyne ligand into the metal coordination sphere of the metal carbene complex prior to CO elimination (associative route). Such a mechanism is not unknown in the field of TM chemistry, e.g., in carbonylmetal complexes with a 17-valence electron shell such as $V(CO)_6$.

The dissociative route has been explored in two independent density functional studies[136,139] using ethyne as the alkyne model. The investigation by Gleichmann, Dötz, and Hess (GDH)[139] shows that the dissociation reaction

$$(OC)_5Cr{=}C(X)(CH{=}CH_2) \rightarrow (OC)_4Cr{=}C(X)(CH{=}CH_2) + CO \quad (11)$$

with X = OH, NH_2 is highly endothermic (125−202 kJ mol^{-1} for X = OH; 115−217 kJ mol^{-1} for X = NH_2), and proceeds without barrier. Similar conclusions were reported by Torrent, Duran, and Solà (TDS)[136] using the same functional and a slightly better basis set (144.7−188.6 kJ mol^{-1} for X = OH). Both studies also found that, as expected, *trans*-CO dissociation requires more energy than dissociation of any of the four *cis*-CO ligands.[136,139] An interesting point, though, is that depending on the particular *cis*-CO ligand removed the resulting species, **31**, can be either suitable to interact with an alkyne molecule or unable to undergo the cyclization reaction. TDS found[136] that the most stable and suitable dissociation product was neither of the two species earlier proposed by GDH[139] (a tetracarbonyl carbene complex, **31a**, and an η^3-allylidene complex, **31b**) but a third one having an agostic interaction between the metal and the H atom on the C_α to the $C_{carbene}$, **31c** (Scheme 12).

Although both theoretical studies[136,139] simulate gas-phase reactions, the benzannulation is generally run in donating solvents (such as THF). There is a possibility, then, that the ligand position of a dissociated *cis*-CO in a pentacoordinate carbene complex **31** is occupied by a solvent molecule. GDH[139] investigated the ligand exchange process for methoxy- and methylaminocarbene complexes by employing a water molecule as a model for the solvent species. A significant heteroatom effect was observed: according to their calculations,[139] a purely σ-electron-donating solvent such as THF will stabilize the vacant coordination site of a tetracarbonyl methoxycarbene much more efficiently than the more electron-rich coordination site of a chromium tetracarbonyl methylaminocarbene complex.

Scheme 12. Different Conformations for the CO-Dissociation Product

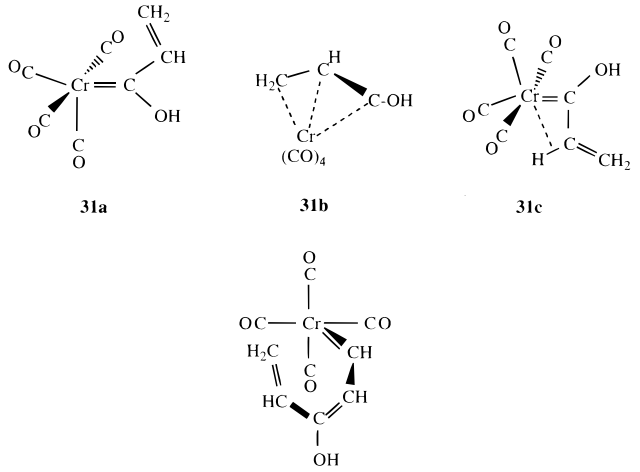

31a **31b** **31c**

32

The next step of the dissociative route is coordination of ethyne to the dissociation product **31**, $(CO)_4Cr{=}C(OH)(CHCH_2)$, followed by ethyne−carbene insertion. GDH found that the approach of ethyne to **31** leads to the formation of two different minima,[139] but only one of them (an η^2-ethyne−carbene complex) is relevant for the subsequent ethyne−carbene insertion step. Such an η^2-ethyne−carbene complex is endothermic by 13 kJ mol^{-1} compared to the water-stabilized tetracarbonyl carbene complex. In the case of an aminophenylcarbene complex, the exchange of a water molecule by an ethyne molecule is even marginally exothermic.[139]

As far as the energetics of the ethyne−carbene insertion are concerned, the nature of the heteroatom is reported to play a significant role.[139] For aminocarbenes, the insertion requires an additional 16 kJ mol^{-1} of activation energy compared to hydroxycarbene complexes. It was also observed that starting from an intramolecularly stabilized tetracarbonyl complex (i.e., a complex where the originally vacant ligand position site is saturated with another fragment/ligand of the same molecule and, therefore, becomes more stable than the coordinatively unsaturated tetracarbonyl carbene complex), the ethyne−carbene insertion requires only a small amount of activation energy.[139] This is in agreement with experimental findings for a morpholino adduct reported by Barluenga.[141] The effect of solvent-stabilized intermediates can be assessed by comparing the calculated energies of the ethyne−carbene insertion in both theoretical studies, starting from $(OC)_4(H_2O)_n$-Cr=C(X)R, −175.7 kJ mol^{-1} (with n = 0, X = OH, and R = vinyl),[136] versus calculated energies ranging from −65 to −116 kJ mol^{-1} (with n = 1, X = OH, NH_2, and R = vinyl, phenyl).[139]

The alternative mechanistic scenario for the initial steps of this reaction (associative route) has been the subject of a recent study by TDS.[136] It considers the possibility that the cycloaddition with alkynes takes place initially by direct reaction of coordinatively saturated chromium carbene complexes. Their calculations reveal that if alkyne addition occurs *before* CO loss, then (i) the initial step becomes clearly exothermic (−163.4 kJ mol^{-1}), and (ii) CO dissociation also becomes easier, occurring at the second step (i.e., taking place at the new pentacarbonyl carbene complex, **30**, instead of the starting carbene, **28**). Such conclusions have been initially regarded with reluctance by some experimentalists.[142] Despite its potential interest, the new alternative does not fit the large body of experimental observations available so far. As pointed out by Fischer and Hofmann,[142] kinetic studies are not consistent with the associative mechanism and are clearly in favor of a dissociative path. However, in a very recent kinetic study, Waters, Bos, and Wulff (WBW)[143] have provided the first example of a bimolecular reaction of a heteroatom-stabilized carbene complex with an alkyne in the absence of CO pressure, supporting TDS's theoretical results.[136] The unprecedented bimolecular mechanism observed by WBW for the reaction of *o*-methoxyphenyl chromium carbene complex with 1-phenyl-1-propyne impelled these authors to investigate whether this was a general phenomenon. Although the kinetics of chromium carbene complexes with substituted acetylenes had been early investigated by Fischer and Dötz,[127] all of their studies were done at 5×10^{-3} M carbene complex, whereas the most typical concentration for running a benzannulation reaction are at 0.1−0.5 M carbene complex, significantly more concentrated than for Fischer's kinetic studies. WBW have found[143] that, under typical reaction conditions, the reaction rates do not depend on alkyne concentration and are first-order in carbene complex only. According to the latest findings, it is not surprising that no bimolecular reaction was observed in the first studies by Fischer and Dötz.[127] As new data become available, also new theoretical studies are necessary. In particular, from a computational point of view, further research should include solvent effects. The present gas-phase calculations clearly fail to account for any stabilizing factor from the solvent.

2. Central Part of the Reaction

Three theoretical papers have been devoted so far to the elucidation of this part of the reaction: the already mentioned study of GDH,[139]and two papers by TDS.[137,138] The former study[139] deals only with the proposal labeled route A in Scheme 11. One of the papers by TDS[137] focuses exclusively on route C in Scheme 11. A thorough analysis and comparison of the three routes can be found in ref 138. In the following paragraphs, the main findings of these three papers are reviewed.

2.1. Route A. Although the starting point for the central part of the reaction is formally the end product of the ethyne insertion (**32**), different studies have proposed slightly different initial structures.[138,139] Also, the inclusion/omission of some of the intermediates has led to distinct descriptions for the path of route A. Thus, GDH[139] reported that the ethyne−carbene insertion leads to the formation of an η^3-vinylallylidene intermediate (**32** in Scheme 12), and that the next step is the intramolecular coupling of the carbene carbon atom of **32** (a former ethyne carbon atom) with a CO ligand. By means of a linear transit, the CO ligand was found to move toward the vinylallylidene ligand until it acquired a favorable position for the subsequent CO insertion.[139] The corresponding activation barrier for this step is only 22 kJ mol^{-1}, and the authors concluded that, due to this small barrier, the isolation of the preceding η^3-vinylallylidene intermediate at the benzannulation would be difficult. Simultaneously with the CO insertion, a ring closure is reported to take place, forming an η^4-cyclohexadienone intermediate **34**. However, no η^4-vinylketene complex intermediate **33** was found in the pathway leading to the η^4-cyclohexadienone,[139] as would be expected.

According to TDS,[136,138] the end product of ethyne−carbene insertion, **32**, lies on a flat region of the PES, and undergoes a small structural rearrangement, turning into its isomer, **32a** (Figure 4), which is 28.0 kJ mol^{-1} more stable. The starting point of the central part of the reaction in that study[138] is assumed to be **32a**. To follow the vinylketene route suggested by Dötz (route A), **32a** has to convert into **33**. Such a conversion takes place in two steps. First, **32a** isomerizes into **32b** through TS**(32a→32b)** (Figure 4), and then turns into **33** via **TS(32b→33)** (Figure 5). No TS directly connecting **32a** and **33** was found.[138] Conversion from **32a** to **32b** involves rotation and folding of the organic chain, which can be expected to occur without many hindrances given the unrestricted mobility of the carbene ligand. The corresponding barrier is 66.9 kJ mol^{-1}. Once **32b** is formed from its precursor **32a**, a CO migration takes place in the step **32b** → **33** followed by a ring closure in the step **33** → **34**. The activation barrier for the conversion **32b** → **33** (28.9 kJ mol^{-1}) corresponds roughly to the energy required for a CO ligand to migrate into the Cr−C double bond.[138] In the next step, conversion from **33** to **34** is notably exothermic (101.7 kJ mol^{-1}) and kinetically very favorable, with a smooth activation barrier of only 1.2 kJ mol^{-1}. Such a remarkable exothermicity is in agreement with the study of GDH,[139] where the η^4-cyclohexadienone intermediate **34** is reported to be the most stable and strongly exothermic intermediate in the phenol formation reaction. However, as mentioned above, GDH[139] did not report any η^4-vinylketene intermediate **33** but a direct conversion from a vinylcarbene similar to **32** to complex **34** (−194.1 kJ mol^{-1}). For the global step, they computed an activation energy of 22.2 kJ mol^{-1}. On the contrary, starting from an η^3-*phenyl*allylidene (i.e, benzannulation of phenylcarbenes instead of vinylcarbenes), GDH did find a minimum corresponding to an η^4-vinylketene. The subsequent ring closure from this η^4-vinylketene to an η^4-cyclohexadienone intermediate was found to involve a small activation barrier (24 kJ mol^{-1}).[139]

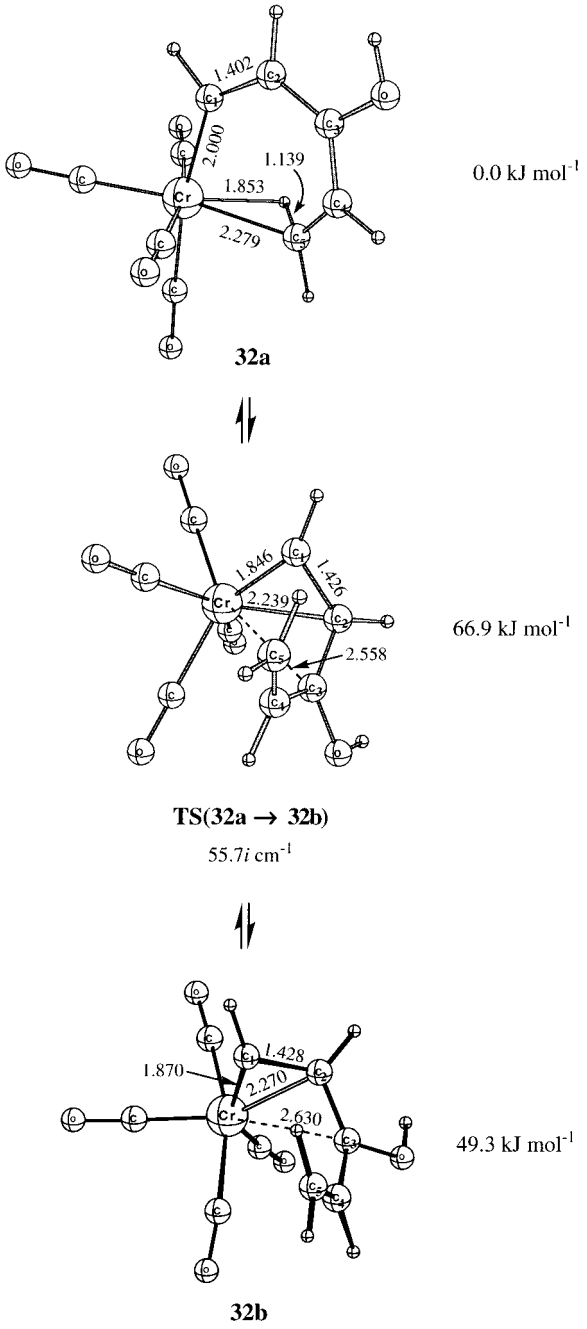

Figure 4. Optimized geometries of η^1-vinylcarbene complex **32a** (top), η^3-vinylketene complex **32b** (bottom), and the TS connecting them (middle). Selected bond distance are given in angstroms. Reprinted from ref 138. Copyright 1999 American Chemical Society.

The last step of the reaction is the keto−enol tautomerization from η^4-cyclohexadienone intermediates (**34**) to aromatic products (**35**). Both theoretical studies coincide in the fact that such a step is accompanied by a considerable gain in energy: about 80 kJ mol^{-1} for vinylcarbenes[138,139] (where a phenol system is formed by the tautomerization step), and about 175 kJ mol^{-1} for phenylcarbenes[139] (where a naphthol system is produced).

2.2 Route B. According to Scheme 11, the main intermediates postulated for the conversion of **32** to **34** through route B are chromacyclohexadiene **36** and chromacycloheptadienone **37**. TDS[138] found no minimum structure having the geometrical traits shown

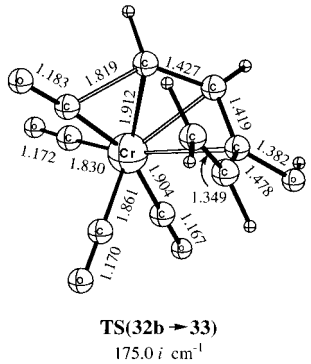

Figure 5. Optimized geometry for the TS connecting intermediates **32b** and **33**. Bond distances are given in angstroms. Reprinted from ref 138. Copyright 1999 American Chemical Society.

by the six-membered species labeled **36**, i.e., a species with two short Cr−C distances. Different input geometries led systematically directly to complex **32a**. Opening of the chain and stabilization through agostic interaction (as in **32a**) were invariably the preferred trends observed along any optimization process. The authors concluded that **36** does not exist as a real stationary point, and that chromacycloheptadienone **37** does directly derive from complex **32a**. This is consistent with a recent isotopic study by Hughes et al.[144] where metallacyclohexadiene complexes similar to **36** were suggested to be excluded as intermediates along the reaction pathway of the Dötz and related reactions.

Conversion of **32a** into **37** was found to be a notably endothermic process (104.6 kJ mol^{-1}). In the next step, reduction of the strain in the seven-membered ring by turning it into a six-membered one (step **37** → **34**) results in a substantial release of energy (−233.0 kJ mol^{-1}). No TSs have been reported for route B;[138] thermodynamic data are conclusive enough to see that route A is more favorable than route B. The reaction energy required for the formation of intermediate **37** is larger than any of the activation energies involved in route A.[138] Calculations reported by TSD indicate that the route initially suggested by Casey for the benzannulation reaction has few (or null) chances to compete against route A in Scheme 11, which would be energetically preferred *both* kinetically and thermodynamically.

2.3. Route C. A novel mechanistic proposal for the central part of the Dötz reaction (route C) has recently been published by TDS.[137] As seen from Scheme 11, the new proposed mechanism invokes formation of a chromahexatriene intermediate **38** through rearrangement of the branch point species **32**, followed by insertion of a CO ligand to yield **34** in the subsequent step.

The structural arrangements involved in this sequence are summarized in Figure 6. Starting with **32a** (which is the preferred isomer arising from **32**), the ring chain evolves to a more stable conformation characterized by a dπ interaction between chromium and the C_4-C_5 olefinic bond. A crucial feature of complex **38** as compared to complex **32a** is the shortening of the distance between C_5 and the CO ligand to be transferred to the $Cr-C_5$ bond (C_5-CO

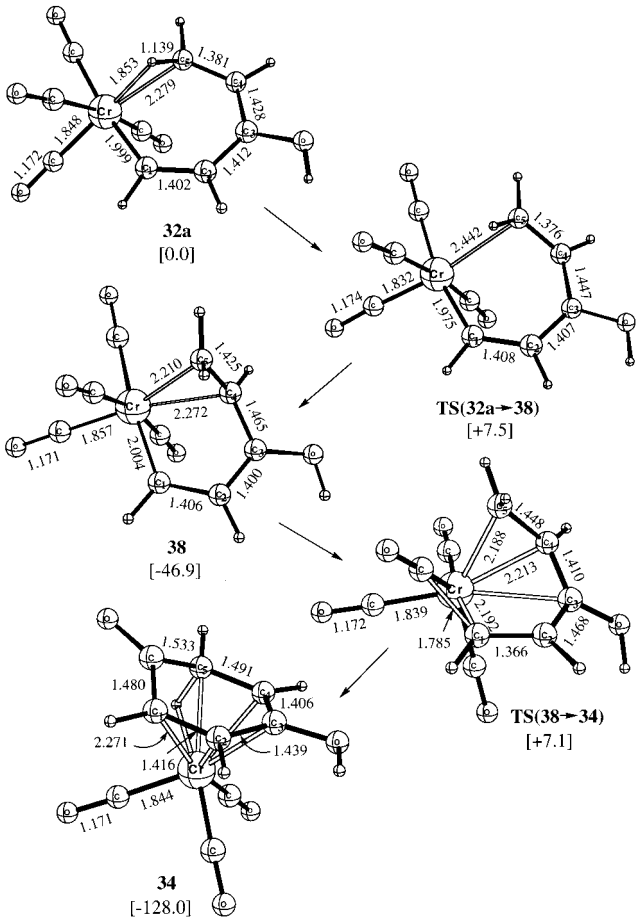

Figure 6. Optimized geometrical parameters for the intermediates and TSs involved in route C. Bond distances are given in angstroms, and relative energies in brackets are given in kilojoules per mole. Reprinted with permission from ref 137. Copyright 1998 The Royal Society of Chemistry.

= 3.517 Å in **32a**, and 2.559 Å in **38**), which facilitates CO insertion in the subsequent step ($C_5-CO = 2.262$ Å in **TS(38→34)**, and 1.533 Å in **34**). Support for the existence of **38** comes from a recent investigation by Barluenga et al.,[141] where a chromahexatriene similar to **38** was isolated and characterized by ^1H and ^{13}C NMR spectroscopy. Experimental data from that study demonstrate that the alkenyl ligand is attached to the metal center through the C_4-C_5 double bond.

Interestingly, chromahexatriene **38** is not an end point of the reaction because it connects to a more stable intermediate, as shown in Figure 6. The fact that the reaction does not terminate at **38** is consistent again with the experimental results reported by Barluenga et al.[141] These authors found that the synthesized chromahexatriene was not stable in solution at room temperature, and decomposed to yield the most common final product in the Dötz reaction with aminocarbenes.[141]

3. Final Remarks

Theoretical calculations indicate that, regardless of the detailed mechanism, the benzannulation reaction is strongly exothermic for hydroxy- and amino-substituted phenyl- and vinylcarbene complexes.[139] It is also found that the global reaction is significantly more exothermic for vinylcarbenes than for phenylcarbenes, since in the former case a new aromatic phenol system is created, whereas in the latter case only an existing phenol system is augmented to an aromatic naphthol system.[139] The exchange of a *cis*-CO with a σ-electron-donating solvent molecule is reported to be significantly less endothermic for metal hydroxycarbene than for aminocarbene.[139] This explains the experimental observation that aminocarbenes react at higher temperatures than their hydroxy analogues.

Beyond thermochemical aspects, the theoretical studies reviewed here have been especially important to determine the kinetics of the benzannulation reaction. The energy profiles[138] for the three postulated mechanisms (Scheme 11) are shown in Figure 7. As seen from the graph, the lowest energy path corresponds to the sequence **28** + **29** → **30** → **32** → **32a** → **38** → **34** → **35**. The rate-determining step (dissociation of a *cis*-CO ligand) occurs at the initial steps of the reaction. Once **32** and **32a** are formed, the ideal mechanistic path for the central part of the reaction is the one that minimizes the amount of energy required to insert a CO ligand into the ring (route C), because CO migration is one of the most costly processes to complete the benzannulation.[138] Interestingly, the particular orientation of the carbene ligand in **38** makes the migration of CO very accessible: During the process each of the two π^* orbitals of CO can interact simultaneously with the $C_4=C_5$ and Cr=C π orbitals. Therefore, CO migration in **38** is favored over CO migration in **32**, and consequently, the energy profile for route C has the advantage of being globally smoother (Figure 7).

From a mechanistic point of view, all data reported so far indicate that the novel route[137] stands out as a potentially suitable alternative to redefine the classical mechanism. However, a word of caution applies here. Given the similarity in energies for the investigated routes, the use of different substrates may alter the relative order of the barriers and, therefore, modify the mechanistic behavior of the reactants, making the reaction proceed through other pathways. New studies will contribute to widen the range of concurrent, competing alternatives, for this intriguing benzannulation reaction whose experimental simplicity (a one-pot reaction) contrasts with its mechanistic complexity.

C. Water–Gas Shift Reaction

Many catalytic reactions described in this review depend on CO and H_2 as feedstock chemicals; hydroformylation and hydrogenation of CO are typical examples. In many cases, CO undergoes side reactions, among which the water−gas shift reaction (WGSR), eq 12, is well studied in terms of the

$$CO(g) + H_2O(g) \rightarrow H_2(g) + CO_2(g) \qquad (12)$$

mechanism. The importance of the WGSR derives from its role both as a means for enriching the H_2 content of water gas (synthesis gas), and as a side reaction of significance in hydroformylation and Fischer−Tropsch processes.[145,146] Moreover, in the

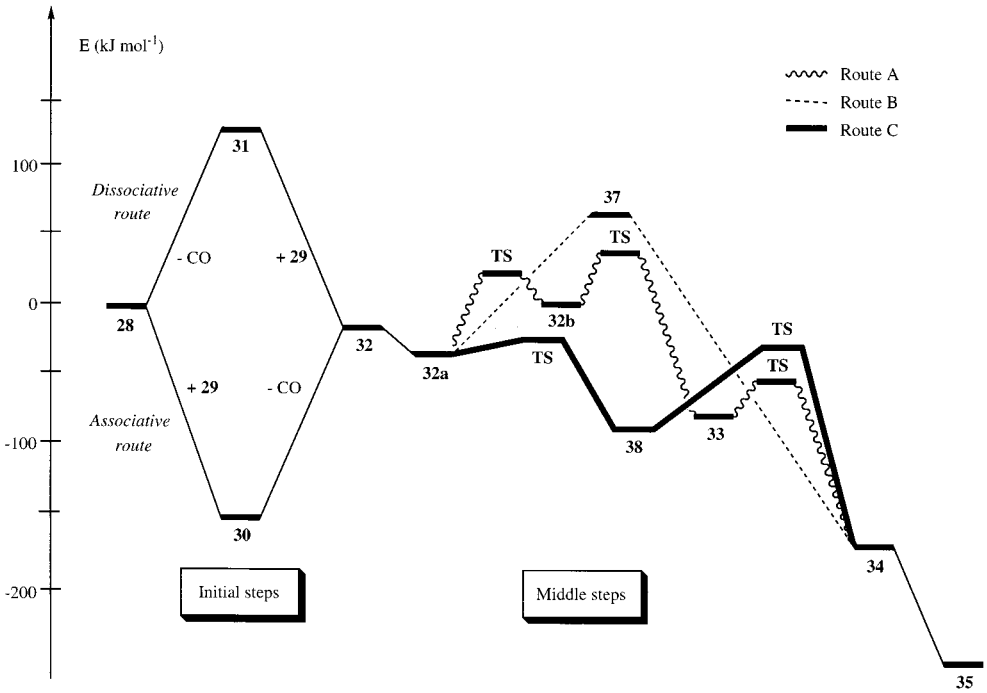

Figure 7. Energy profile for the whole benzannulation reaction: comparison of the profiles for the three reviewed mechanisms (route A, wavy line; route B, dotted line; route C, bold line). Relative energies are in kilojoules per mole. Reprinted from ref 138. Copyright 1999 American Chemical Society.

presence of water, CO can be used to hydrogenate substrates such as olefins, nitroaromatics, and other unsaturated organic compounds. However, in certain industrial processes (e.g., the hydrocarboxylation of ethylene), this is an unwanted side reaction.[147]

Homogeneous catalysis of the WGSR by TM carbonyls has received considerable attention since the first examples were reported 50 years ago.[148−155] The $Fe(CO)_5$-catalyzed WGSR was initially proposed[155] to proceed via a cycle displayed in Scheme 13. Due to

Scheme 13. Initially Proposed Mechanism for the WGSR Catalysis Using Iron Pentacarbonyl

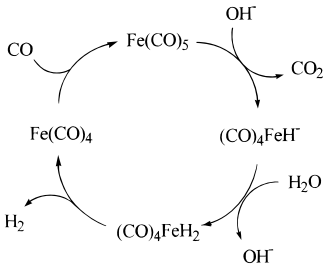

further investigations,[156,157] an improved approach to the catalytic cycle can be formulated as follows:

$$Fe(CO)_5 + OH^- \rightarrow (CO)_4FeCOOH^- \quad (13)$$

$$(CO)_4FeCOOH^- \rightarrow (CO)_4FeH^- + CO_2 \quad (14)$$

$$(CO)_4FeH^- + H_2O \rightarrow (CO)_4FeH_2 + OH^- \quad (15)$$

$$(CO)_4FeH_2 \rightarrow Fe(CO)_4 + H_2 \quad (16)$$

$$Fe(CO)_4 + CO \rightarrow Fe(CO)_5 \quad (17)$$

Support has been provided for most of steps 13−17 taken as individual reactions;[158−163] however, the majority of these reactions have been reported to proceed either in solution or under conditions which are different from the ones in the catalytic cycle. Moreover, only indirect evidence exists that the postulated reactions should occur in the sequence 13−17 given above since these steps have only been studied individually. For instance, from a computational point of view, step 13 has been the subject of two works by Dedieu and Nakamura (DN),[164,165] where a computed SCF reaction energy of −298.3 kJ mol^{-1} was reported. DN also explained the high exothermicity encountered in this nucleophilic addition in terms of MOs. The reverse of step 17, i.e., CO dissociation from $Fe(CO)_5$, has been even more extensively studied,[166] especially as a benchmark for first-bond dissociation energies in TM carbonyl chemistry. However, none of those studies go beyond a single step in the reaction. A complete picture of the whole catalytic cycle including both kinetical and thermodynamical data seems to be necessary to determine the validity of the suggested mechanism for the WGSR catalysis. Very recently, experimental data from a gas-phase ion study combined with other thermochemistry have been reported by Sunderlin and Squires[167] to derive a model-reaction energy profile for this chemical process. Although their investigation is very interesting for comparison to solution-phase results, experimental difficulties with the identification and characterization of the transient intermediate species believed to be involved are self-evident.

As of this writing, only one computational study on the whole mechanism of the $Fe(CO)_5$-catalyzed WGSR has been reported.[168] By means of quantum chemical calculations using gradient-corrected density functional theory (B3LYP) and ab initio methods at the CCSD(T) level, Torrent, Solà, and Frenking[168]

Table 5. Calculated and Experimental Reaction Energies ΔE (kJ mol^{-1}) for the Postulated Steps 13−17 and Other Related Reactions Involved in the WGSR Catalytic Cycle[a−c]

reaction	ΔE(B3LYP/II++)			ΔE(CCSD(T)/II++)			exptl
$CO + H_2O \rightarrow CO_2 + H_2$	−47.3	(−59.4)	*−72.1*	−15.5	(−27.6)	*−40.2*	−41.0[d]
$Fe(CO)_5$ (**39**) + OH^- → $(CO)_4FeCOOH^-$ (**40a**)	−295.0	(−275.3)	*−258.6*	−297.5	(−277.8)	*−261.1*	−254.4 ± 135.6[e]
$(CO)_4FeCOOH^-$ (**40a**) → $(CO)_4FeOCOH^-$ (**40b**)	−14.2	(−18.4)	*−20.9*				
$(CO)_4FeCOOH^-$ (**40a**) → $(CO)_4FeH^-$ (**41**) + CO_2	−16.3	(−30.5)	*−46.9*	26.8	(12.6)	*−3.8*	−17 ± 29[e]
$(CO)_4FeH^-$ (**41**) + H_2O → $(CO)_4FeH^-{\cdot}H_2O$ (**42**)	−29.3	(−22.6)	*−13.8*				
$(CO)_4FeH^-{\cdot}H_2O$ (**42**) → $(CO)_4FeH_2$ (**43**) + OH^-	345.6	(328.4)	*307.9*				
$(CO)_4FeH^-$ (**41**) + H_2O → $(CO)_4FeH_2$ (**43**) + OH^-	316.3	(305.8)	*294.1*	300.8	(290.4)	*278.6*	299.2[e]
$(CO)_4FeH_2$ (**43**) → $(CO)_4FeH_2$ (**44**)	33.0	(32.2)	*32.6*	50.2	(49.4)	*49.8*	
$(CO)_4FeH_2$ (**44**) → $Fe(CO)_4$ (**45**) + H_2	73.3	(55.2)	*42.3*	102.1	(84.1)	*71.1*	
$(CO)_4FeH_2$ (**43**) → $Fe(CO)_4$ (**45**) + H_2	106.3	(87.4)	*74.9*	152.3	(133.5)	*120.9*	109 ± 8[f]
$Fe(CO)_4$ (**45**) + CO → $Fe(CO)_5$ (**39**)	−158.6	(−146.8)	*−135.6*	−197.9	(−186.2)	*−175.3*	−173.6[g]

[a] Numbering of the species as in Scheme 14. [b] Numbers in parentheses include the ZPE correction computed at B3LYP/II. Basis set II uses a small-core ECP with a (441/2111/41) split-valence basis set for Fe and 6-31G(d,p) all-electron basis sets for C, O, and H. Basis set II++ is the same as II plus the addition of an s diffuse function on H and a set of three sp diffuse functions on C and O atoms. [c] Numbers in italics include ZPE + thermal corrections computed at B3LYP/II. [d] Reference 195. [e] Reference 167. [f] Reference 178. [g] Reference 196.

(TSF) have recently scrutinized step by step the classically assumed reaction path of this catalytic process, and have enlarged it with novel mechanistic proposals.

Table 5 summarizes the reported thermochemical data regarding steps 13−17 and other related reactions relevant for a complete description of the catalytic cycle.[168] The numbering of the complexes is given in Scheme 14. The most relevant features

Scheme 14. New Proposed Scheme for the Mechanism of the $Fe(CO)_5$-catalyzed WGSR Derived from the Study of TSF[a]

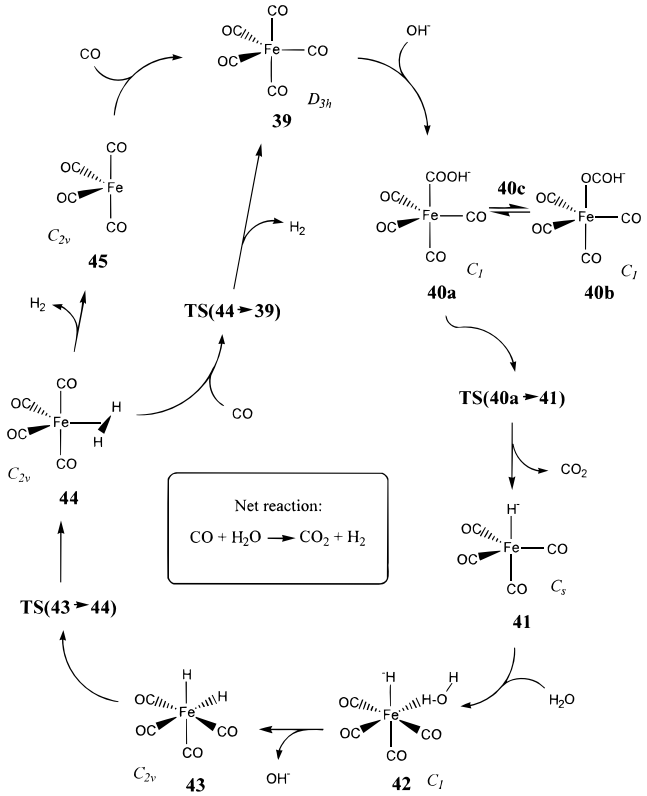

[a] Reprinted from ref 168. Copyright 1999 American Chemical Society.

reported by TSF[168] are (i) investigation of a metalloformate complex, **40b**, besides the metallocarboxylic acid **40a**, (ii) elucidation of the decarboxylation process **40a** → **41** + CO_2 followed by acidification of hydride **41** with H_2O to yield species **43**, (iii) analysis of the dichotomy between dihydride **43** and an unprecedented dihydrogen complex **44**, and (iv) exploration of an alternative path, **44** → **39**, to the classical route involving **45**.

1. Metalloformate Complexes versus Metallocarboxylic Acids

The homogeneous WGSR catalysis by group 6 metals has been recently found to involve formate complexes[169−174] analogous to surface-bound formates observed in heterogeneous WGSR.[173] Although metal formates have not been generally regarded as key intermediates in catalytic reactions of carbon oxides, their intermediacy has been observed in a number of catalysis-related reactions,[146a,175] as well as on magnesia, alumina, and iron−chromia catalysts for the heterogeneous WGSR.[173] Prompted by these results, TSF[168] explored the possibility that (besides acid **40a**) a formate intermediate could also take part in the $Fe(CO)_5$-catalyzed WGSR. The point is that, since its reported formation and chemical characterization in the gas phase,[157] $(CO)_4FeCOOH^-$ has been proposed as the only reactive intermediate in the initial step of this reaction. TSF showed that the optimized molecular structure of the formate complex $(CO)_4FeO_2CH^-$, **40b**, corresponds to a real minimum on the PES, and that it is even *more* stable than its isomer, the metallocarboxylic acid.[168] However, since the formate anion **40b** has not been observed, TSF suggested[168] that the exchange between the two isomers must have a high energy barrier so that the carboxylic species derived from the nucleophilic addition, **40a**, cannot undergo isomerization into the more stable form, **40b**. Their hypothesis has been confirmed by finding that the lowest energy path connecting **40a** and **40b** involves a highly energetic intermediate, **40c**, which actually prevents the interconversion of the two isomers under reaction conditions (Scheme 15).[168]

These calculations[168] are in good agreement with experimental evidence recently discussed in the literature[167] concerning the identification of the species produced from the OH^- attack on **39**, and are

Scheme 15. Schematic Structures of Some Intermediate Species and TS(40a→41)

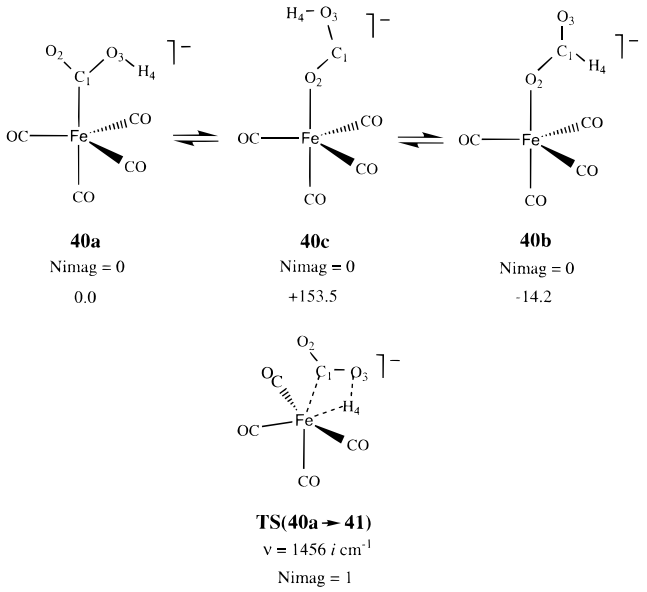

also in line with the experimental work of Darensbourg and Rokicki,[176] who found that for the chromium triad the intermediate afforded from OH^- addition to $M(CO)_6$, $M(CO)_5COOH^-$, and its structural isomer, $M(CO)_5O_2CH^-$, do not interconvert intramolecularly.[176]

2. Elucidation of the Decarboxylation Process

The experimentally reported reaction enthalpy[167] for the decarboxylation process **40a** → **41** + CO_2 (−17 ± 29 kJ mol^{-1}) suggests that the reaction is close to thermoneutral, the error range of the experimental value being rather high. The enthalpies calculated by TSF[168] (Table 5) indicate an exothermic reaction. Concerning the mechanism for the decarboxylation of $(CO)_4FeCOOH^-$, at least three different proposals have been made in the literature: (i) a path involving addition of OH^- to the hydroxycarbonyl group[177] to give a $C(OH)_2O$ function that subsequently decomposes via loss of HCO_3^-, (ii) a deprotonation mechanism[178] similar to the ones that had been earlier proposed for the decarboxylation of other hydroxycarbonyls,[179] and (iii) a mechanism which involves β-elimination of M−H from the M−CO_2H functionality.[180,181] The latter proposal is the most accepted, especially after the work by Pettit and co-workers,[156] where a concerted elimination of CO_2 was suggested for the reaction rather than loss of CO_2 via a metallocarboxylic anion.[156] Both mechanisms have been proposed for other systems in which decarboxylation of metallocarboxylic acids is inferred.[182] However, before the investigation of TSF[168] no theoretical studies had been reported to support such a concerted mechanism.

TSF reported[168] the optimized geometry for the TS that connects **40a** and **41**. Inspection of the four-centered **TS(40a→41)** shows that elimination of CO_2 and formation of the metal hydride occur simultaneously.[168] In a previous study,[183] it had been shown that the HCOOH decarboxylation reaction, which has a rather high energy barrier in the gas phase, is facilitated by the mediation of water.[183] The structure of the TS is therefore changed from a four-membered ring to a less energy-demanding six-membered ring. These facts suggested that the decarboxylation of **40a** could also be regarded as being water-mediated instead of proceeding as formulated above,[168] owing to the isolobal analogy[184] between $(CO)_4Fe^-$ and H. The assistance of a base bearing a hydrogen atom has already been invoked as a possible reaction pathway for the hydroxycarbonyl decarboxylation reaction in solution.[177,178,180] To test whether decarboxylation can be catalyzed by a neutral base in the gas phase as well, Lane and Squires[185] examined the reaction of $(CO)_4FeCOOH^-$ with NH_3. No measurable shift in the threshold for decarboxylation was observed with NH_3 as the target gas, indicating that NH_3 *does not lower* the barrier for loss of CO_2 in the gas phase.[185] Also, $(CO)_4FeCOOD^-$ was found not to exchange with NH_3 during decarboxylation to form $(CO)_4FeH^-$, as would be expected if base catalysis involved a concerted six-center reaction.[185,186] It follows that the reaction is most likely to occur through a four-membered TS, such as the one reported by TSF[168] involving rearrangement of the acetyl ligand via a concerted mechanism with a moderate activation barrier (104.2 kJ mol^{-1}).

3. Analysis of a Dichotomy: Dihydride or Dihydrogen Complexes?

The intermediacy of isomer **44** in the catalytic cycle has been also explored by TSF. The short H−H distance found in **44** (0.894 Å)[168] indicates that such a species is not dihydride **43** but actually the isomer containing H_2. Typical hydrogen atom separation for dihydrogen complexes is ca. 0.8 Å,[187] very close to the free H_2 value of 0.74 Å.[187,188] According to eq 16, $(CO)_4FeH_2$ decomposes into H_2 and $Fe(CO)_4$. Prior to the work of TSF[168] the species believed to undergo H_2 decomposition in the catalyzed reaction had always been assumed to be isomer **43**. Table 5 reveals that isomers **43** and **44** are very close in energy, the former being more stable by about 35−45 kJ mol^{-1}. Such a difference is low enough to be surmounted under reaction conditions, and therefore, an equilibrium between the two isomers should be expected to take place provided kinetics do not prevent it. Since the isomerization reaction **43** → **44** is also found[168] to proceed via smooth rearrangement (the activation barrier is computed[168] to be about 40 kJ mol^{-1}), the interconversion between the two isomers is concluded to be feasible both thermodynamically and kinetically, and the two species to coexist in the catalytic cycle.[168]

The molecular configuration of η^2-dihydrogen iron tetracarbonyl **44** has been reported for the first time in the work by TSF.[168] No previous structural data existed in the literature for such a complex prior to that study,[168] although there is now indirect evidence for its existence.[189] The theoretical findings by TSF[168] confirm a very recent study on the PES of the H−Fe−H symmetric bend in the dihydride $(CO)_4FeH_2$, where it has been shown[189] that, at an angle of 27°, the two H atoms approach to approximately the distance of a molecular hydrogen bond. Moreover, at

that angle, there is a local minimum in energy which lies 35.9 kJ mol^{-1} above the dihydride, which is the most stable isomer.[189] Although no structure has been reported for such a local minimum, the authors of the experimental study[189] point out that it would correspond to a "dihydrogen" complex,[189] which is in excellent agreement with the theoretical results of TSF[168] for species **44**. The global minimum (called "classical dihydride") in the experimental study corresponds to species **43** in the theoretical work.[168]

4. Exploration of an Alternative Path to the Classical Route

Contradictory arguments exist both *for* and *against* reactions 16 and 17 being the last steps in the catalytic cycle as classically assumed to operate.[63,178,190−192] Preliminary rate studies with an alkaline solution, ruthenium-based catalyst, indicated a first-order rate dependence on P_{CO}.[193] Since CO addition to an unsaturated complex seems an unlikely rate-limiting step for this cycle, the classically assumed mechanism may not fit the reported evidence.[193] Experiments rather seem to suggest that an alternative pathway should exist where CO participates in a rate-limiting dihydrogen elimination pathway.

TSF have explored an alternative path that could take into account the role of CO during H_2 elimination.[168] Such a path can be conceived to proceed by means of an S_N2-type mechanism which involves (1) approach of CO to $(CO)_4FeH_2$ from the side opposite H_2, and (2) simultaneous ejection of H_2. A linear transit has been performed by TSF to model this TM-containing S_N2-type mechanism, but all attempts to locate a TS by fully optimizing the found upper-bound structure failed.[168] The system systematically decomposes into $Fe(CO)_4 + CO + H_2$.[168] Since the estimated upper bound derived from the linear transit was still larger than the computed enthalpy for the rate-limiting step of the classical path, it was concluded[168] that the novel proposal has no chance to compete with the classical route, and that the reaction has to proceed through the less-energy-demanding path despite not being fully consistent with the experimental facts.[193] In a recent study on the model reaction system $Pd + CH_3Cl$, the question of whether nucleophilic substitution could be competitive in the formation of the oxidative insertion product, CH_3-PdCl, has been addressed.[194] Likewise, it was found that the high endothermicity of the S_N2 process prevents that route from being a competitive alternative to oxidative insertion.[194]

5. Final Remarks

Figure 8 shows the thermochemical profile for the model reaction as reported by TSF.[168] Even after the very endothermic step **42** → **43**, the overall reaction is energetically still *below* the reactants. The exothermicity of the net reaction is 72.1 kJ mol^{-1} (Table 5). Since formation of **42** from the reactants is *very* exothermic (319.3 kJ mol^{-1}), the following step can still take place despite being notably endothermic (307.9 kJ mol^{-1}). As pointed out by the authors,[168] the activation barrier for the overall reaction is only

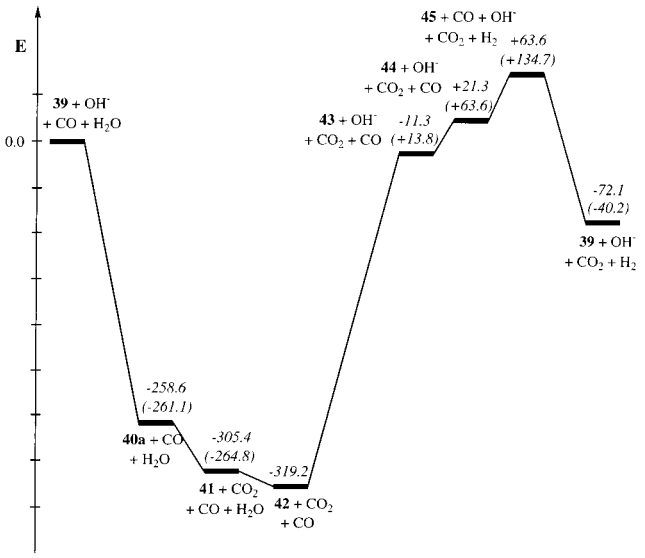

Figure 8. B3LYP thermochemical profile for the model $Fe(CO)_5$-catalyzed WGSR in the gas phase (enthalpies in kilojoules per mole) as reported by TSF. CCSD(T)//B3LYP enthalpies are given in parentheses. Reprinted from ref 168. Copyright 1999 American Chemical Society.

63.5 kJ mol^{-1}, although some energy has to be added thermally along the pathway because the intermediates will lose some energy via decomposition (loss of CO_2 and H_2), and the dissociated particles will take some energy vibrationally, rotationally, and translationally.

D. Hydrogenation of CO_2

The use of carbon dioxide as a C_1 building block in organic synthesis is of great interest because of the vast amounts of carbon that exist in this form. CO_2 is cheap, easy to handle, and nontoxic. To enhance the reactivity of this inert, highly oxidized, thermodynamically stable compound, electroreductive techniques or TM catalysts are used (see ref 197 for a recent review on activation of CO_2 by TM). In particular, the homogeneous catalytic hydrogenation of CO_2 to formic acid catalyzed by TM complexes, usually biphosphine rhodium complexes, is one of the most promising approaches to CO_2 fixation.[198−213] Remarkably, hydrogenation of CO_2 is an endoergonic and exothermic process under standard conditions (eq 18).[70] However, by a suitable choice of the reaction

$$H_2 + CO_2 \rightleftarrows HCOOH$$

$$\Delta H°_{298} = -31.6 \text{ kJ mol}^{-1} \text{ and}$$

$$\Delta G°_{298} = 32.9 \text{ kJ mol}^{-1} \quad (18)$$

parameters (elevated pressure, base addition, etc.), the equilibrium can be shifted to the right.[198,199] In addition, the very large kinetic barrier can be overcome using a suitable catalyst.[198−213]

The first detailed mechanistic study of the hydrogenation of CO_2 to HCOOH catalyzed by Rh(I) complexes was carried out by Tsai and Nicholas using $[(NBD)Rh(PMe_2Ph)_3][BF_4]$ (NBD = norbornadiene) as a catalyst.[202] From their work and subsequent studies (see refs 198−200 and 206 for recent reviews), it has

been established that the reaction mechanism for this hydrogenation catalyzed by rhodium complexes consists of four steps shown in Scheme 16:[198,202−208] (1)

Scheme 16. Schematic Representation of the Suggested Mechanism for the Hydrogenation of CO_2 Catalyzed by $HRhP_2$ Complexes (P = Phosphine)[a]

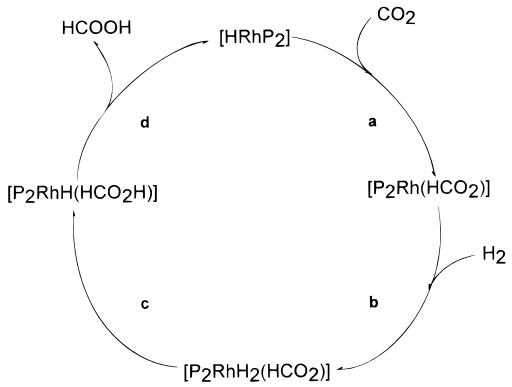

[a] Reprinted from ref 234. Copyright 1998 American Chemical Society.

insertion of the incoming CO_2 molecule into the Rh−H bond of the unsaturated T-shape neutral 14-electron active species[198,201,206−209,212,214] $HRhP_2$ to yield $P_2Rh(HCO_2)$, (2) oxidative addition of H_2 to the vacant site of this complex, (3) reductive elimination from $P_2RhH_2(HCO_2)$ to yield $P_2RhH(HCOOH)$, and (4) release of HCOOH to recover the catalytically active species $HRhP_2$. Experiment demonstrates the full reversibility of this Rh-catalyzed hydrogenation of CO_2.[206,215] The experimental kinetic data are consistent with a mechanism in which the rate-determining step is the reductive elimination of HCOOH from an intermediate that is formed via two reversible reactions of the catalytically active species $HRhP_2$ first with CO_2 and then with H_2.[202,215] The following sections review theoretical studies on the whole catalytic cycle and also on some of the four steps present in Scheme 16.

1. Insertion of CO_2

The first step of the catalytic cycle corresponds to the insertion of CO_2 into the Rh−H bond of the active species $HRhP_2$. This insertion may proceed via formation of a precursor complex where CO_2 is coordinated to the vacant site of $HRhP_2$. Different coordination modes can be considered for the interaction of CO_2 with a TM.[216] As a monodentate ligand, CO_2 can interact through the carbon atom, leading to an η^1-C complex, or through an oxygen atom, resulting in an η^1-O species. As a bidentate ligand, CO_2 can form η^2-C,O complexes when the metal interacts with the C−O bond and η^2-O,O complexes when the bond occurs with the two oxygen atoms (see Scheme 17). Examples of η^1-C and η^2-C,O coordination modes have been confirmed by X-ray crystallography.[216,217]

Sakaki and Dedieu[218] performed partial optimizations at the HF level to analyze the coordination mode of CO_2 in $[Co(alcn)_2(CO_2)]^-$ (alcn = HNCHCHCHO$^-$). The authors derived the following rule for predicting the preference for the η^1-C or the η^2-C,O

Scheme 17

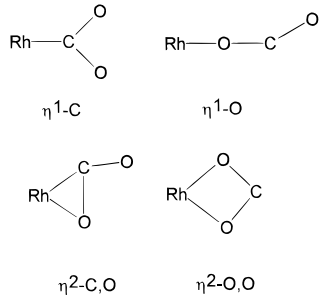

coordination mode of CO_2. When the metal has a d_σ orbital as the HOMO and a low oxidation state, the η^1-C mode is favored, whereas the best situation for the η^2-C,O coordination mode is the presence of a HOMO mainly composed of a d_π orbital and an empty d_σ orbital pointing to the CO_2 ligand. In agreement with this conclusion, the η^1-C mode is the most stable in the $[Co(alcn)_2(CO_2)]^-$ complex[218] and in $RhCl(AsH_3)_3(CO_2)$,[219] while the η^2-C,O coordination mode is favored in $Ni(CO_2)(PCy_3)_2$.[220] In the η^1-C coordination mode, the CO_2 ligand acts as a Lewis acid accepting electrons from the metal. Consequently, in this mode CO_2 is activated in front of electrophiles.[219] In the η^2-C,O coordination mode the main interaction is the π back-donation from the TM to the CO_2 ligand.[221]

In three different works, Sakaki and Musashi (SM)[222−224] studied the insertion of CO_2 into the Rh^I−H bond of the SPl $HRh(PH_3)_3$ complex and into the Rh^{III}−H bond of the SPy *cis*-$[H_2Rh(PH_3)_3]^+$ species. For the latter complex, two possible conformations with H or PH_3 in the apical position of the SPy structure were considered. In all cases, a precursor complex between CO_2 and $HRh(PH_3)_3$ or *cis*-$[H_2Rh(PH_3)_3]^+$ is formed. In these precursor complexes, the CO_2 is not directly coordinated to Rh, the position of the CO_2 molecule being parallel to the Rh−H bond. At the MP2 level, the Rh−O bond lengths are larger than 2.4 Å and the stabilization energies for the formation of the precursor complex are rather small, ranging from 13.8 kJ mol^{-1} for $HRh(PH_3)_3$ to 59.4 kJ mol^{-1} for *cis*-$[H_2Rh(PH_3)_3]^+$ with apical phosphine.

Hutschka, Dedieu, Eichberger, Fornika, and Leitner (HDEFL)[215] found that, in contrast to $HRh(PH_3)_3$, CO_2 directly coordinates to the $HRh(PH_3)_2$ complex **46** (Figure 9), forming an η^2-C,O complex with a remarkable binding energy of 102.0 and 82.8 kJ mol^{-1} at the MP2 and QCISD(T)//MP2 levels, respectively. The presence of occupied d_π orbitals of high energy and the existence of an unoccupied low-lying d_σ pointing toward CO_2[225] makes the η^2-C,O coordination mode of CO_2 the most favored in complex **46**.[218]

Sakaki, Musashi, and Okhubo studied the CO_2 insertion into the Rh−H bond of the $HRh(PH_3)_3$ and *cis*-$[H_2Rh(PH_3)_3]^+$ complexes,[222−224] and also the insertion into the Cu−H bond of $HCu(PH_3)_2$.[30,226−229] Some of their results together with the values for the CO_2 insertion into the Rh−H bond of the $HRh(PH_3)_2$ complex **46** discussed by HDEFL[215] are gathered in Table 6. In this table, the stabilization energy E_{stab} corresponds to the energy difference between the

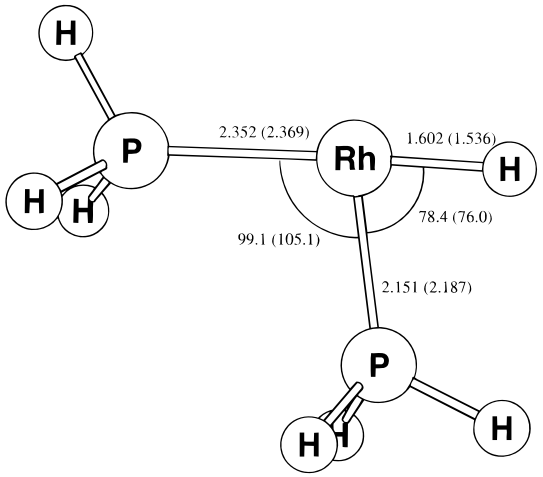

46

Figure 9. B3LYP-optimized structure for complex **46**.[234] MP2-optimized parameters are given in parentheses.[215] Bond distances in angstroms and angles in degrees. Reprinted from ref 234. Copyright 1998 American Chemical Society.

Table 6. Stabilization Energy of the Precursor Complex E_{Stab}, Activation Energy E_a, and Reaction Energy ΔE for the Insertion of CO_2 into Rh−H and Cu−H Bonds Computed at the MP2 Level (kJ mol^{-1})

	E_{stab}	E_a	ΔE^a	ref
$HRh^I(PH_3)_2$	−102.0	18.0	−84.4	215
$HRh^I(PH_3)_3$	−13.8	75.7 (85.7)[b]	−4.2	222
cis-$[H_2Rh^{III}(PH_3)_3]^+$ [c]	−89.2	221.1	−13.8	223
$HCu^I(PH_3)_2$		53.9 (29.7)[b]	−69.8	227

[a] The η^1-O coordination mode in the product complex has been considered everywhere, except for the product complex in the insertion to *cis*-$[H_2Rh(PH_3)_3]^+$, for which the η^2-O,O coordination mode in the product has been taken into account. [b] MP4(SDQ) values in parentheses from ref 222. [c] With the hydride ligand trans to CO_2.

precursor complex and the separated reactants, the activation energy E_a is the energy difference between the TS and the precursor complex, and ΔE is the reaction energy, i.e., the energy difference between reactants and products.

The insertion of CO_2 into the Rh^{III}−H bond of *cis*-$[H_2Rh(PH_3)_3]^+$ is characterized by an electrophilic attack of CO_2 on *cis*-$[H_2Rh(PH_3)_3]^+$.[223,224] The electronic charge flows basically from the HOMO of *cis*-$[H_2Rh(PH_3)_3]^+$ to the π^* orbital of CO_2. Values in Table 6 show that the CO_2 reaction with *cis*-$[H_2Rh(PH_3)_3]^+$ requires the highest activation energy and has a small exothermicity. This is because in this positively charged complex the charge transfer to the π^* orbital of CO_2 is the weakest, and CO_2 must closely approach the H ligand to break the bond. Actually, the stronger charge-transfer interaction is one of the characteristic features of the CO_2 insertion reaction. The CO_2 population of the TS is nearly the same as that of the product, clearly indicating that the formate anion is almost formed in the TS. In this TS, the formate strongly interacts with the Rh in an η^1-O coordinating mode at the trans position of the hydride. This location of the ligands is unfavorable for the insertion because of the strong trans influence of the H ligand. If the ligand trans to CO_2 is PH_3 in the same *cis*-$[H_2Rh(PH_3)_3]^+$ complex, the barrier is lowered by ca. 40 kJ mol^{-1} because of the weaker trans influence of PH_3 with respect to hydride.[224] Finally, the insertion of CO_2 into the *cis*-$[H_2Rh(PH_3)_2(H_2O)]^+$ complex with H_2O trans to CO_2 takes place even more easily with an activation barrier of 100 kJ mol^{-1}.[224] In the product, the formate anion coordinates to Rh in an η^2-O,O mode, due to the Rh(III) tendency to form octahedral complexes because of its d^6 electron configuration.

The insertion of CO_2 into the Rh^I−H bond of $HRh(PH_3)_3$ proceeds more easily than into the Rh^{III}−H bond of the positively charged *cis*-$[H_2Rh(PH_3)_3]^+$ complex.[222−224] The interaction between the HOMO of $HRh(PH_3)_3$ and the π^* orbital of CO_2 is more favorable in this neutral complex. As expected from the d^8 electronic configuration of Rh(I), the most stable structure for the final product corresponds to a SPl four-coordinated complex with the formate anion coordinating in an η^1-O mode.

Results in Table 6 by HDEFL[215] indicate that the insertion of CO_2 into the complex $HRh(PH_3)_2$, **46**, has the largest exothermicity and the lowest energy barrier. Figure 10 depicts the MP2-optimized geometries of the precursor complex, the TS, and the coordinately saturated η^2-O,H product for the CO_2 insertion into the Rh^I−H bond of complex **46**. All calculations reported by HDEFL[215] were performed on the singlet PES. For the 14-electron complex **46**, MP2 calculations favor the singlet over the triplet by 69.4 kJ mol^{-1},[215] while, for instance, $RhCl(PH_3)_2$ has a triplet ground state more stable than the singlet by 8−33 kJ mol^{-1}.[230] As one can see from Figure 10, the geometry of the TS reveals that it has product-like character. The four-center-type interaction in the TS **48** is hardly present in $HRh(PH_3)_3$ and *cis*-$[H_2Rh(PH_3)_3]^+$. The Rh−H bond distance in **48** is much shorter than in the TSs found by Sakaki and Musashi[222−224] for the insertion into the Rh−H bond of $HRh(PH_3)_3$ or *cis*-$[H_2Rh(PH_3)_3]^+$ owing to the propensity of the hydrogen atom to fill the vacant fourth coordination site of rhodium through an agostic interaction. The other geometrical parameters are similar. The most stable structure for the final product corresponds to a SPl four-coordinated complex (as expected for the d^8 configuration of Rh(I)) with η^2-O,O coordination of the formate anion. This structure is lower in energy than the η^2-O,H configuration by 50.6 kJ mol^{-1}. For that reason it is considered an unproductive "shunt" in the catalytic cycle.[202−215] Insertion of CO_2 into the Cu^I−H bond of the complex $HCu(PH_3)_2$ affords comparable structures for the stationary points and rather similar energetics.[30,226−229] Remarkably, the CO_2 insertion into the Cu^I−H bond of the complex $HCu(PH_3)_2$ takes place with a lower activation barrier and a higher exothermicity than the insertion of ethylene. The lower activation energy was attributed to the smaller exchange repulsion (probably as a result of smaller overlaps between the HOMOs of the two fragments in the TS) in the approach of CO_2 with respect to that of C_2H_4. The reason for the higher exothermicity is the stronger Cu−OC(O)H bond as compared to the Cu−CH_2CH_3 bond.[229] Finally, the insertion of CO_2

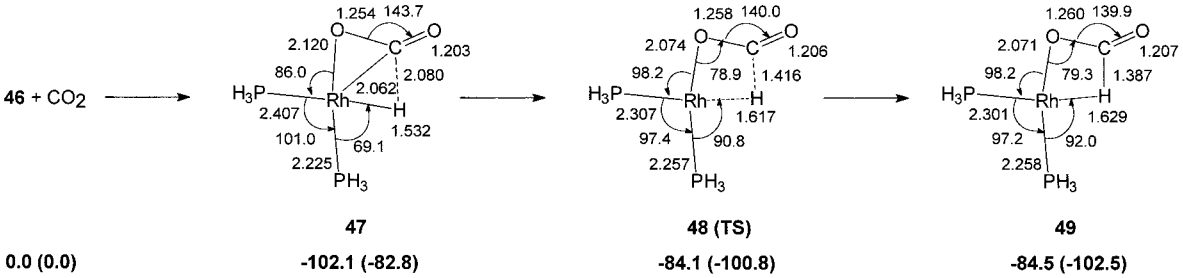

Figure 10. MP2-optimized geometries and relative energies (kJ mol^{-1}, QCISD(T)//MP2 values in parentheses) for the precursor complex, TS, and product of the CO_2 insertion in $HRh(PH_3)_3$. Bond distances in angstroms and angles in degrees. Reprinted from ref 215. Copyright 1997 American Chemical Society.

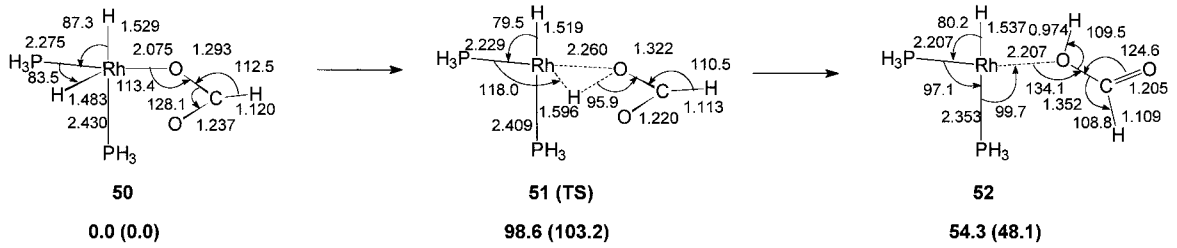

Figure 11. MP2-optimized geometries and relative energies (kJ mol^{-1}, QCISD(T)//MP2 values in parentheses) for the formate intermediate complex **50**, TS, and product of the reductive elimination of HCOOH.[215] Bond distances in angstroms and angles in degrees. Reprinted from ref 215. Copyright 1997 American Chemical Society.

into the Fe−H bond of $Fe(CO)_4H^-$ is more difficult, being endothermic by 46.9 kJ mol^{-1} and having a remarkable barrier of 151.1 kJ mol^{-1}.[168] The larger repulsions between CO_2 and the negatively charged $Fe(CO)_4H^-$ account for this higher energy barrier.

As a whole, the low energy barriers obtained for CO_2 insertion into neutral complexes (in particular, that of $HRh(PH_3)_2$) point to the conclusion that step **a** is not rate-determining in the catalytic cycle of the hydrogenation of CO_2 catalyzed by rhodium complexes.

2. Oxidative Addition of H_2

The second step in the catalytic cycle of the hydrogenation of CO_2 to yield HCOOH, step **b** in Scheme 16, corresponds to the oxidative addition of H_2 to complex **49** to form the $(PH_3)_2RhH_2(HCO_2)$ complex **50** (see Figure 11). Dedieu and co-workers[215,231] in two different works studied this step performing MP2 optimizations followed by QCISD(T)//MP2 single-point energy calculations in selected points of the PES. No stable nonplanar η^2-H_2 precursor complex was found, as one could expect from the fact that, among the second-row TMs, rhodium is very effective in H_2 oxidative addition.[27] The only stable η^2-H_2 precursor complex is a planar dihydrogen complex, **53**. However, when H_2 approaches complex **49** perpendicular to the plane of the molecule, it directly produces the dihydrido formate complex **50** of SPy structure with an axial hydride. This **49** + H_2 → **50** process is barrierless and is exothermic by 36.4 and 20.9 kJ mol^{-1} at the MP2 and QCISD(T)//MP2 levels, respectively.[215] Multiple isomers of complex **50** exist. Among them, the most stable is the η^2-O,O dihapto isomer, which is more stable than the structure **50** in Figure 11 by 83.6 kJ mol^{-1}. Further calculations are needed to determine the precise role of this η^2-O,O dihapto isomer in the catalytic cycle. It may be that either this bidentate isomer is an unproductive "shunt", or it is kinetically inaccessible, or calculations are at fault providing a too stable η^2-O,O dihapto isomer. In any event, it is expected that the reaction continues from **50**.

3. Reductive Elimination of HCOOH

Figure 11 depicts the dihydrido formate complex **50**, the TS **51**, and the product **52** of the reductive elimination of *trans*-HCOOH from complex **50** (step **c** in Scheme 16). At the QCISD(T)//MP2 level, this process is endothermic by 48.1 kJ mol^{-1} and has an energy barrier of 103.2 kJ mol^{-1}.[215]

This relatively high energy requirement for the reductive elimination step prompted the authors to analyze an alternative [2+2] σ bond metathesis reaction between H_2 and the formate intermediate **49** to form product **52**. σ bond metathesis of H_2 is a well-established process among electron-poor early TMs,[95,232] and it has been invoked for middle and late TMs as well. The initial interaction of H_2 and complex **49** in the same plane yields a stable η^2-H_2 precursor complex which is stabilized by −23.7 kJ mol^{-1} at the QCISD(T)//MP2 level. Rather surprisingly, the TS for this σ bond metathesis from this dihydrogen complex was found to be 17.6 kJ mol^{-1} lower in energy than the TS **51** corresponding to the reductive elimination process.[215] The low energy barrier for this σ bond metathesis was attributed, first, to the involvement of the low-lying unoccupied $d_{x^2-y^2}$ orbital of Rh in the σ bond that is broken and in the σ bond that is formed and, second, to the existence of a lone pair in the oxygen atom bonded to Rh that is directed toward the incoming H atom.[215]

In a subsequent work, Hutschka and Dedieu showed that this σ bond metathesis pathway was further favored by the presence of an additional Lewis base.[233] The authors found that the assistance of an

ammonia molecule is very effective for the kinetics of this process, the barrier being reduced from 45.6 to 8.8 kJ mol^{-1} at the MP2 level.[233] In this mechanism, the ammonia molecule acts as a relay, first withdrawing a proton from the coordinated H_2 molecule and afterward releasing it to the formate anion. Experimentally, it is usual to add triethylamine to the reaction to facilitate the catalysis and to get higher formic acid yields.[199,207,208] From the calculation by Hutschka and Dedieu, one can expect that, in the presence of triethylamine, the σ bond metathesis will be the operative pathway for the transformation of the formate intermediate **49** into the product complex **52**. This process is associated with a very smooth energy profile.

4. Dissociation of HCOOH

Experimental[202] and more precisely theoretical[215,231] studies have shown that the release of formic acid from complex **52** is the rate-determining step of the process. In particular, the energy for surpassing this last step is 98.6, 94.5, and 91.5 kJ mol^{-1} at the MP2,[215,231] QCISD(T)//MP2,[215,231] and B3LYP levels.[234] The dative-type interaction between rhodium and oxygen accounts for the large energy requirement for the dissociation of **52** into HCOOH and $HRh(PH_3)_2$. Such a relatively high energy requirement for the release of HCOOH does not meet the expected standards for a process that occurs rapidly at moderate temperatures, and that is fully reversible.[206,215] It has been suggested that the presence of a base may facilitate the release of HCOOH,[199,207,233] although no conclusive data on this point have been reported to date. On the other hand, it has also been pointed out[231] that substitution of HCOOH by CO_2 may follow an associative mechanism which should be less energy demanding than the dissociative one depicted in Scheme 18.

Scheme 18

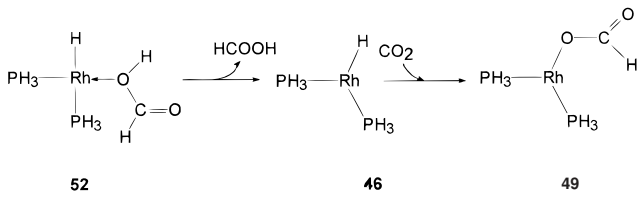

Two possible associative mechanisms can be conceived. First, the incoming CO_2 molecule may occupy a vacant coordination site of the 16-electron complex **52**. It is expected that the presence of this new ligand may facilitate the liberation of formic acid in the last step of the hydrogenation process (Scheme 19).

Scheme 19

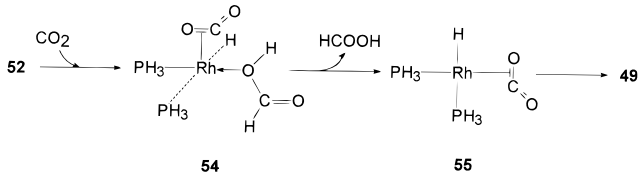

Alternatively, the CO_2 molecule may bind the hydride ligand through a donor−acceptor interaction[235] to yield the complex **56a** in Scheme 20, which, in turn, can rearrange to complex **56b** which after release of HCOOH may form complex **49**, closing the catalytic cycle. These associative mechanisms can be especially relevant when the hydrogenation is performed in supercritical CO_2 ($scCO_2$)[236] owing to the high concentration of CO_2.

Scheme 20

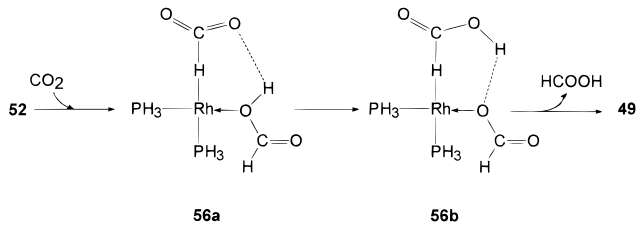

These two associative paths were studied by Pomelli, Tomasi, and Solà (PTS)[234] at the B3LYP level in the gas phase and in $scCO_2$. The authors found that both associative processes favor release of HCOOH. The lowest energy requirement for the dissociation corresponds to the **52** → **54** → **55** → **49** associative pathway. In this case, PTS found that the interaction of the unsaturated 16-electron complex **52** with CO_2 to yield the 18-electron complex **54** (see Figure 12) is exothermic by 58.1 kJ mol^{-1} in the gas phase and by 58.9 kJ mol^{-1} in $scCO_2$, in line with earlier experimental[200,209,217] and theoretical[215,219−223,231] studies of coordination of CO_2 in rhodium complexes. Dissociation of HCOOH from complex **54** to yield complex **55** is endothermic by 54.3 kJ mol^{-1} in the gas phase. Therefore, release of HCOOH from complex **54** is 37.2 kJ mol^{-1} less endothermic than dissociation from complex **49** at the B3LYP level.[234] Dissociation of HCOOH from complex **54** is even slightly more favored in $scCO_2$, where the energy requirement for the dissociation of HCOOH is only 53.5 kJ mol^{-1}. The insertion of CO_2 into the Rh−H bond of complex **55** to yield complex **49** is a slightly endothermic process by 37.6 kJ mol^{-1} in the gas phase and 31.4 kJ mol^{-1} in $scCO_2$. From the calculations by HDEFL,[215] one can expect that the insertion of CO_2 into the Rh−H bond that forms complex **49** from complex **55** will possess a small energy barrier (only slightly larger than 37.6 kJ mol^{-1}, which is the endothermicity of the **55** → **49** transformation).

5. Final Remarks

The entire energy profile for the catalytic cycle at the QCISD(T)//MP2 level computed by HDEFL[215] is depicted in Figure 13. As one can see, the whole energy profile is rather smooth, the dissociation of HCOOH from complex **52** in the last step of the catalysis being the rate-determining step. Associative mechanisms, such as those studied by PTS,[234] reduce the energy needed for the release of HCOOH by about 40 kJ mol^{-1}. This notwithstanding, the energy requirement for this last step is still high enough, as compared to the barriers for the rest of the catalytic cycle, to indicate that the dissociation of formic acid corresponds to the rate-determining step, in agreement with experimental results.[202,215]

Despite these important theoretical contributions to the understanding of the mechanism of the hy-

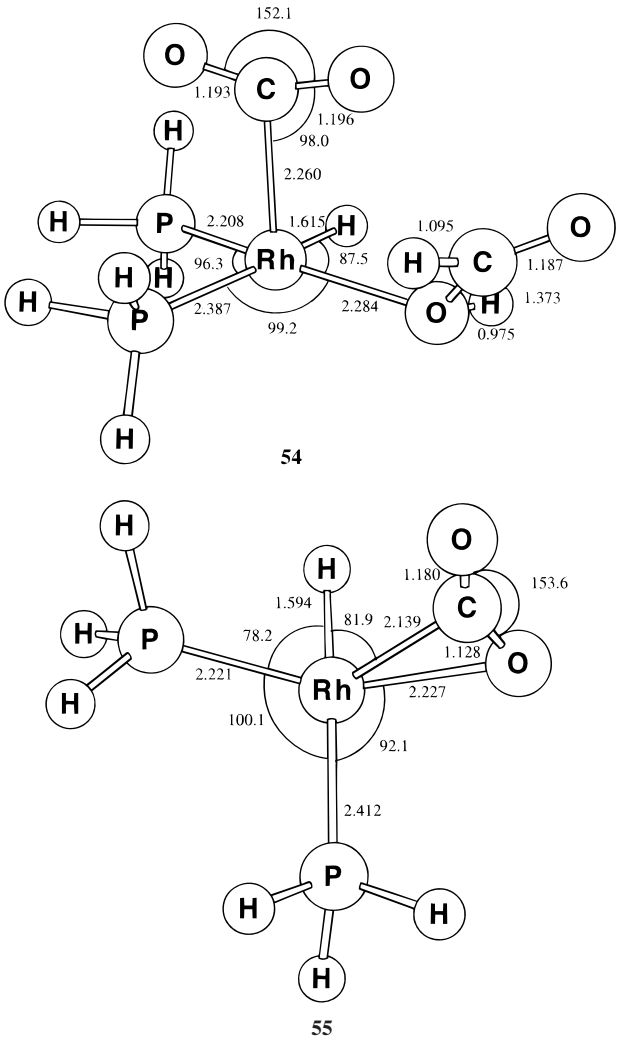

Figure 12. B3LYP-optimized structures for complexes **54** and **55**.[234] Bond distances in angstroms and angles in degrees. Reprinted from ref 234. Copyright 1998 American Chemical Society.

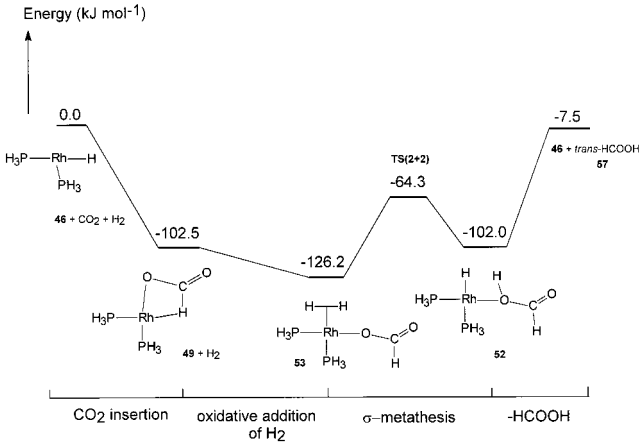

Figure 13. QCISD(T)//MP2 energy profile (kJ mol^{-1}) for the entire catalytic cycle of the hydrogenation of CO_2 to yield *trans*-HCOOH as computed by HDEFL.[215] (This energy profile does not take into account the beneficial effects of the presence of amine in the σ-metathesis process and the possible involvement of associative mechanisms in the release of HCOOH.)

drogenation of CO_2 catalyzed by rhodium complexes, there are still some open questions that should be discussed in forthcoming years. It will be interesting to analyze whether the presence of a Lewis acid favors the thermodynamics of the last step. Further, although it is true that gas-phase results are very important for the understanding of the reaction mechanism, it is also true that an inherent problem of the corroboration of ab initio studies with experimental observations in homogeneous catalysis is the extrapolation of results obtained for gas-phase structures to the situation in solution. For that reason, a further step will be to take into account the solvent effects in the whole catalytic cycle. Finally, it will be interesting to analyze theoretically the effect of the ligands on the energy profile, both from an electronic point of view by looking at different phosphine ligands with different basicities and from a steric point of view. This last point has already been addressed by Angermund et al.[208] by defining the so-called accessible molecular surface (AMS) for the active species $HRhP_2$. The authors found that a small AMS has a beneficial effect because it prevents the undesired stabilization of the species $HRhP_2$ by addition of donor molecules and facilitates the release of HCOOH.

E. Hydrogenation of CO

The hydrogenation of CO became an important process for the synthesis of motor fuels and other liquid hydrocarbons during the World War II, when German scientists developed heterogeneously catalyzed methods which are collectively called the Fischer−Tropsch process.[237] The poor selectivity and the lower prices for the alternative resources mineral oil and natural gas made the Fischer−Tropsch reaction become less important in the past decades. However, facing declining resources in liquid and gaseous chemical raw materials, the controlled hydrogenation of CO has become of renewed interest for the chemical industry.[238] Efforts were made to find homogeneous variants of the catalytic CO hydrogenation.[239] It turned out that homogeneous rhodium catalysts and most prominently $HRh(CO)_4$ (**4**) are particularly suited for the synthesis, which leads to a variety of oxygenated C_1 and C_2 products (Scheme 21).[90a,240]

Despite enormous efforts on the experimental side, the homogeneously catalyzed hydrogenation of CO has not found any large-scale industrial applications yet. The most carefully investigated process is the Union Carbide method for the conversion of CO and H_2 into ethylene glycol.[241−243] It was concluded that for a systematic development of effective catalysts for CO hydrogenation reactions a better understanding of the fundamental mechanistic processes is necessary,[239] but despite the industrial importance of the reaction, very few theoretical studies were devoted to the mechanism of the catalyzed CO hydrogenation.

Most previous investigations focused on the initial step of the TM-catalyzed CO hydrogenation, i.e., the hydrogen migration from the metal hydride to the carbonyl ligand, yielding the formyl complex:[43,244]

$$L_nMH(CO) \rightarrow L_nM(CHO) \qquad (19)$$

Earlier theoretical studies of reaction 19 have been

Scheme 21. Reaction Products of the $HRh(CO)_4$-Catalyzed CO Hydrogenation

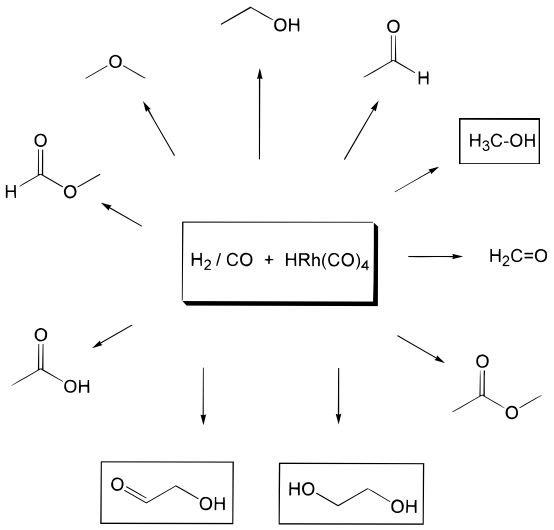

Table 7. Relative Energies (kJ mol^{-1}) of MH(CO) and M(CHO) Species and Transition States MCHO‡ for the Interconversion[a]

M	MH + CO	MH(CO)	MCOH‡	M(CHO)
Y	0.0	−14.2	−7.5	−68.6
Zr	0.0	−89.1	−56.9	−89.1
Nb	0.0	−104.6	−79.9	−61.1
Mo	0.0	−68.2	58.2	−0.8
Tc	0.0	−100.4	32.6	−10.0
Ru	0.0	−144.3	−12.6	2.5
Rh	0.0	−146.0	−82.4	−22.2
Pd	0.0	−74.9	32.2	−20.5

[a] Reference 60a.

reviewed by Koga and Morokuma (KM).[23,24] The most important findings were the following: (i) Reaction 19 is endothermic for neutral complexes of the middle and late TMs, but it is exothermic for early TM compounds. (ii) The reaction proceeds for middle and late TMs via hydride migration to CO, while for early TMs the hydride inserts into the M−CO bond. (iii) The formyl complexes of the middle and late TMs exhibit η^2-coordinated formyl ligands with rather weak metal−oxygen interactions, while the early TM complexes have shorter M−O than M−C bonds. The difference between the early and the later TMs was explained with the electron deficiency of the early TMs, which have energetically low-lying empty d orbitals and thus are strong Lewis acids.[23,24]

An important theoretical work on the CO insertion into the M−H bond of ligand-free TMs was published by Blomberg, Karlsson, and Siegbahn (BKS) in 1993.[60] BKS made a complete TM second-row sweep of reaction 20, which was calculated at the MCPF level using HF-optimized geometries.

$$MH + CO \rightarrow MH(CO) \rightarrow M(CHO) \qquad (20)$$

Table 7 shows the summary of the calculated energies. The formation of the formyl complex from the carbonyl hydrido complex is exothermic for M = Y, thermoneutral for M = Zr, and clearly endothermic for the other metals. There are substantial activation barriers for M = Mo to Pd. Note that among Mo to Pd, Rh has the highest overall exothermicity, lowest activation barrier, and highest (of all metals) CO binding energy.

In 1988, Rosi, Sgamellotti, Tarantelli, and Floriani (RSTF) investigated some postulated intermediates of the CO hydrogenation catalyzed by $Fe(CO)_2(PH_3)_2$ at the HF level of theory with partial geometry optimization of the molecules.[245] They found that the reaction starting from $Fe(CO)_2(PH_3)_2H_2$ + CO and yielding $Fe(CO)(PH_3)_2(CHO)_2$ is exothermic by 98 kJ mol^{-1}. The reaction proceeds via symmetry-allowed hydrogen addition, yielding the intermediate $Fe(CO)(PH_3)_2(CH_2O)$, while the formation of $Fe(CO)(PH_3)_2(CHO)H$ is not allowed.[245]

Versluis and Ziegler (VZ) published in 1990 a DFT study of the insertion of formaldehyde into the H−$Co(CO)_3$ bond of a model catalyst, which is a possible reaction step in the later stage of the catalytic CO hydrogenation.[100] The calculations predict the initial formation of a π complex $HCo(CO)_3(H_2CO)$ with formaldehyde in the equatorial position. The axial isomer is 50 kJ mol^{-1} higher in energy. The reaction profile for the hydride migration was modeled by a linear transit procedure. It was found that the formation of the methoxy complex $Co(CO)_3(H_3CO)$ is kinetically (activation barrier <5 kJ mol^{-1}) and thermodynamically (reaction enthalpy 6 kJ mol^{-1}) more favorable than the formation of the hydroxymethyl complex $Co(CO)_3(H_2CHO)$, which has an activation barrier of 15 kJ mol^{-1} and a reaction enthalpy of 40 kJ mol^{-1}.[100]

The C−C coupling reaction of the heterogeneously catalyzed Fischer−Tropsch reaction was modeled by Koga and Morokuma in 1991 in a theoretical study at the MP2 level of theory using HF-optimized structures.[246] These authors took reaction 21 as a model for the C−C coupling step, which had previously been investigated in experimental studies of related complexes.[247]

$$(CpRh)_2(\mu\text{-}CH_2)_2(CH_3)H \rightarrow (CpRh)_2(\mu\text{-}CH_2)(C_2H_5)H \qquad (21)$$

The symmetry-restricted optimization of the equilibrium structures and TSs showed that the reaction probably takes place via reductive elimination and not via a dinuclear replacement. The calculated activation barrier was rather high (175 kJ mol^{-1}), but it was clearly lower than the corresponding C−C coupling step of the mononuclear complex, which had a barrier of 275 kJ mol^{-1}.[246] Mechanistic details of the heterogeneously catalyzed CO hydrogenation have also been modeled in three studies at the EHT level of theory.[248]

The most comprehensive theoretical study in this field has recently been published by Pidun and Frenking (PF), who carried out a systematic ab initio study of the $HRh(CO)_4$-catalyzed CO hydrogenation.[66] The calculations were performed at the MP2 level of theory using an ECP for Rh with a double-ζ plus polarization quality basis set and 6-31G(d,p) basis sets for the other atoms. All optimized structures were characterized as either minima or saddle points on the PES by numerical calculation of the Hessian

matrixes. Using up to 32 starting structures per intermediate, a total of 29 energy minima, 17 TSs, and 2 higher-order saddle points were located for reaction 22.

$$HRh(CO)_4\ (\mathbf{4}) + H_2 \rightarrow Rh(CO)_3(C,O,H_3) \quad (22)$$

The most relevant results of this work are shown in Figure 14, which gives the calculated reaction energies and activation barriers for the numerous reaction steps of reaction 22 yielding different compounds. Two major reaction channels with similar energies which lead to the methoxy complex **64a** and hydroxymethyl complex **63b**, respectively, were found. This is in agreement with the experimental findings that methanol and hydroxymethyl compounds are the major products of the rhodium-catalyzed CO hydrogenation (Scheme 21). The formation of a hydroxycarbene complex, which had been suggested as a possible intermediate in reaction 22, can be excluded because of the large activation barrier for the formation of **62a**.

III. Organometallic Reactions Involving Unsaturated Hydrocarbon Compounds

A. Olefin Hydrogenation

One of the simplest and most fundamental catalytic reactions of olefins is hydrogenation. Many TM complexes can catalyze the homogeneous hydrogenation of olefins,[249] although as yet the most thoroughly studied catalyst has been the Wilkinson's catalyst,[250] $RhCl(PPh_3)_3$, discovered in 1965.[251] Terminal olefins are rapidly hydrogenated at room temperature and atmospheric pressure by this catalyst, while internal olefin hydrogenation proceeds more slowly. Such a property has been used in organic synthesis to selectively hydrogenate a targeted double bond.[249] The homogeneous hydrogenation of prochiral alkenes, which gives rise to enantiomerically enriched products, has found important applications in the pharmaceutical industry and in organic synthesis.[249,252−256]

At least four different mechanistic pathways have been proposed for olefin hydrogenation. The most widely accepted one is the so-called Halpern mechanism derived through detailed kinetic[250,254,257] and NMR and IR spectroscopic[258] studies. It involves the following steps (Scheme 22): (a) ligand dissociation, (b) oxidative addition of H_2, (c) olefin coordination, (d) olefin insertion, (e) isomerization, and (f) reductive elimination of the alkane and regeneration of the active species. Although the isomerization step was not originally proposed by Halpern, Morokuma and co-workers[259] showed that the isomerization of **70** to **71** has to occur to facilitate the reductive elimination of the alkane. In this mechanism, the olefin insertion step is believed to be the rate-determining step.[254,257c] Scheme 23 depicts the Brown mechanism.[252,260] The main difference between the Halpern and the Brown mechanisms is the presence of key intermediates having *cis*-phosphines in the latter. Thus, this mechanism requires isomerization of species **68** to **72** prior to olefin coordination. Remarkably, a complex equivalent to **73** with *cis*-phosphines and *cis*-hydrides has been observed during olefin hydrogenation by means

Scheme 22. Schematic Representation of the Halpern Mechanism for the Hydrogenation of Olefins Catalyzed by Rh Complexes

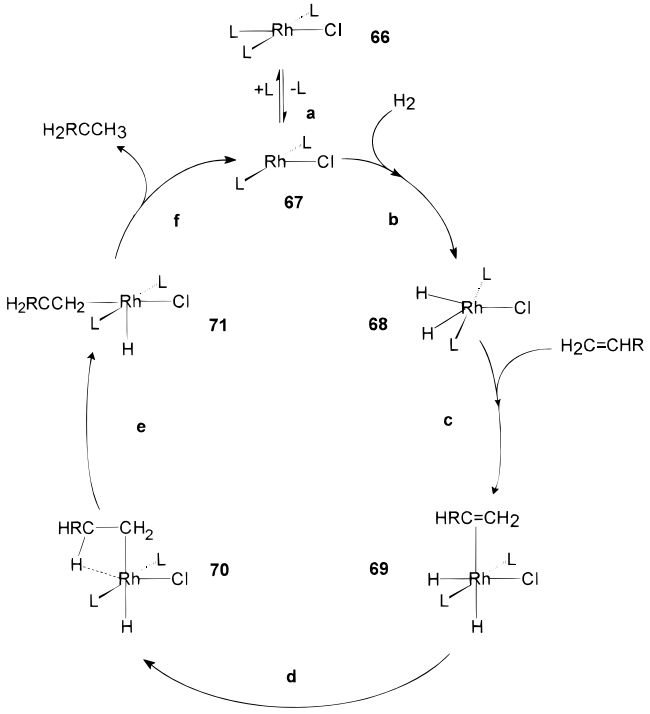

Halpern mechanism

Scheme 23. Schematic Representation of the Mechanism Proposed by Brown for the Hydrogenation of Olefins Catalyzed by Rh Complexes

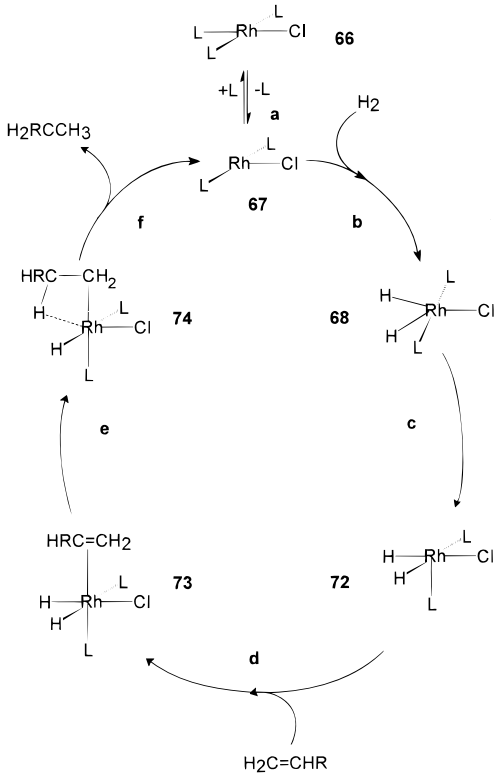

Brown mechanism

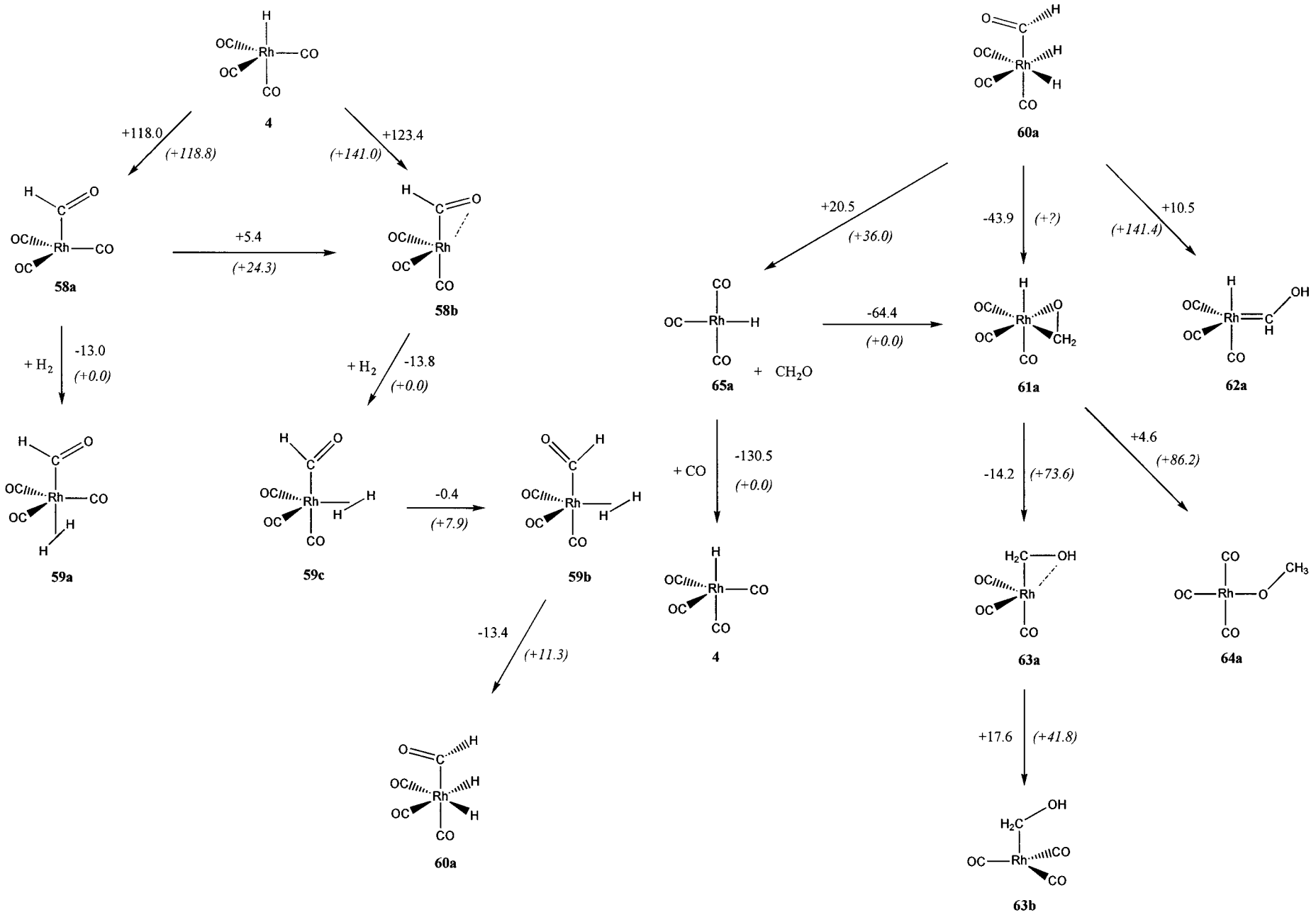

Figure 14. Calculated reaction energies and activation barriers (*in parentheses*) at the MP2 level of theory for the $HRh(CO)_4$-catalyzed CO hydrogenation. Reprinted with permission from ref 66. Copyright 1998 Wiley-VCH. The values are in kilojoules per mole.

of the para-hydrogen induced polarization technique.[261] A mechanism for hydrogenation by $HRh(PPh_3)_3$ that differs from that proposed for the catalysis by $RhCl(PPh_3)_3$ was discussed by Strauss and Shriver.[262] In this mechanism ligand dissociation before olefin coordination is not a prerequisite and the olefin coordinates directly to $HRh(PPh_3)_3$. The $HRh(C_2H_4)(PPh_3)_3$ thus formed rearranges to $Rh(C_2H_5)(PPh_3)_3$, which in turn reacts with dihydrogen to produce ethane and release the catalyst. Finally, in the hydrogenation of olefins catalyzed by $[Rh(diphos)]^+$ [diphos = 1,2-bis(diphenylphosphinoethane)] it was found that the sequence of reactions of the catalyst with H_2 first and then with olefin is reversed.[253,255] Interestingly, in this latter mechanism the rate-determining step is the oxidative addition of H_2, except at low T, where the product-forming reductive elimination becomes rate-limiting.[253,254]

Despite the numerous kinetic and spectroscopic studies performed, the only species observed when **66** reacts with H_2 and/or olefins have been intermediates **67**, **68**, and a stereoisomer of **73** with *cis*-hydrides and *cis*-phosphines.[250a,257a,260b,261,263] The solvated hydridoalkyl intermediate **74** has also been characterized at low T in a homogeneous hydrogenation of an olefin catalyzed by the $[Rh(diphos)]^+$ complex.[253] The rest of the intermediates in the catalytic cycle have been postulated but never detected during the reaction. Other species directly observed in olefin hydrogenation include $RhH_2Cl(PPh_3)_3$, $Rh_2Cl_2(PPh_3)_4$, $Rh_2H_2Cl_2(PPh_3)_4$, and $Rh_2H_2Cl(PPh_3)_3$,[250a,254,257a,258,260b,261,263] although it seems that none of these species play a relevant role in the catalytic cycle. Finally, no evidence has been found for the participation of dihydrogen−rhodium complexes.[264]

The different mechanisms proposed for this catalysis incorporate all the main reaction types encountered in catalysis. Thus, not surprisingly, from the early 1980s this homogeneous catalysis attracted the attention of theoreticians, and in fact, it was the first full catalytic cycle studied using ab initio methods locating all TSs and intermediates involved in the elementary steps of the mechanism.[259]

Earlier theoretical works by Dedieu et al.[265,266] on olefin hydrogenation catalyzed by the model rhodium complex $RhCl(PH_3)_3$ were carried out performing partial optimizations at the SCF ab initio level. For each intermediate in the Halpern mechanism, Dedieu and co-workers calculated the relative stabilities of the most probable stereoisomers. The authors compared two possible mechanisms for the initial steps of the reaction, a dissociative mechanism corresponding to the Halpern mechanism shown in Scheme 22 and an associative one in which oxidative addition takes place before phosphine dissociation. From the collected thermodynamic data, the authors were unable to decide which pathway is the most favorable one. It is worth mentioning that more recent experimental studies have shown that the oxidative addition of H_2 to $RhCl(PPh_3)_2$ takes place ca. 10^4 times faster than to $RhCl(PPh_3)_3$[257a,263] and that excess PPh_3 inhibits the catalysis,[250b,261] thus indicating that the associative mechanism is not operative. A more careful analysis of the olefin insertion step was carried out by Dedieu et al. to conclude that this process is not a H migration but rather an olefin insertion into the Rh−H bond, followed by rearrangement of the nonreacting H. The insertion process is calculated to be exothermic with a moderate activation barrier of 59 kJ mol^{-1}, not far from the experimental value of 54 kJ mol^{-1} found for the insertion in the *cis*-$HRh(C_2H_4)(P\text{-}i\text{-}Pr_3)_2$ complex.[267]

To date the most comprehensive study of the homogeneous catalytic hydrogenation of olefins by the Wilkinson catalyst has been performed by Morokuma and co-workers.[259,268] The results of their calculations at the HF and MP2//HF levels using ECPs for Rh have been reviewed in several publications.[22,23,28,87] The most important findings in regard to the Halpern mechanism (Scheme 22, L = PH_3 and R = H) were the following: (i) oxidative addition of H_2 to $RhCl(PH_3)_2$ is exothermic by 110 kJ mol^{-1}, and it is almost barrierless, (ii) ethylene coordination to form the octahedral **69** complex is also an easy and exothermic process, (iii) the insertion of ethylene into the Rh−H bond is endothermic and has a large activation barrier of about 77 kJ mol^{-1} despite the additional stabilization of **70** due to the agostic interaction,[269] (iv) the isomerization from **70** to **71** by sequential migration of hydride and chlorine is exothermic and exhibits an energy barrier of ca. 17 kJ mol^{-1}, and (v) reductive elimination of ethane is almost thermoneutral and has a moderate energy barrier of 64 kJ mol^{-1}. The authors conclude that the combination of the olefin insertion and the isomerization of the *trans*-ethyl hydride complex to the cis complex is the rate-determining step, in agreement with experimental results.[254,257c]

Comparison of the energy profile for the Halpern mechanism catalyzed by $RhCl(PH_3)_2$ with that obtained for the $HRh(PH_3)_2$ catalyst revealed that substitution of chlorine by hydride makes the olefin insertion process easier.[259b] The reduction in the energy barrier was attributed to the larger trans effect of H as compared to Cl. The Rh−H bond trans to Cl in $H_2RhCl(PH_3)_2(C_2H_4)$ is stronger by ca. 84 kJ mol^{-1} than that in $H_2RhH(PH_3)_2(C_2H_4)$ and, therefore, requires a large energy to break. Not only is the insertion reaction easier for the $HRh(PH_3)_2$ catalyst, but also the reverse β-hydride elimination is facilitated, resulting in unwanted olefin isomerization. In this respect, Morokuma and co-workers concluded that the larger barrier of the β-hydride elimination as compared to the barrier of reductive elimination for the $RhCl(PH_3)_2$ catalyst prevents olefin isomerization and makes this complex a more convenient catalyst for olefin hydrogenation than $HRh(PH_3)_2$. Noteworthy, Siegbahn reached a different conclusion[270] by comparing the insertion reaction of ethylene to the rather simple RhH_2 and RhHCl models. He carried out MCPF//HF calculations with relativistic ECPs for Rh to find out that there is a significant lowering of about 44 kJ mol^{-1} of the ethylene insertion barrier for RhHCl as compared to RhH_2. This was mainly attributed to the cationic nature of Rh when Cl is present, which translates into a more important contribution of the $5s^0$ state that is less

repulsive for the incoming ethylene. The origin of the difference in the conclusion drawn by Morokuma and Siegbahn is not obvious.

In a subsequent work,[268] Koga and Morokuma (KM) discussed the Brown mechanism (Scheme 23, L = PH_3, R = H). The main difference between the Halpern and Brown mechanisms is that the latter requires isomerization of $H_2RhCl(PH_3)_2$ with *trans*-phosphines to $H_2RhCl(PH_3)_2$ with *cis*-phosphines. KM demonstrated that this step has a large activation barrier of 113 kJ mol^{-1}. In sharp contrast to the Halpern mechanism, ethylene coordination and insertion from **72** have low-energy requirements. Apart from isomerization, the final release of ethane has the highest energy barrier in the Brown mechanism (ca. 60 kJ mol^{-1}). The authors concluded that whenever olefin insertion is found to be rate-determining, the Halpern mechanism is more likely. However, KM do not rule out the possibility that olefin hydrogenation occurs through the Brown mechanism in the case where olefin is too bulky to coordinate to the **68** complex. In this particular case, isomerization of **68** to **72** will probably take place by ligand exchange (loss of PPh_3 in the Wilkinson catalyst is endothermic by only 52 kJ mol^{-1}).[271] This study shows that the kinetics expected for the Brown mechanism is quite different from that of the Halpern mechanism: the rate-determining step in the former is reductive elimination and in the latter olefin insertion. Remarkably, the reductive elimination step in the olefin hydrogenation catalyzed by $Rh(diphos)^+$ was found to be the rate-determining step below −40 °C with an activation barrier of 71 kJ mol^{-1}.[253,254]

There are still many unresolved questions about the mechanism of olefin hydrogenation catalyzed by TMs that could be clarified by means of computational studies. For example, the mechanisms proposed for the catalysis by $HRh(PPh_3)_2$[262] and by $Rh[diphos]^+$ [253,255] have not been yet discussed from a theoretical point of view. Further, we do not know whether dinuclear species can efficiently act as a catalyst for the olefin hydrogenation or not,[258] nor do we know whether the Brown mechanism[252,260] is a real alternative in the case of bulky olefins. With respect to this latter point, preliminary calculations of van der Waals repulsions indicated that the trans complex is a viable intermediate only for small olefins,[260b] although more reliable theoretical studies are necessary to confirm this result. Moreover, the importance of correlation energy and the effect of the solvent on the calculations of TSs and intermediates have not been sufficiently explored. Obviously, the use of HF geometries may introduce important distortions into the calculated energy profile. In particular, the HF geometry for the π complex obtained in the olefin coordination step was shown to not be reliable.[270a] Another topic that has not been sufficiently addressed is the origin of stereoselectivity in asymmetric catalytic olefin hydrogenation.[272] To our knowledge only two works devoted to this question have been published.[273,274] In these studies, the authors employed computer-driven molecular graphics and van der Waals energy calculations for identifying the steric interactions of the enantioselective step. In this way, they were able to predict the prevailing enantiomer.

Table 8. Selected Geometrical Parameters of the C_{2v} Structure of the Closed-Shell $^1A_1$ *trans*-$RhCl(PH_3)_2$ Complex Calculated at Different Levels of Theory (Å and deg)

method	*R*(Rh−Cl)	*R*(Rh−P)	∠P−Rh−Cl
RHF[a]	2.436	2.441	85.3
MP2[b]	2.384	2.394	86.9
MP2[c]	2.392	2.393	
MP2[d]	2.381	2.394	86.9
BP86[e]	2.301	2.303	85.7

[a] Reference 230. [b] Reference 276. [c] Reference 277. [d] Reference 97. [e] Reference 275.

Despite the apparent need for more theoretical works on this process, few contributions to this topic have been published after the seminal papers by Dedieu[265,266] and Morokuma.[259,268] Among these studies one can include those aimed to elucidate the molecular and electronic structures of the active species *trans*-$RhCl(PH_3)_2$.[97,230,275−277] For this complex, the closed-shell $^1A_1$ and the $^3A_1$ states have similar energies. Thus, while MP4SDTQ//HF calculations[230] favor the triplet state by 28 kJ mol^{-1}, at the BP86 level[275] the closed-shell singlet is more stable than the triplet by 20 kJ mol^{-1}. Calculations at a higher level of theory are necessary to unequivocally determine the ground state for *trans*-$RhCl(PH_3)_2$. Nonetheless, it is expected that the closed-shell singlet state becomes the ground state as soon as $RhCl(PH_3)_2$ interacts with H_2 or with the olefin.[276] Such a crossover from the triplet surface to the singlet surface should be possible for such a complex through spin−orbit coupling.[278] On the other hand, the closed-shell $^1A_1$ state of the *cis*-$RhCl(PH_3)_2$ stereoisomer is found to be more stable than the closed-shell $^1A_1$ of *trans*-$RhCl(PH_3)_2$ by 69 kJ mol^{-1} at the BP86 level.[275] However, for bulkier phosphines such as PPh_3 the trans isomer might become more stable. In addition, from the point of view of olefin hydrogenation, the trans isomer is more relevant, at least in the hydrogenation of unhindered olefins. Table 8 contains the most relevant geometric parameters for *trans*-$RhCl(PH_3)_2$ computed at different levels of theory. As expected, inclusion of correlation energy reduces the metal−ligand bond lengths. The differences between HF and correlated methods are less remarkable than those found for $HCo(CO)_4$ (see Table 1) in line with the well-known fact that electron correlation effects are less important for the second- and third-row than for the first-row TM complexes.[41,45,60,69]

Benson and Cundari (BC)[279] studied ethane dehydrogenation catalyzed by $HIr(PH_3)_2$ at the MP2//HF level using ECPs for Ir and P. The energy profile for the reverse reaction, which is the ethylene hydrogenation catalyzed by $HIr(PH_3)_2$, is depicted in Figure 15. As one can see in this figure, some TSs located by means of the HF method are more stable at the MP2//HF level than either reactants or products. This notwithstanding, the conclusions reached by BC are similar to those obtained by Morokuma et al.[259] for the ethylene hydrogenation by the $RhCl(PH_3)_2$ complex. Thus, oxidative addition and olefin coordination are exothermic and almost barrierless processes,

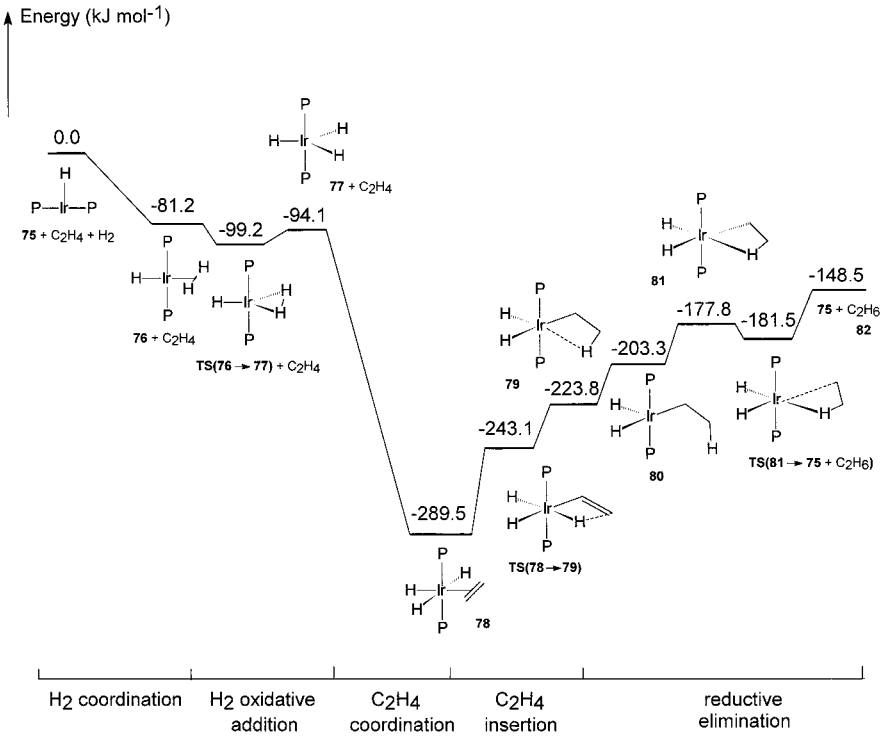

Figure 15. MP2//HF energy profile (kJ mol^{-1}) for the catalytic cycle of the hydrogenation of ethylene catalyzed by $HIr(PH_3)_2$. Adapted from ref 279.

while ethylene insertion and reductive elimination are endothermic and have relatively high barriers. In particular, the endothermicity for the insertion of ethylene is 66 kJ mol^{-1}, while the reductive elimination has a endothermicity of 75 kJ mol^{-1}. Thus, reductive elimination is predicted to be the rate-determining step in this particular case.

Finally, a Monte Carlo method has been used recently to simulate the olefin hydrogenation catalysis on a platinum surface.[280] The authors showed that it is possible to discuss the effect of changing various model parameters such as the size of the catalyst matrix or the pressure of reactants on the kinetic properties of the catalysis. These simulations can be useful in the design of the most appropriate conditions for the catalysis.

B. Epoxidation and Dihydroxylation

1. Dihydroxylation

The reaction mechanism of olefin oxidation mediated by TM oxides yielding diols or epoxides has been the topic of several high-level theoretical studies in the recent past. In particular, the question of whether the addition of osmium tetroxide to olefins proceeds as a concerted [3+2] reaction as originally suggested by Criegee[281] or in a two-step process via initial [2+2] addition yielding a metallaoxetane as intermediate followed by ring expansion as suggested by Sharpless[282] (Scheme 24) was hotly debated. It was a triumph of theory that this question could unequivocally be answered with the help of quantum chemical calculations.

The formation of metallaoxetanes as intermediates in the osmylation reaction had been postulated because kinetic studies of the base-catalyzed reaction

Scheme 24. Schematic Representation of the Suggested Mechanisms for the Osmylation Reaction: Concerted [3+2] Mechanism and Two-Step Pathway via Initial [2+2] Addition of OsO_4 to Ethylene

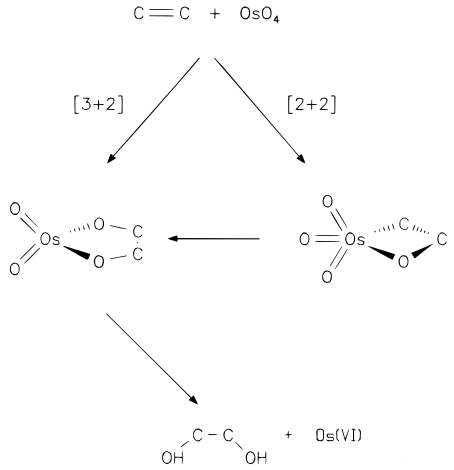

revealed a nonlinear correlation between the temperature and the enantioselectivity of the products which is observed when chiral bases and prochiral olefins are used.[283] There was no direct evidence for the two-step mechanism, and an alternative explanation of the kinetic data was given in favor of the [3+2] mechanism.[284] An orbital analysis of the [2+2] and [3+2] additions using EHT calculations could not discriminate between the two alternatives, but the [3+2] mechanism was suggested to be more likely.[285] Calculations at the QCISD(T) level of theory using HF-optimized geometries by Veldkamp and Frenking showed that the osmaoxetane intermediate **84** is indeed a minimum on the potential energy surface, albeit 127.6 kJ mol^{-1} higher in energy than the

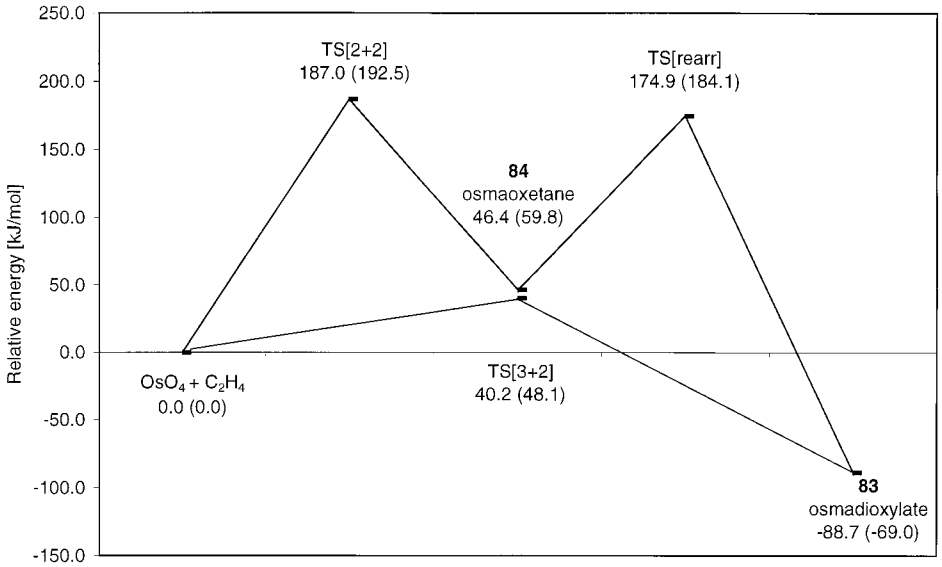

Figure 16. Calculated reaction profile of the addition of OsO_4 to ethylene at CCSD(T)//B3LYP using a quasi-relativistic ECP and a (441/2111/21) basis set for osmium in conjunction with a 6-31G(d) basis for the other atoms. (Values in parentheses include ZPE contributions.) Reprinted with permission from ref 288. Copyright 1996 Wiley-VCH.

osmadioxylate **83**.[286] The two-step mechanism via initial [2+2] addition could still be possible for kinetic reasons, provided that the activation energies were lower than the barrier for the [3+2] addition. A similar conclusion was reached in another theoretical study at the DFT level using RuO_4 instead of OsO_4 as the model compound.[287]

Four independent theoretical studies showed clearly that the barrier for [2+2] addition of OsO_4 to ethylene yielding the osmaoxetane **84** and the activation energy for ring expansion to the osmadioxylate **83** are substantially higher than the barrier for the [3+2] cycloaddition.[288−291] Figure 16 shows the calculated reaction profile at the CCSD(T) level of theory using DFT (B3LYP) optimized geometries.[288] The activation barriers for the [2+2] addition (187.0 kJ mol^{-1}) and for the ring expansion (174.9 kJ mol^{-1}) are much higher than the barrier for the [3+2] addition (40.2 kJ mol^{-1}). Other theoretical studies at different levels of theory gave very similar results.[289−291] The theoretically predicted barriers rule out the assumption that the osmylation reaction proceeds via a two-step mechanism. Calculations which include NH_3 as a model base showed that the relative energies change only slightly.[288,290] Additional support for the [3+2] mechanism came from theoretical kinetic isotope effects, which agreed very nicely with experimental data.[291]

Once the question concerning the operative mechanism had been answered, further details on the osmium-catalyzed dihydroxylation of olefins could just recently be provided by QM/MM calculations.[292−294] In particular, the origin of enantioselectivity in the dihydroxylation of styrene catalyzed by $OsO_4(NR_3)$ (NR_3 = bis(dihydroquinidine)-3,6-pyridazine) has been investigated. The selectivity is found to be essentially governed by stacking interactions between aromatic rings, with a leading role for the face-to-face interaction between the substrate and one of the quinoline rings of the catalyst.[292]

The next issue in the field was the question of whether there are TM oxides other than OsO_4 which add to C=C double bonds in a [2+2] reaction. Kinetic studies of the extrusion of alkenes from Cp*−rhenium(V)−dioxylates yielding olefins and metal oxides, which is the reverse reaction of the addition reaction, led Gable and Phan (GP) to conclude that "these data are inconsistent with a concerted mechanism for interaction of alkenes with Cp^*ReO_3 but consistent with a stepwise mechanism with a metallaoxetane intermediate".[259a] Kinetic evidence for a stepwise reaction came from several experimental studies, but a direct proof for the putative formation of the metallaoxetane could not be given.[259]

The reaction of $LReO_3$ compounds with C=C double bonds has been investigated in many experimental studies, particularly by Herrmann.[296] Depending on the nature of L, the reaction products may be metalladioxylates or the alkene C=C bond is cleaved, while in the presence of H_2O_2 epoxides may be formed. The selectivity of this reaction is found depending on the nature of L in $LReO_3$.[296−298] Theoretical studies of the latter reaction will be discussed below. The large variation of the reaction products of $LReO_3$ addition to olefins has been the topic of a theoretical study by Rappé et al.,[299] who calculated the geometries and energies of the rhenium−dioxylate and −oxetane compounds $LReO_3-C_2H_4$ for L = Cl, CH_3, OH, OCH_3, O^-, Cp, and Cp* at the B3LYP level of theory using relativistic ECPs for Re and fairly large valence basis sets. These authors found that for L = Cp and Cp* the dioxylate structure is lower in energy than the oxetane form. For L = Cl, CH_3, OH, OCH_3, and O^- the four-membered ring is more stable than the five-membered isomer. The focus of the study was the thermodynamics of the $LReO_3 + C_2H_4$ addition reaction. The authors mention that they also calculated the TS for the addition of $CpReO_3$ to ethylene. The theoretically predicted value is 113.8 kJ mol^{-1}, which is in good agreement with the experimental value of 117.2 kJ mol^{-1} for L = Cp*.[295a] The authors point out that their calculated barriers tend to support the [3+2] pathway.[299] Also the value for the deuterium kinetic isotope effect

Table 9. Calculated Relative Energies (B3LYP/III+) of the Stationary Points for the [3+2] and [2+2] Addition of Metal Oxides (MO) to Olefins (kJ mol^{-1})[a]

MO	olefin	MO + olefin	TS [3+2]	TS [2+2]	oxetane	TS [rearr]	dioxylate
OsO_4	ethylene	0.0	49.4	200.4	53.1	190.0	−79.9
ReO_4^-	ethylene	0.0	187.2	211.7	113.8	452.3	128.9
$ClReO_3$	ethylene	0.0	128.0	144.3	38.5	251.0	61.5
$CpReO_3$	ethylene	0.0	86.6	125.1	3.8	243.9	−36.4
Cp^*ReO_3	ethylene	0.0[b]	70.3[b]	168.6[b,c]			
$(H_3PN)ReO_3$	ethylene	0.0	150.2	186.2	38.5	271.1	82.0
$(H_3PN)ReO_3$	Ketene	0.0	154.4	88.3	−45.6	180.7	8.4
$(Me_3PN)ReO_3$	Ketene	0.0	152.3	90.4			
$(H_3PN)ReO_3$	diphenylketene	0.0[d]	150.6[d]	130.5[d]	1.7[d]		30.1[d]

[a] References 300 and 301. Basis set III+ has a small-core ECP at the metal with a totally uncontracted valence basis set augmented with one f-type polarization function in conjunction with 6-31+G(d) basis sets for the other atoms. [b] Using the smaller valence basis set II for Re. Basis set II has a small-core ECP for the metal with a DZ+P-quality valence basis set and 6-31G(d) basis sets for the other atoms. [c] TS [2+2] was approximated from TS [2+2] of $CpReO_3$. [d] The geometries are only partially optimized, using the frozen structure of the ketene addition and optimized values for the diphenyl ligands.

calculated from the TS for the [3+2] addition (1.09) was in accordance with the experimental data (1.06−1.07).

The thermodynamics and the kinetics of the addition of $LReO_3$ to ethylene have been the topic of a very recent theoretical study of Deubel and Frenking (DF)[300] which was carried out at the B3LYP level of theory using similarly large basis sets as in the work of Rappé et al.[299] Table 9 shows the calculated energies of the TSs for the [2+2] and [3+2] additions and for the ring expansion as well as the reaction energies for OsO_4 and $LReO_3$ with L = O^-, Cl, Cp, and Cp*. As previously found by Rappé et al.,[299] the metallaoxetane intermediate is more stable than the dioxylate when L = O^- and Cl, while the opposite holds true for L = Cp and Cp*. The calculated activation energies predict, however, that the [2+2] addition always has a higher barrier than the [3+2] reaction. In particular the activation energy for the [2+2] addition of Cp^*ReO_3 to ethylene (168.6 kJ mol^{-1}) is much higher than the barrier for [3+2] addition (70.3 kJ mol^{-1}). It seems unlikely that the extrusion of olefins from Cp*−rhenium(V)−dioxylates proceeds indeed in a two-step mechanism via [2+2] cycloreversion as suggested by Gable et al.[295]

The first report about a [2+2] cycloaddition of a TM oxide across a C=C double bond was recently given by Schlecht, Deubel, Dehnicke, and Frenking (SDDF).[301] These authors reported theoretical and experimental evidence that $(R_3PN)ReO_3$ adds in a [2+2] fashion across the C=C bond of ketenes $R_2C{=}C{=}O$, yielding the four-membered metallalactone as the reaction product (Scheme 25). Previous

Scheme 25. Addition of $LReO_3$ to Ketenes for Different Substituents L[a]

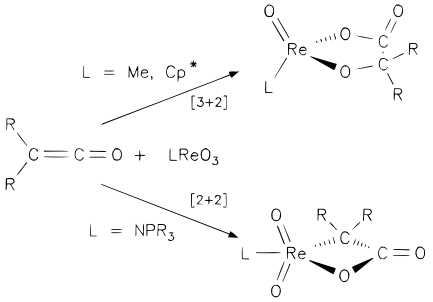

[a] Reprinted with permission from ref 301.

experimental work has shown that the addition of Cp^*ReO_3 to ketenes gives the [3+2] product.[302] The calculated energies of the stationary points for the [2+2] and [3+2] additions are also shown in Table 9. It was concluded that the ligand L of $LReO_3$ has a strong influence on the reaction course. SDDF also pointed out in their paper that the activation energies for [3+2] addition of $(H_3PN)ReO_3$ to ethylene (150.2 kJ mol^{-1}) and ketene (154.4 kJ mol^{-1}) are nearly the same, while the reaction energy for the ketene addition (8.4 kJ mol^{-1}) is much more favorable than for the ethylene addition (82.0 kJ mol^{-1}).

2. Epoxidation

The oxidation of olefins with TM oxides may in the presence of H_2O_2 or other peroxides yield epoxides (oxiranes) rather than diols. TM-catalyzed epoxidation reactions have become important industrial processes for the synthesis of a variety of epoxides.[303] It is generally assumed that the oxygen transfer to the olefin is a two-step process. The first step is the oxidation of the TM oxide to a peroxide, hydroperoxide, or alkylhydroperoxide. The second step is the oxygen transfer from the TM bonded peroxide group to the olefin. Three different mechanisms have been suggested for this process (Scheme 26). The olefin may directly attack either (a) the distal[304] or (b) the proximal[305] oxygen atom of the peroxo group, which gives the epoxide and the metal alkoxide as reaction products. In the case of metal peroxides the two mechanisms a and b are the same. In a third mechanism (c) the initial coordination of the olefin takes place at the metal, which is followed by insertion into the TM−oxygen bond, yielding a five-membered cyclic intermediate. This intermediate then decomposes into the epoxide and the metal alkoxide.[306] The formation of metallaoxetanes as possible intermediates in the epoxidation has also been discussed, but there is no evidence that these species are involved in the reaction mechanism.[306,307] The structures of metallaoxetanes $M{-}CH_2CH_2O$ with M = Cr to Ag and their relative energies with regard to M = O + C_2H_4 and M + ethylene oxide have been calculated by Bäckvall, Bökman, and Blomberg at the MCPF level of theory.[308]

There are very few theoretical studies of the reaction mechanism of TM-catalyzed epoxidation

Scheme 26. Three Different Mechanisms Which Were Suggested for the Epoxidation of Olefins with Metal−Peroxide Complexes

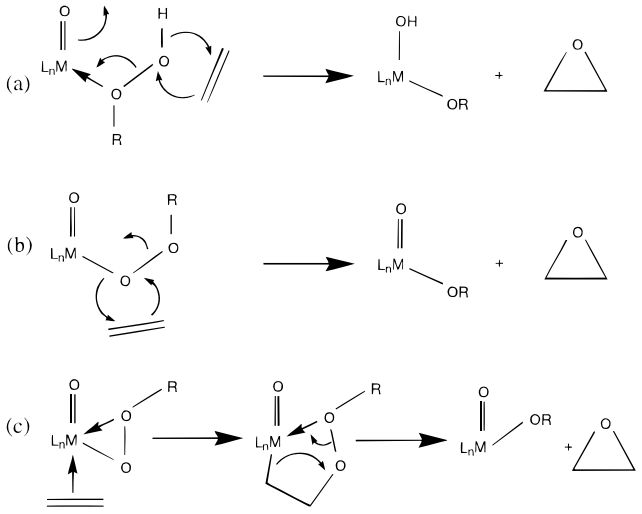

reactions. Bach et al. carried out a frontier orbital analysis of the bonding in peroxo−metal complexes which were used as a model catalyst in metal-catalyzed epoxidation reactions.[309] Jørgensen and Hoffmann (JH) published a frontier orbital investigation using EHT calculations of the reaction mechanism (c) using $Mo(O)(O_2)_2 + C_2H_4$ as the model system.[310] It was found that the formation of the five-membered cyclic intermediate involves a slipping motion of the π-coordinated ethylene ligand. The calculations of JH suggested that the best initial approach corresponds to the coordination of the olefin to the metal (Scheme 26c), but the TS obtained in a further step was close to the proposed mechanism where the olefin directly attacks the distant oxygen atom (Scheme 26b).[310] Two more theoretical studies at the EHT level came to a different conclusion. Filotov, Shalyaev, and Talsi (FST) investigated the mechanism of ethylene epoxidation with ligand-supported Mo(VI) peroxo complexes.[311] These workers found that the direct nucleophilic attack of the olefin on an electrophilic oxygen of the peroxo group should be preferred over the initial metal coordination. The same conclusion was drawn in an EHT study of the epoxidation reaction by Salles et al. using a dinuclear tungsten(VI) peroxo complex as the oxidizing agent.[312]

A very recent theoretical study by Rösch et al.[313] focused on the epoxidation reaction with CH_3ReO_3, which is known to be a highly efficient catalyst for the reaction.[296] The authors reported the structures and energies of the educts and TSs for addition of ethylene to the mono- and bisperoxo complexes $MeRe(O)_2(O_2)$ and $MeRe(O)(O_2)_2$ with and without an additional water molecule as the supporting ligand.[313] The calculations were carried out at the B3LYP level of theory using an ECP for Re and large TZ+2P valence basis sets. Figure 17 shows the calculated TSs and activation barriers.

The most important findings of this paper can be summarized as follows. There is no precursor π complex with ethylene as a rhenium-bonded ligand. The [2+2] TSs for insertion of ethylene into the metal−peroxo bond (**85A**, **88A**, **88B**) which lead to a

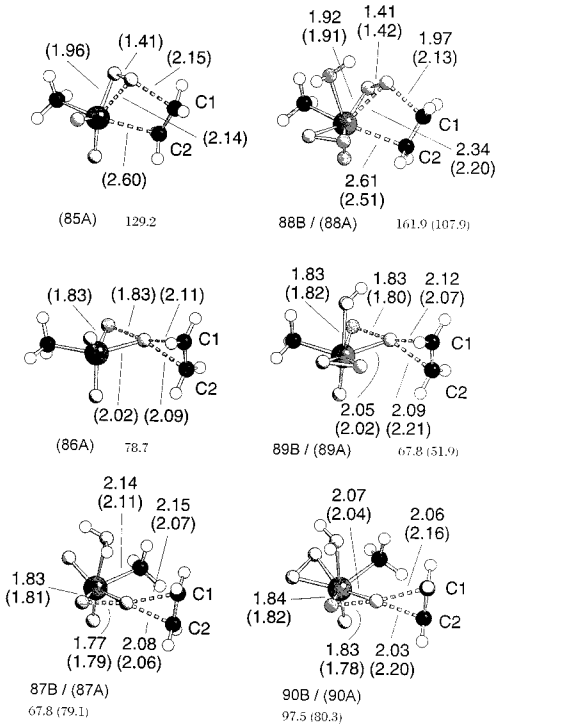

Figure 17. Calculated TSs of the addition of ethylene to the monoperoxo complexes $(CH_3)Re(O)_2(O_2)$ and $(CH_3)(H_2O)Re(O)_2(O_2)$ (left side) and to the diperoxo complexes $(CH_3)Re(O)(O_2)_2$ at the B3LYP level. Interatomic distances are given in angstroms. Activation energies (kJ mol^{-1}) are given relative to those of the respective educts. The values in parentheses refer to the water-free complexes. Reprinted with permission from ref 313. Copyright 1998 Wiley-VCH.

five-membered intermediate are much higher in energy than the [2+1] TSs for direct attack of a peroxo oxygen atom by ethylene. Thus, reaction mechanism c (Scheme 26) can be ruled out. The oxygen atoms of the peroxo groups in $MeRe(O)_2(O_2)$ and $MeRe(O)(O_2)_2$ are not equivalent because of the methyl group. Rösch et al. located [2+1] TSs where ethylene attacks either the proximal oxygen atom (spiro forms **86A**, **89A**, and **89B**) or the distal oxygen atom (backspiro forms **87A**, **87B**, **90A**, and **90B**).[313] The TSs **85B** and **86B** were not found because the water molecule dissociates during the optimization. The calculations show (Figure 17) that **89A** has the lowest activation barrier. However, the additional water ligand stabilizes the bisperoxo complex (not shown in Figure 17) by 59.4 kJ mol^{-1}, which makes the reaction course of the water-free compounds **A** energetically less favorable than the process involving the complexes **B** which are stabilized by one water ligand. The TSs **89B** and **87B** have similar activation energies. Since the monohydrated bisperoxo complex (not shown in Figure 17) is only 10.9 kJ mol^{-1} lower in energy than the monohydrated monoperoxo complex (not shown in Figure 17), it is concluded that the actual reaction pathway may be a competition between spiro attack via **89B** and backspiro attack via **87B**. The authors also report calculations of an alternative mechanism where ethylene attacks a hydroperoxo group of the rhenium complex $MeRe(O)(O_2)(OOH)(OH)$, which may be formed via formal proton transfer from $MeRe(O)(O_2)_2(H_2O)$. The calculated energies of the hydroperoxo

complex and the related TSs are clearly higher than those which are found for the other structures.[313]

Finally, a preliminary contribution about the mechanism of the epoxidation reaction was recently reported by Fantucci et al.[314] These authors calculated at the MP2 level of theory the reaction profile of the epoxidation of ethylene with hydroperoxides YOOH where Y is either an organic group or a TM fragment $(PH_3)_2PtCl$ or $(PH_3)_2Pt(CF_3)$. The authors suggest that the reaction may possibly proceed via an oxywater-like species, YHOO. The calculated activation barrier for rearrangement YOOH → YHOO was found to be significantly lower when Y is a TM fragment. However, the basis sets used in this study are rather small (4-31G), and the activation barrier for the novel reaction path which involves oxywater-like species is still rather high (>150 kJ mol^{-1}).[314]

An interesting TM−oxo compound which in reactions with olefins, even in the absence of peroxides, yields epoxides rather than diols is chromyl chloride, CrO_2Cl_2. The unique behavior of CrO_2Cl_2 is in contrast with the general tendency of other TM−oxo compounds[315] to yield diols whenever peroxides are not present. Diols seem not to be a product in the reaction of chromyl chloride and olefins;[316] instead, an often complex mixture is produced, with epoxide and *cis*-chlorohydrin as the main products, and, sometimes, vicinal dichloride.[282a] The mechanism by which these products are formed has been the subject of extensive studies since as early as 1893;[317] however, it was not revealed until 1998.[316,318]

In the past, complex mechanisms were put forward for the oxidation of olefins with CrO_2Cl_2 that attempted to explain the great variety of products obtained on the basis of widely differing intermediates such as chromaoxetanes, chromium alkoxides, and epoxide complexes.[282a,317] None of these intermediates have ever been proven. Thus, to explain the formation of the above-mentioned products, Sharpless et al.[282a] originally proposed a mechanism involving organometallic intermediates with Cr−C σ bonds. In particular, the key feature in the formation of epoxide was claimed to be the involvement of a chromaoxetane, i.e., a four-membered cyclic compound formed via a [2+2] interaction between the olefin and an oxo group on the chromium atom.[282a] This mechanism was very much contrary to the previously suggested mechanisms for this reaction, in which a direct interaction between the alkene and the oxo groups of CrO_2Cl_2 had been postulated.[317]

Although the new idea was suggested as an alternative path based only on the observed products of the reaction (no evidence for a chromaoxetane intermediate was established), it was quickly adapted within a few years in the discussion of many types of oxygen-transfer reactions involving high-valent oxochromium compounds[319] and other oxo−transition metal species.[320] The advantage of the novel proposal[282a] was that experimental observations concerning cis addition could now be more easily accommodated. Sharpless et al.,[282a] however, introduced their hypothesis with reserve because some mechanisms involving direct interaction with the ligands were able to account for experimental facts as well. Particularly, neither a direct addition of the olefin to one oxygen atom nor a [3+2] addition of the olefin to two heteroatom ligands could be excluded at that time as operative routes for the mechanism of epoxidation. Some years later, Samsel et al.[321] argued for a direct interaction between the alkene and the oxygen in OCr(V)−salen complexes in the epoxidation of alkenes, rather than a chromaoxetane. Some interesting results that cast doubt on the metallaoxetane reaction path were also reported by Barret et al.,[322] and later by Groves et al.[323] To date experimental input has not been sufficient to rule out either of the mechanistic channels.

To obtain further insight into the sequence of this reaction, some theoretical contributions started to appear. The most notable earlier computational study is that of Rappé et al.[324,325] where a thermodynamic analysis by means of the generalized valence bond method was performed, with attention being devoted to the energies of the intermediates in the oxidation of ethylene with CrO_2Cl_2 and MoO_2Cl_2. Unfortunately, due to limitations in methodology and computational facilities at that time, these authors were not able to fully optimize the geometrical structures of the different species involved. Their results favored a [2+2] cycloaddition path involving a four-centered intermediate, and confirmed the (as seen later, false) proposal that the metallaoxetane is a likely common precursor for all of the observed oxygen-containing products.[324]

Further theoretical support for a chromaoxetane was provided[326] later by an ab initio study of the addition of ethylene to $Cr{=}O^{n+}$ ($n = 1-3$). Several gas-phase investigations have also supported the chromaoxetane as an intermediate in the reaction of oxochromium species with alkenes.[327] In fact, the metallaoxetane intermediate derived from a [2+2] cycloaddition had been proposed in many other studies of oxygen-transfer reactions from oxomanganese and oxoiron porphyrins to alkenes,[320] but often without detailed mechanistic investigations or without any direct experimental evidence to support it.[307] A few isolated metallaoxetanes are known for Rh,[328] Ir,[329] Pd,[330] and Pt.[331] However, none of these species were synthesized by direct addition of olefin to a M=O bond. Also to date no chromaoxetane has been isolated.

At least three different reaction modes have been used to explain the formation of epoxide (Scheme 27): (1) a direct addition of ethylene to one oxygen atom, (2) a [2+2] addition of ethylene to one Cr=O linkage, and (3) a [3+2] addition to two Cr=O bonds. However, what appears to have been forgotten, at least in some of the proposed mechanisms, is that the reaction $CrO_2Cl_2 + C_2H_4 \rightarrow CrOCl_2 + C_2H_4O$ is endothermic with an experimental heat of reaction[332] given by 103.7 kJ mol^{-1}. Thus, the intermediates formed in the three mechanisms will not spontaneously decompose to epoxide. In fact, experimentally epoxide is only isolated after the original reaction mixture in an organic solvent (such as CH_2Cl_2) is extracted into aqueous solution. Thus, it is likely that epoxide is formed from the reaction of water with one or more of the precursors in Scheme 27. Regarding

Scheme 27. Different Mechanisms for the CrO_2Cl_2-Mediated Formation of Epoxide[a]

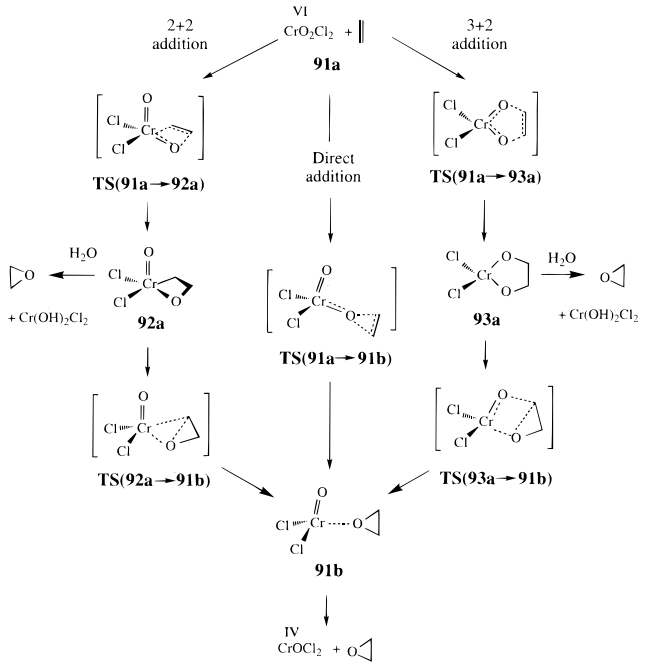

[a] Reprinted with permission from ref 318a. Copyright 1999 National Research Council of Canada.

the formation of the chlorine-containing products (Scheme 28), a [2+2] and/or a [3+2] cycloaddition pathway can account in principle for the mechanisms

Scheme 28. Different Mechanisms for the Formation of Chlorohydrin (Left) and Dichloride (Right)[a]

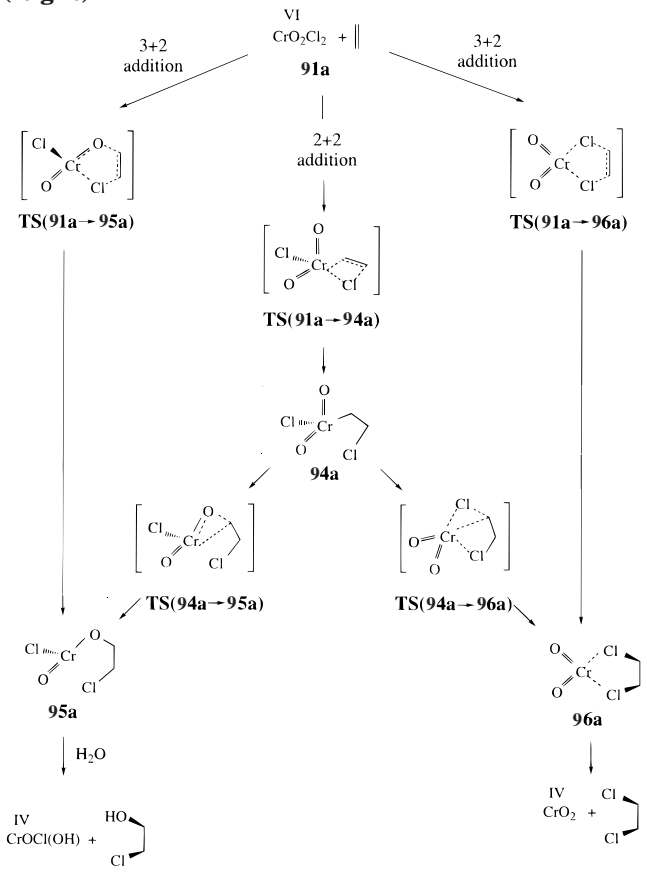

[a] Reprinted with permission from ref 318a. Copyright 1999 National Research Council of Canada.

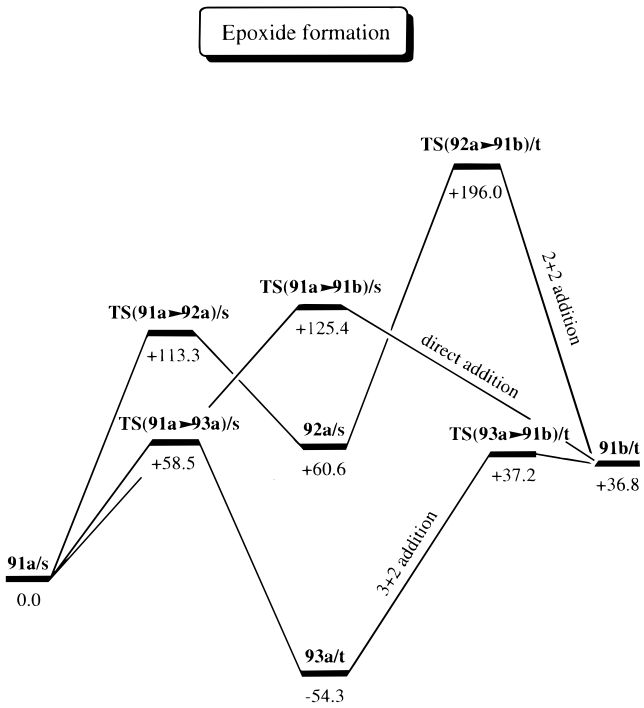

Figure 18. Reaction profile of the three suggested mechanisms for the formation of epoxide precursor from the addition of CrO_2Cl_2 to ethylene. The notations "/s" and "/t" stand for singlet and triplet, respectively. Energies (kJ mol^{-1}) are relative to that of **91a**. Reprinted with permission from ref 318a. Copyright 1999 National Research Council of Canada.

leading to a chlorohydrin precursor (left) and dichloride precursor (right). However, again for the chlorohydrin precursor (left), a hydrogen-containing agent such as water is needed to release $CH_2(OH)CH_2Cl$.

The pathways outlined in Schemes 27 and 28 have been recently explored in terms of reaction energies and activation barriers by Torrent et al.[318a,b] in a DFT study. More specifically, the triple objective of that study was (i) to examine the energetics and kinetics of the mechanism leading to the epoxide precursors of Scheme 27 when ethylene is oxidized by CrO_2Cl_2, (ii) to provide an interpretation for the formation of chlorohydrin precursor of Scheme 28 as one of the main products in the reaction of CrO_2Cl_2 with ethylene, and (iii) to rationalize why only in some cases dichloride is observed among the products. Also, the thermochemistry of the reaction between H_2O and the precursors in Schemes 27 and 28 was briefly discussed.[318a,b] This is the first time that mechanistic insight has been given into the formation of epoxide, chlorohydrin, and dichloride using optimization procedures, and TS search schemes.

As far as the first goal is concerned, the formation of the epoxide precursor ($Cl_2(O)Cr—OC_2H_4$) was found to take place via a [3+2] addition of ethylene to two Cr=O bonds followed by rearrangement of the five-membered diol to the epoxide product.[318a,b] The activation barriers for this two-step process were computed to be 58.5 kJ mol^{-1} for the **91a** → **93a** reaction step (for the same OsO_4-catalyzed process, the energy barrier had been reported to be 7.5 kJ mol^{-1}),[290] and 91.5 kJ mol^{-1} for the **93a** → **91b** reaction step (Figure 18). The former step involves a

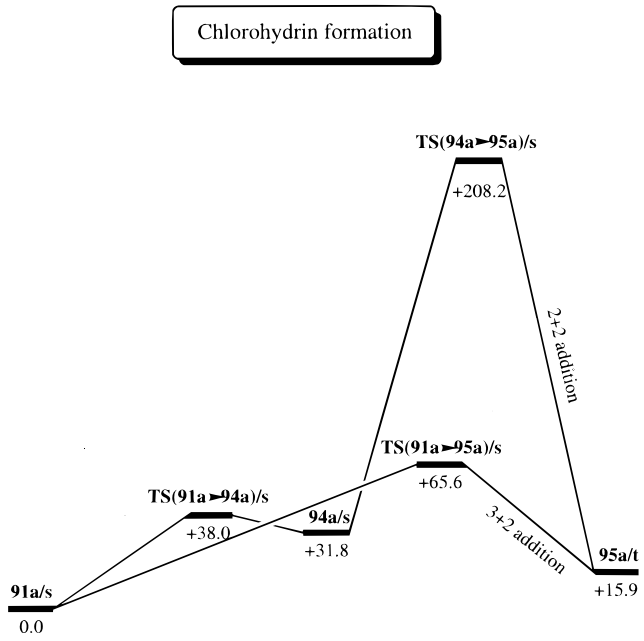

Figure 19. Reaction profile of the two possible mechanisms for the formation of the 1,2-chlorohydrin precursor from the addition of CrO_2Cl_2 to ethylene. The notations "/s" and "/t" stand for singlet and triplet, respectively. Energies (kJ mol^{-1}) are relative to that of **91a**. Reprinted with permission from ref 318a. Copyright 1999 National Research Council of Canada.

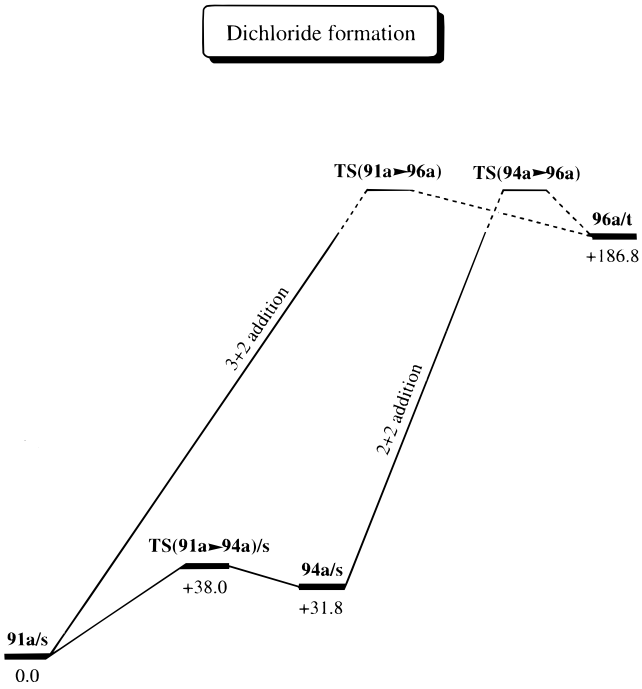

Figure 20. Reaction profile for the formation of the 1,2-dichloride precursor from the addition of CrO_2Cl_2 to ethylene. The notations "/s" and "/t" stand for singlet and triplet, respectively. Energies (kJ mol^{-1}) are relative to that of **91a**. Reprinted with permission from ref 318a. Copyright 1999 National Research Council of Canada.

crossover from the singlet surface in **91a** to the triplet surface in **93a**. Such a crossover had been analyzed in detail in a previous study[333] by means of IRC calculations (see below). The alternative mechanisms involving (1) a direct addition of oxygen to ethylene or (2) the [2+2] addition of the olefin to a Cr=O bond were found to have higher activation energies (above 125.0 kJ mol^{-1} in both cases).[318a,b] It was concluded that, contrary to the findings reported in the pioneering computational studies of Rappé et al.,[324,325] epoxides originate from an ester intermediate. Such an intermediate is clearly formed via a [3+2] cycloaddition.

In the second part of the study,[318a,b] the formation of the chlorohydrin precursor (Cl(O)Cr−OCH_2=CHCl) was found to take place via a [3+2] addition to one Cr−Cl bond and one Cr=O bond. Pathways involving initial [2+2] addition to a Cr−Cl or Cr=O bond had much higher activation barriers (Figure 19).[318a,b]

Finally, regarding the question of why epoxidation and oxychlorination are more favorable than dichlorination, the study showed[318a,b] that the generation of 1,2-dichloroethane is highly unfavorable with an endothermicity of +186.8 kJ mol^{-1} and an even higher activation barrier (Figure 20).

Comparison of the reactivity patterns for CrO_2Cl_2 and OsO_4 has been the subject of another DFT study,[333] where eqs 23−26 were investigated in detail. That study[333] showed that the unique product distribution from the reaction between CrO_2Cl_2 and C_2H_4 cannot be explained in terms of a preference for a [2+2] addition, as initially suggested by Sharpless,[282a] and later supported by Rappé.[324] On the contrary, DFT calculations reveal that the [3+2] addition of ethylene to metal−oxygen bonds in tetrahedral d^0 oxo complexes such as CrO_2Cl_2 and OsO_4 are favored over the [2+2] addition to a M=O linkage both kinetically and thermodynamically. Qualitative

$$CrO_2Cl_2 + C_2H_4 \rightarrow TS_1^{\ddagger}([2+2]) \rightarrow Cr(OCl_2)OC_2H_4 \quad (23)$$

$$CrO_2Cl_2 + C_2H_4 \rightarrow TS_2^{\ddagger}([3+2]) \rightarrow Cr(Cl_2)O_2C_2H_4 \quad (24)$$

$$OsO_4 + C_2H_4 \rightarrow TS_3^{\ddagger}([2+2]) \rightarrow Os(O_3)OC_2H_4 \quad (25)$$

$$OsO_4 + C_2H_4 \rightarrow TS_4^{\ddagger}([3+2]) \rightarrow Os(O_2)O_2C_2H_4 \quad (26)$$

considerations have also been given to rationalize why this addition is more prone to proceed by a [3+2] mechanism.[333] It was found that the [3+2] addition process has a relatively low barrier due to a good π-type overlap between the ethylene π orbital and the LUMO on the metal complex. The barrier is predicted to be especially low for d^0 oxo complexes with a covalent (rather than polar) bond, as in the case of OsO_4. On the other hand, the qualitative analysis of the [2+2] addition underlines that this process has a high barrier due to a poor overlap between the ethylene π orbital and the LUMO on the metal complex since the LUMO acts as a π^* orbital in the [2+2] approach with a nodal plane through the M=O bond.[333]

3. Final Remarks

The above-reviewed studies represent significant improvement in an area of the organometallic field

where computational chemistry has been shown to be particularly useful. More specifically, these examples show that theoretical calculations have been able to do what many decades of experimental studies had failed to achieve, namely, to provide conclusive answers to the question, Which is the operative mechanistic channel for a given TM-mediated oxidation reaction of olefins?

Despite the remarkable progress made, however, many aspects still remain unsolved or have only begun to be explored very recently. For instance, in the osmium-catalyzed asymmetric dihydroxylation of alkenes it is not clear yet which is the exact dependence of the base on the enantioselectivity, and which are the factors responsible for enhancing the reaction rates.[292] Hopefully, further QM/MM studies should be capable of offering more clues in the forthcoming years. Also, it is not clear yet why diols are absent among the products of the reaction between CrO_2Cl_2 and olefins whereas the corresponding reaction between OsO_4 and olefins generates exclusively diols with little epoxide as a product. To unravel this mystery, upcoming investigations cannot neglect the role of water as the reaction mixture preceding epoxide formation is extracted from an organic solvent into aqueous solution. Complexation energies might be crucial to turn endothermicities into exothermic reactions (or, at least, into more feasible processes). Moreover, as seen above, CrO_2Cl_2 is unique in that the diester (**93a** in Scheme 27) is a triplet whereas the [3+2] diester product from addition to OsO_4 (and MnO_4^-, and others) is a singlet.[318a,b,333] Also intermediates **91b** (Scheme 27) and **95a** (Scheme 28) are triplets.[318a,b] The question remains whether **93a**, **91b** or **95a** would be able to react with another olefin, inserting into the Cr−O bond and eliminating epoxide (or directly abstracting the olefin).

Needless to say, dihydroxylation and epoxidation by TM compounds promise to be a very active area during the coming years, and we can foresee that the assistance of computational chemistry to rationalize experimental facts will prove as useful as it has been so far.

C. Hydro-, Di-, and Thioboration

A renewed interest in the synthesis, characterization, and reactivity of metal−boryl compounds in recent years has provided the first structural data for these catalytically important species.[334,335] In particular, TM-catalyzed alkene and alkyne boration reactions are found to be attractive methods to produce alkyl- or alkenylboron derivatives with defined regio- and stereochemistry, which increased the potential applications of boron derivatives in synthetic organic chemistry.[336−338] In this work, attention will be given to theoretical studies regarding the mapping of reaction paths for the proposed catalytic cycles, with special emphasis on mechanistic aspects, for three groups of TM-catalyzed "boration" reactions: hydroboration, diboration, and thioboration.

The TM-catalyzed *hydroboration* of alkenes and alkynes with catecholborane or polyhedral boranes has been studied extensively by both experimental[336,337] and theoretical[25,26,276,277,339,340] methods; theoretical works will be reviewed in section III.C.1. More recently, interest has moved to metal-catalyzed *diboration* of alkynes, alkenes, 1,3-dienes, α,β-unsaturated ketones, and allenes[341] and, more particularly, to Pd(0)- and Pt(0)-catalyzed alkyne and alkene diboration reactions with pinacol ester derivatives.[342] In general, it has been shown that Pt(0) complexes catalyze cis addition of the B−B bond in pinacol ester derivatives, $(OCH_2)_2B-B(OCH_2)_2$, to alkynes but not to alkenes. Also, it has been found that Pd(0) complexes, the best catalysts for the silyl- and stannylmetalation,[343] do not catalyze alkyne and alkene diboration reactions. The origins of the observed differences in the catalytic activity of Pt(0) and Pd(0) complexes for alkyne diboration reactions remained unclear until the first high-level quantum chemical calculations were reported,[344,345] as will be discussed in section III.C.2. Finally, the contribution of theoretical chemistry to elucidate unsolved aspects concerning *thioboration*[346] will be analyzed in section III.C.3.

1. Hydroboration

During the past decade, the uncatalyzed hydroboration of alkenes was extensively studied.[347] In the early 1990s, the synthetic usefulness of the Rh(I)-catalyzed hydroboration reaction was demonstrated by Evans et al.[348] The TM-catalyzed hydroboration displays potential for altering chemo-, regio-, and diastereoselectivity relative to the uncatalyzed hydroboration, as well as for achieving enantioselectivity in the presence of a chiral TM catalyst.[337,349] That the diastereoselectivity of the reaction is opposite that observed for uncatalyzed hydroborations was found to be of particular interest.

1.1. Transition Metal−Boryl Bonding Energies. Before mechanistic studies concerning metal−boryl compounds in hydroboration reactions are properly discussed, it is worth mentioning first a recent theoretical paper by Rablen, Hartwig, and Nolan (RHN), where the first TM−boryl bond energies have been reported.[350] TM−ligand covalent bond energies are important in understanding catalysis;[351] however, it is difficult to measure borane BDEs experimentally, and only average BDEs are typically quoted for B−H and B−C bonds.[352] RHN have calculated B−H and B−C BDEs for a series of boranes including catecholborane, the reagent most commonly used in metal-catalyzed processes, and demonstrated the importance of using BDEs from a single B−H bond instead of average BDEs when considering catalysis with boranes. With an accurate single B−H BDE for catecholborane in hand, RHN have also measured the enthalpy for oxidative addition of a borane B−H bond to *trans*-$[Ir(CO)(PPh_3)_2Cl]$, obtaining the first estimate of a TM−boryl bond energy.[350] The value for the iridium−catecholboryl linkage was found to exceed those of either the corresponding alkyls or hydrides. Interestingly, the B−H oxidative addition reaction is found to cleave a bond that is stronger than that in methane. According to the authors, it is the strength of the iridium−boron bond that provides the necessary driving force for this reaction.[350]

1.2. Mechanistic Studies. Recently, Morokuma and co-workers,[25,276,339] and Dorigo and Schleyer[277] (DS) presented ab initio studies on the mechanism of the Rh(I)-catalyzed hydroboration of alkenes. These investigations were prompted by a recent surge of experiments in this field.[336d,e,kk] A number of TM complexes have been found to catalyze the olefin hydroboration with catecholborane, HBcat (cat = catecholato; 1,2-$O_2C_6H_4$), and TMDB (4,4,6-trimethyl-1,3,2-dioxaborinane). This process has shown a variety of promising features, including chemo-, regio-, and diastereoselectivity, and has attracted a substantial interest in connection to organic synthesis.[336d,e,kk] In general, it has been found that (i) the reductive elimination step is the slowest step in the overall transformation, (ii) Rh complexes are the most suitable catalysts and, among them, the Wilkinson catalyst appears to be the most efficient, (iii) boron hydrides bearing oxygen ligands are the most successful reagents, and (iv) the rate of catalyzed hydroboration reaction is very sensitive to the olefin substitution pattern, with terminal alkenes more reactive than highly substituted olefins.

The mechanism proposed in early papers[336d,e] for the Wilkinson catalyst involves oxidative addition of a B−H bond to the metal center, followed by olefin coordination to the metal center accompanied by dissociation of one of the two PPh_3 ligands, further followed by migratory insertion of olefin into the Rh−H bond and subsequent reductive elimination of the B−C bond. Several important questions not resolved in those earlier papers were (1) whether the reaction occurs with phosphine dissociation or not, (2) which of the Rh−B and Rh−H bonds is energetically more favorable for the olefin to be inserted into, and (3) how competitive the "σ bond metathesis" pathway is involving coordination of the HBcat and olefin to the complex followed by simultaneous cleavage of the Rh−C and B−H bonds with formation of the Rh−H and B−C bonds. Scheme 29 shows some of the proposed mechanisms of the Rh(I)-catalyzed olefin hydroboration.

Detailed experimental and theoretical studies have been (and still are) highly desirable on the mechanism of the TM-catalyzed olefin hydroboration reactions, as well as on the role of the TM center, substrates, and electronic and steric factors in the mechanism. Morokuma and co-workers[276] presented the first detailed ab initio MO study of possible reaction pathways illustrated in Scheme 29 for the reaction of C_2H_4 with boranes $HB(OH)_2$ and $HBO_2(CH_2)_3$ catalyzed by the model Wilkinson catalyst $RhCl(PH_3)_2$.

The calculated overall potential energy profile of the reaction with $HB(OH)_2$ is given in Figure 21.[276] The mechanism **I.1.B** has been found to be the most favorable pathway of the catalytic hydroboration of C_2H_4 of $HB(OH)_2$ with the model for the Wilkinson catalyst $RhCl(PH_3)_2$. Since the potential energy profile for the **I.1.B** mechanism for $HBO_2(CH_2)_3$ is nearly quantitatively the same as that for $HB(OH)_2$, the same conclusion should be applicable for reactions of real boranes experimentally studied. It involves oxidative addition of the B−H bond of borane to the

Scheme 29. Possible Mechanisms for Olefin Hydroboration Mediated by $RhCl(PPh_3)_2$[a]

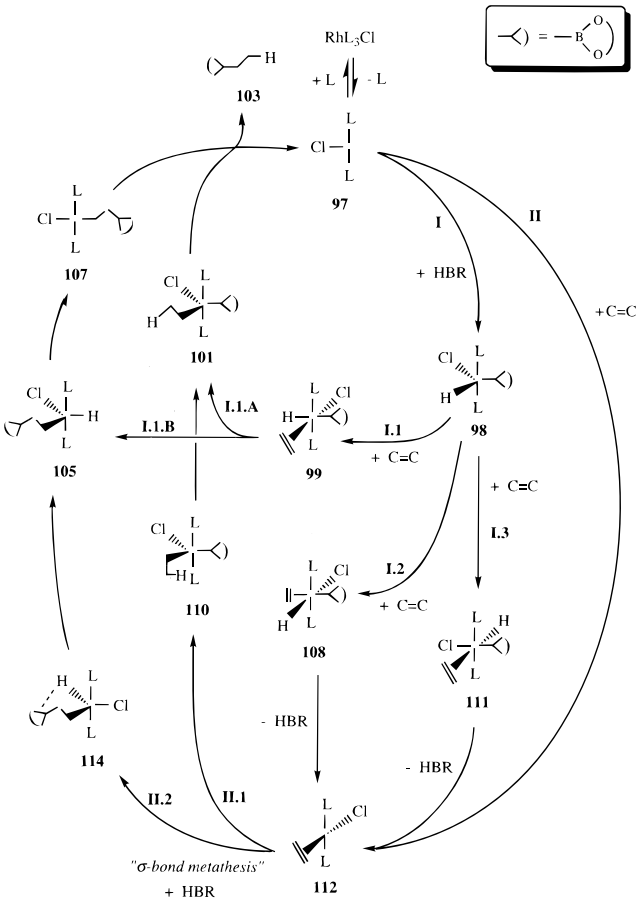

[a] Adapted from ref 276.

catalyst (**97** → **98**), followed by coordination of olefin to the complex between B and H ligands (→**99**). The reaction further proceeds by insertion of C=C into the Rh−B bond (→**105**), followed by the coupling of H and $C_2H_4BR_2$ (i.e., dehydrogenative reductive elimination of $C_2H_5BR_2$ to give the product complex, **107**), and eventual dissociation of $C_2H_5BR_2$. The activation energy for the last two steps of the mechanism, reductive elimination and dissociation, is calculated to be about 84 kJ mol^{-1}. Since the endothermicity for the dissociation in solution would be reduced by solvation of the regenerated catalyst, the coupling of H and $C_2H_4BR_2$ should be the rate-determining step. This conclusion agrees with the experimental observation that the reductive elimination step is the slowest in the overall transformation.[336e] The coordination of the olefin to complex **98** between Cl and H ligands or between Cl and B ligands gives a stable complex (**108** or **111**, respectively) and cannot proceed further without reductively eliminating borane first (→**112**); otherwise the reaction goes back to **98** (olefin dissociation).

The other competitive mechanism (**II**) begins with coordination of the olefin to the catalyst (**97** → **112**). The next step is "σ bond metathesis" (i.e., coordination of borane to complex **112**, accompanied by simultaneous cleavage of Rh−C and B−H bonds with formation of B−C and Rh−H bonds). After an internal rotation (**114** → **105**), which does not require high activation energy, dehydrogenative reductive elimi-

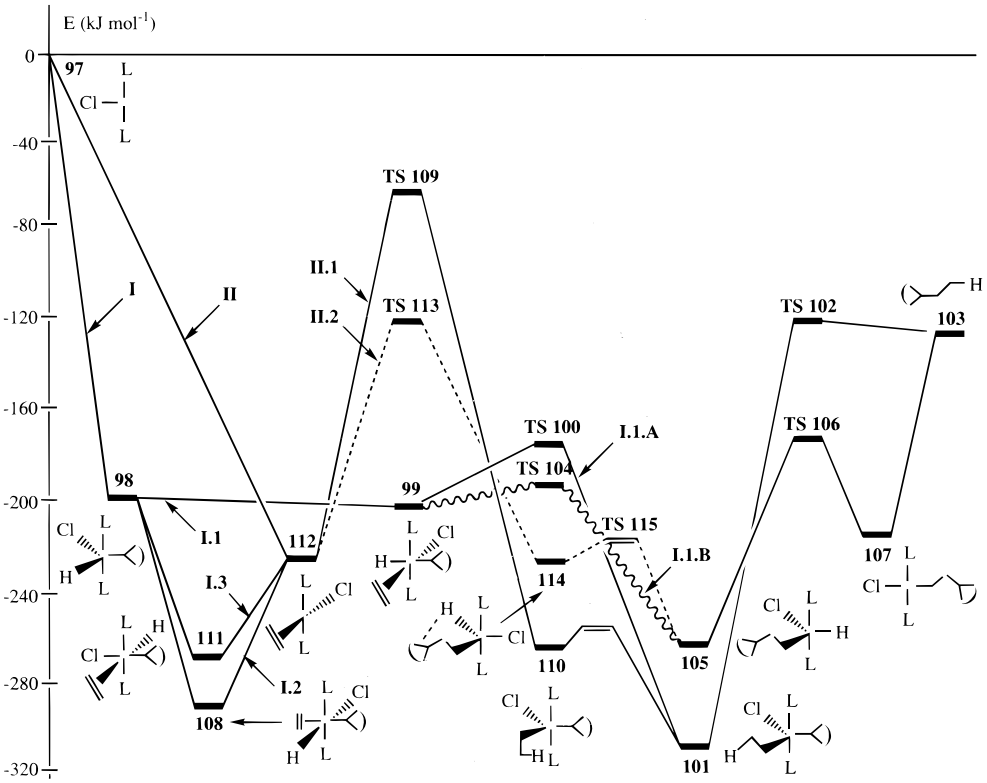

Figure 21. Overall profiles of the reaction $HB(OH)_2 + C_2H_4 + C_2H_5B(OH)_2$ catalyzed by $ClRh(PH_3)_2$. Labels such as **I.1.A** refer to different mechanisms, and labels such as **98** refer to TSs and intermediates. The double lines mean that the TSs were not calculated, but the barriers are expected to be low. Adapted from ref 276.

nation of $C_2H_5BR_2$ takes place. The final steps for the mechanism **II.2** coincide with those for the mechanism **I.1.B**. The rate-determining barrier for **II.2** corresponding to the metathesis process, 100.0 kJ mol^{-1}, is not much higher than the barrier for **I.1.B**, 93.7 kJ mol^{-1}. However, for the **II.2** pathway, the system has to overcome both of these barriers.

In complex **99**, the olefin has a choice of inserting into the Rh−B bond or the Rh−H bond. The latter process (**I.1.A**, **99** → **101** → **103**) requires higher barriers than the former (**I.1.B**) discussed above. Likewise, in the σ bond metathesis pathway starting at **112**, the insertion into the Rh−B bond (mechanism **II.2**) is preferred to that into the Rh−H bond (mechanism **II.1**).

DS[277] studied the mechanism for the $RhCl(PH_3)_2 + C_2H_4 + BH_3 \rightarrow RhCl(PH_3)_2 + C_2H_5BH_2$ catalytic reaction with dissociation of one of the PH_3 ligands upon coordination of olefin. It was shown that the insertion of the olefin into the Rh−H bond is more favorable than that into the Rh−B bond by 55.1, 44.5, 66.7, and 52.6 kJ mol^{-1}, at the MP2/lanl1dz, MP4(SDQ)/II//MP2/lanl1dz, MP2/lanl1dz(pol)//MP2/lanl1dz, and MP4(SDQ)/lanl1dz(pol) //MP2/lanl1dz levels of theory, respectively (basis set II denotes lanl1dz but with the 4s and 4p electrons of Rh included in the valence space instead of being described by the ECP). This result indicates that H migration is favored both kinetically and thermodynamically over BH_2 migration, in good agreement with experimental proposals.[336g]

Using ab initio MO methods, the reaction path for Sm(III)-catalyzed olefin hydroboration reaction by catecholborane has recently been investigated.[340] The stationary structures on the model reaction path considering ethylene as the alkene, Cp_2SmH as an active catalyst, and $HB(OH)_2$ as the model borane were obtained at the RHF and MP2 levels, and the MP4SDQ energy calculations were carried out at the MP2 structures. It was found[340] that, in the initial steps of the reaction, ethylene coordinates to the active catalyst to form a π complex. Then, ethylene insertion into the Sm−H bond takes place, leading to stable $Cp_2SmC_2H_5$ after passing through a barrier of 1 kJ mol^{-1}. In the following step the model borane adds to $Cp_2SmC_2H_5$ to form a borane complex which thereafter passes through a small barrier of 0.3 kJ mol^{-1} giving rise to a product complex. In the final step, the dissociation of the hydroborated product, $C_2H_5B(OH)_2$, takes place with a large endothermicity of 9.7 kJ mol^{-1}. The activation energies are so small that the final step of the dissociation is believed to be rate-determining, different from the reaction catalyzed by a Rh(I) complex. According to the authors,[340] the small electronegativity and oxophilicity of the Sm atom (compared to Rh) affect these features of the PES. The former makes the Sm−C bond ionic to result in the easy formation of the B−C bond assisted by the large exothermicity of this step due to the oxophilicity of the Sm atom. Also, it was pointed out that the oxophilicity makes the last step of the product dissociation very endothermic.[340]

2. Diboration

The uncatalyzed addition reactions of diborane H_2B-BH_2 to alkenes and alkynes are well documented[353] to have two drawbacks which hamper their

utility as synthetic reagents: (a) the difficulties in preparation and (b) the inherent instability of these compounds. Therefore, the catalytic versions of these reactions have begun to be explored with great interest.[342,354,355]

Sakaki and Kikuno (SK) have theoretically investigated the insertion of $M(PH_3)_2$ into BX_2-BX_2 (M = Pd, Pt; X = H, OH) with the ab initio MP4(SDQ), SD-CI, and CCD methods.[356] The MP4(SDQ) method provides an activation energy and an exothermicity similar to those of the SD-CI and CCD methods.[356] The reaction of BX_2-BX_2 exhibits interesting features: around the TS, not only the σ^* orbital of the B−B bond but also the unoccupied π and π^* orbitals can form the charge-transfer interaction with the occupied d_σ and d_π orbitals of Pt, which stabilizes the TS. According to SK, this is the reason, although the B−B bond is much stronger than the Si−Si bond, the insertion of $Pt(PH_3)_2$ into BX_2-BX_2 can still occur.[356] Such a reaction is computed to proceed with a moderate activation energy of ca. 63 kJ mol^{-1} and a considerable exothermicity of ca. 84 kJ mol^{-1} for X = OH and M = Pt, and a higher activation energy of 84 kJ mol^{-1} and a higher exothermicity of 138.1 kJ mol^{-1} for X = H and M = Pt. These results indicate that the B−B bond, as well as the Si−Si bond, undergoes insertion reaction of $Pt(PH_3)_2$ more easily than the C−C bond.[356] However, the insertion of $Pd(PH_3)_2$ into $B(OH)_2-B(OH)_2$ is difficult: The Pt−BH_2 and Pt−$B(OH)_2$ bond energies have been estimated to be ca. 251 kJ mol^{-1} (similar to the Pt−SiH_3 bond energy, and much greater than the Pt−CH_3 bond energy), whereas the Pd−$B(OH)_2$ bond energy (205 kJ mol^{-1}) is calculated to be much smaller than the Pt−$B(OH)_2$ bond energy.[356]

Morokuma and co-workers[344] have reported a study of Pt(0)-catalyzed alkyne (C_2H_2) and alkene (C_2H_4) diboration reactions with $(OH)_2B-B(OH)_2$ as a model of $(OCH_2)_2B-B(OCH_2)_2$ used in the experiments.[342] According to these authors, the Pt(0)-catalyzed alkyne/alkene diboration reaction may proceed, in principle, via two different paths (A and B in Scheme 30).[344] Path A involves the following steps: (1) coordination of the diborane, (2) oxidative addition of the B−B bond to the Pt(0) complex, (3) endothermic dissociation of one of the phosphine ligands, (4) coordination of alkyne/alkene to Pt, (5) insertion of the alkyne/alkene to the Pt−B bond, (6) isomerization of the resulting complex acompanied by recoordination of a phosphine ligand, and (7) reductive elimination of the alkenyl/alkane−diboron products. In path B, the initial step is coordination of alkyne/alkene to the Pt complex, followed by dissociation of one of the phosphine ligands and oxidative addition of the B−B bond to $Pt(PR_3)(C_2H_x)$ ($x = 2$ or 4) in either a planar (where atoms B, B, C, C, and P are on the same plane) or perpendicular (where BPtB and PPtC planes are perpendicular to each other) fashion, leading to a square-planar or tetrahedral intermediate, $(BR_2)_2Pt(PR_3)(C_2H_x)$ ($x = 2$ or 4), respectively. The tetrahedral intermediate lies 18.4 kJ mol^{-1} lower than the planar cis intermediate, which is also involved in path A and is separated from the latter by a small barrier. However, the barrier from the tetrahedral to the planar trans intermediate is high. Therefore, it has been concluded[344] that the tetrahedral intermediate $(BR_2)_2Pt(PR_3)(C_2H_x)$ rearranges to the square-planar cis intermediate and paths A and B merge. By comparing these two paths and calculating the binding energies of $Pt(PR_3)_2$ with bulkier diboranes B_2R_2 and substituted alkynes/alkenes used in the experiments, the authors have also concluded that path A is energetically more favorable than path B in the real Pt(0)-catalyzed alkyne/alkene diboration reaction.[344]

Scheme 30. Proposed Mechanism of Alkyne and Alkene Diboration by the $Pt(PR_3)_2$ Catalyst[a]

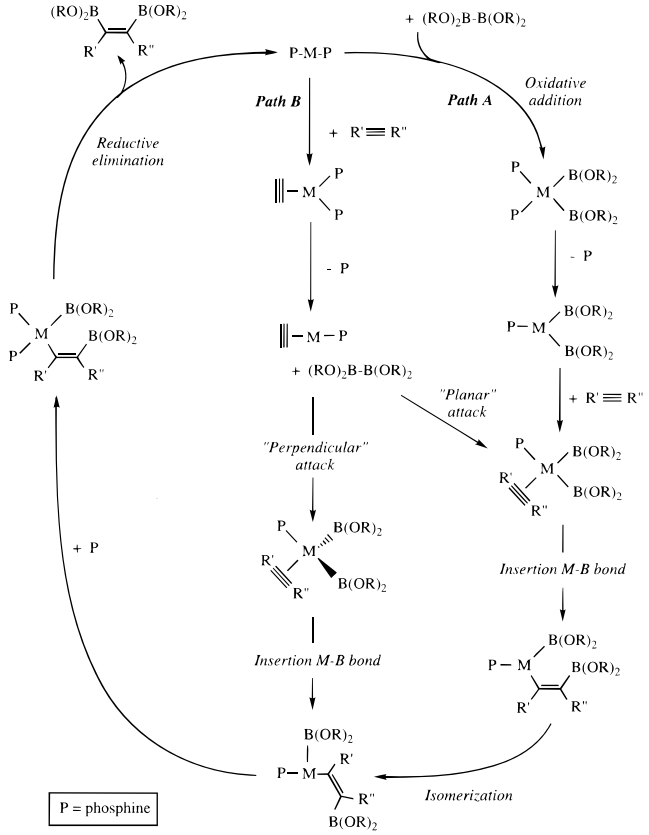

[a] Adapted from ref 344.

Morokuma and co-workers[344] also reported that the observed different catalytic behavior of $Pt(PH_3)_2$ on the two substrates, C_2H_2 (reactive) and C_2H_4 (nonreactive), is the result of the differences in the barrier heights for insertion of hydrocarbons into the Pt−B bond, which are calculated to be 37.7 and 95.8 kJ mol^{-1} for C_2H_2 and C_2H_4, respectively. This difference is essentially dictated by the thermochemistry of the insertion process, $Pt(PH_3)[BR_2]_2(C_2H_x) \rightarrow Pt(PH_3)(BR_2C_2H_xBR_2)$, which is found to be 117.6 kJ mol^{-1} exothermic for C_2H_2, but 17.1 kJ mol^{-1} endothermic for C_2H_4, and has been explained in terms of a smaller substrate deformation energy and a larger B−C "σ bond" energy in $Pt(PH_3)(BR_2C_2H_xBR_2)$ for $x = 2$ (C_2H_2) than for $x = 4$ (C_2H_4).[344]

To understand why $Pt(PR_3)_2$ complexes catalyze the alkyne diboration reaction, but their Pd(0) analogues do not, Morokuma and co-workers[345] have performed a theoretical study where the mechanisms of the Pd(0)- and Pt(0)-catalyzed alkyne diboration reactions have been analyzed and compared. In particu-

lar, they investigated the model reaction

$$M(PH_3)_2 + C_2H_2 + R_2B{-}BR_2 \rightarrow M(PH_3)_2 + (HR_2B)C{=}C(HBR_2)\ (M = Pd, Pt) \quad (27)$$

According to their study,[345] the Pd(0)-catalyzed reaction should proceed via the same mechanism as in the Pt(0)-catalyzed reaction (path A in Scheme 30). However, the reason the Pd(0) complex (unlike the Pt(0) complex) cannot catalyze alkyne diboration reaction is the difference in the oxidative addition processes of the B−B bond to $M(PH_3)_2$.[345] For M = Pt, this step takes place because it is clearly exothermic (30.1 kJ mol^{-1}) despite having a 58.6 kJ mol^{-1} activation barrier. For M = Pd, the process is 35.6 kJ mol^{-1} endothermic; although it has a lower barrier (36.0 kJ mol^{-1}), the addition product is not stable due to the very small reverse barrier of 0.4 kJ mol^{-1}! Therefore, the reaction is likely to go back to the reactant complex before the next step can take place.[345] For Pt, the next step can occur due to the thermodynamic driving force, i.e., the high reverse barrier. The origin of the inactivity of Pd(0) is reported to be the promotion energy from the d^{10} to the s^1d^9 configuration, which is not required for Pt(0) with the s^1d^9 ground state.[345]

3. Thioboration

Experimental studies involving heteroatom−boron compounds[357−359] are not as numerous as those of hydroboration (section III.C.1) and diboration (section III.C.2) reactions. Among them, those regarding B−X species with X = S[358,359] rapidly attracted the interest of theoretical chemists, so that it is in the area of thioboration (and not silaboration, X = Si, stannaboration, X = Sn, or others)[357] where the first theoretical studies[346] have appeared.

Recently, Suzuki and co-workers[359] have reported the Pd(0)-catalyzed addition of the 9-(alkylthio)-9-BBN (BBN = borabicyclo[3.3.1]nonane) derivatives to terminal alkynes to produce (alkylthio)boranes, which are known as versatile reagents to introduce thio groups into organic molecules.[335] It has been found[359] that (i) with the presence of $Pd(PPh_3)_4$, the addition of a B−S bond to terminal alkynes proceeds efficiently with high regio- and stereoselectivity, (ii) *Z* isomers of the addition products are dominant, (iii) among the various metal compounds tested in the experiment, only Pd(0) complexes exhibit high catalytic behavior, (iv) there is basically no difference in the reactivities of the various (alkylthio)- and (arylthio)boranes used in the experiment, except for the very sterically hindered *tert*-butylthio derivatives, and (v) the thioboration reaction is specific for terminal alkynes; thus, the double bonds in the conjugated alkynes remain intact during the reaction.

On the basis of these experimental facts, Suzuki and co-workers[359] proposed a mechanism for the present reaction, which involves an oxidative addition of the B−S bond to the Pd(0) complex, the insertion of an alkyne into the Pd−B or Pd−S bond, and the reductive elimination of the alkenylthioboron products. However, the first step of this proposed mechanism is not supported by their experiment: the oxidative addition product of B−S to the Pd(0) complex has not been observed, and attempts to detect an intermediate by ^{11}B and ^{31}P NMR were unsuccessful.[359]

To clarify the operative reaction mechanism of the Pd(0)-catalyzed alkyne thioboration process, Morokuma and co-workers have carried out a DFT study[346] on the model reaction

$$Pd(PH_3)_2 + C_2H_2 + (OR)_2B{-}SR' \rightarrow Pd(PH_3)_2 + (OR)_2B{-}CH{=}CH{-}SR' \quad (28)$$

In this theoretical study, no oxidative-addition product of the S−B bond to $Pd(PH_3)_2$ has been found,[346] which is in agreement with the experimental observation.[359] Therefore, the authors conclude that the oxidative addition mechanism proposed by Suzuki et al.[359] is not the proper one for the thioboration reaction of alkynes. Alternatively, they propose a new mechanism (Scheme 31)[346] involving (1) acetylene coordination to $Pd(PH_3)_2$, (2) dissociation of a phosphine ligand, (3) addition of the S−B bond to the metal center via a metathesis-like TS, (4) isomerization of the resultant complex, accompanied by recoordination of the phosphine ligand, and (5) reductive elimination of the alkenylthioboron product, R′S−CH=CH−$B(OR)_2$. The rate-determining stage of the entire reaction is found to be the addition of the S−B bond to the metal center via a metathesis-like TS, which takes place with a barrier of 77.8 kJ mol^{-1}.[346]

Scheme 31. Proposed Mechanism of the $M(PR_3)_2$-Catalyzed Alkyne Diboration (XR′ = $B(OR)_2$) and Thioboration (XR′ = SH) Reactions[a]

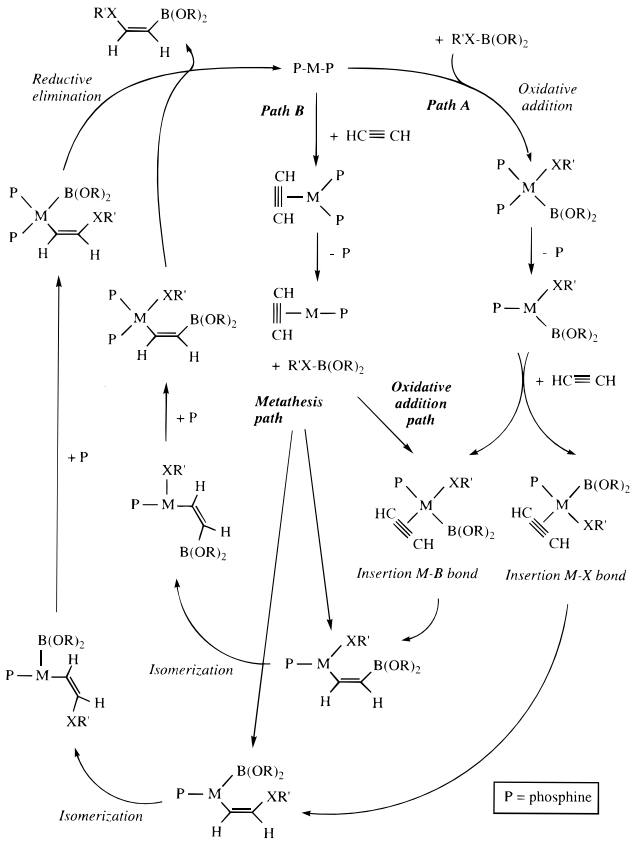

[a] Adapted from ref 346.

In this study,[346] Morokuma and co-workers also compare diboration and thioboration reactions, and conclude that the Pd(0) complexes do catalyze alkyne thioboration but not the diboration reaction because the rate-determining barrier at the metathesis-like TS is much lower for the former than for the latter. This fundamental difference is explained by the authors in terms of the hypervalency character of sulfur compared to boron. Due to the weaker C−S bond energy (compared to C−B), the reductive elimination step is highly exothermic for diboration but only slightly exothermic for thioboration. The reductive elimination step proceeds with a high barrier for thioboration but is barrierless for diboration.[346]

Finally, Morokuma and co-workers have also predicted whether Pt(0) complexes can serve as active catalysts for the thioboration of alkynes or not.[346] On the basis of their calculations, the Pt(0) complex is not expected to be a good catalyst for thioboration (while it is found to be an efficient catalyst for the alkyne diboration reaction).[346] The reason behind this is the high reductive elimination barrier of ca. 116.7 kJ mol^{-1}, which in part comes from the promotion energy required for the metal during the process.

4. Final Remarks

From an experimental point of view, activation of thermally stable bonds between main-group elements such as boron, silicon, and tin is a subject of growing interest.[360−365] Nowadays, in addition to the homometallic compounds with B−B,[360] Si−Si,[361] and Sn−Sn[362] bonds, heterometallic compounds containing B−Si,[357b−d,363] B−Sn,[357,364] and Si−Sn[365] bonds are also employed for the TM-catalyzed bismetalation of unsaturated hydrocarbons. It is expected, therefore, that in coming years theoretical studies will also extend to the mechanisms of silaboration, stannaboration, and silastannation of alkenes and alkynes.[3]

IV. Critical Assessment of the Present Methods for Calculating Transition-Metal Compounds

The review of the theoretical studies of TM-mediated reactions has shown that different methods have been used to gain information about the reaction profiles. The number of theoretical studies which focus on TM compounds has significantly increased in the past decade, and as a result of the efforts standard levels of theory evolved in the course of time. It is appropriate to make a critical assessment of the accuracy of the theoretical approaches which are presently employed for calculating TM compounds.

There are two different quantum chemical methods which have been proven to give geometries, bond energies, activation barriers, vibrational frequencies, and other chemically important properties of *electronically saturated* TM compounds in the *electronic ground state*, i.e., compounds which obey the 16- or 18-electron rule and have a sufficiently large HOMO−LUMO gap, with an accuray that is generally sufficient for synthetic chemistry. They are ab initio methods at various levels of theory and density functional theory (DFT) methods. The accuracy of both methods strongly depends on the chosen parameters of the calculations, which shall briefly be discussed.

Most ab initio methods use Hartree−Fock (HF) theory as the starting point of the theoretical procedure. It is important to realize that the HF approximation can only be used if the electronically excited states are clearly higher in energy than the ground state. This is not always the case for TM compounds, because the energy levels of the occupied and empty valence s and d orbitals are much closer to each other than the s and p valence orbitals of the main group elements. Most theoretical studies focused on diamagnetic (closed-shell) TM compounds for which the HF method is usually but not always a good starting point. This does not hold, however, for compounds of the first TM row which have a partly filled d shell. Such molecules require an MCSCF wave function instead of a HF wave function. MCSCF calculations are much more expensive than HF calculations and should only be used by experts, because the choice of the active space of MCSCF wave functions is not trivial.

Three parameters determine the level of theory of an ab initio calculation: (a) the size of the basis set; (b) the treatment of correlation energy; (c) the treatment of relativistic effects.

(a) The question about the size of the basis set concerns mainly the valence electrons and the outermost core electrons. The inner core electrons are frequently replaced by a pseudopotential or effective core potential (ECP). One important point concerns the size of the ECP, i.e., the number of electrons that are described by the core potential. There is general agreement now that the outermost core electrons of the transition metals should *not* be replaced by an ECP but should be retained and should be explicitely calculated. Small-core ECPs demand more computer time than large-core ECPs, but the latter are clearly less accurate than the former. A second important point concerns the size of the valence basis set. It has been shown that the basis set for the (n)s and (n − 1)d valence electrons and for the outermost (n − 1)p core electrons should have double-ζ quality.[366,367] However, there is evidence that basis sets which have functions for the lowest lying (n)p empty orbitals of the metals yield significantly improved geometries and energies.[366,368] This result is important, because the standard contraction scheme LANL2DZ of the ECPs by Hay and Wadt[369] in the Gaussian program series,[370] which is very popular in the computational chemistry community, does not have p functions for the empty (n)p orbitals of the first TM row. The LANL2DZ basis set for the second and third TM row elements has one additional p function than originally published (6 rather than 5),[369] which leads to improved results. The original valence p basis set of the Hay and Wadt ECPs must be more decontracted than in LANL2DZ to provide a function for the lowest lying empty p orbital.[366] Alternatively, a set of (n)p functions which was developed for TMs by Couty and Hall[368] may be added to the double-ζ valence basis set. The valence basis set may further be improved by adding f-type polar-

ization functions[371] and by decontracting the basis set, yielding triple-ζ quality for the s and d valence electrons. The latter augmentation may become too expensive for geometry optimizations, but it can become important for more accurate single-point energy calculations. The basis set is then still far away from a quality which gives very high accuracy,[372] but it is usually sufficient for problems in synthetic chemistry. As a standard, the quality of the valence basis sets with increasing accuray should be DZ+p → DZ+p+f → TZ+p+f.

(b) The treatment of correlation energy has mostly been carried out at the MP2 level, although it is well-known that Møller−Plesset perturbation theory can lead to significant errors for TM compounds. This is particularly true for metals of the first TM row which have a partly filled d shell.[367,373] MP2 should *not* be used for molecules containing the elements Sc to Zn unless they have a d^0 or d^{10} valence shell. The reason for the peculiar failure of MP2 for the first TM row but not for the second and third TM rows is due to the different ratio of the radii of the s and d valence orbitals.[367] MP2 performs better for the heavier TMs, but it should be used with caution and by experts who know the pitfalls of the method. An excellent method for the calculation of correlation energy is coupled-cluster theory[374] at the CCSD(T)[375] level, which may be used as a benchmark for cheaper methods and for DFT results. Unfortunately, CCSD-(T) calculations are very expensive and may be employed only for molecules which are usually not relevant for synthesis. In some cases it can be possible to achieve reliable results without calculating correlation energy at all. For example, the geometries of TM compounds in high oxidation states are predicted surprisingly well at the HF level.[367] However, results of energy calculations without treatment of correlation energy should be taken with caution, although the cancellation of errors may lead to fortuitously accurate numbers. To justify pure HF calculations of TM compounds requires an expert and much experience.

(c) The calculation of relativistic effects is necessary to achieve accurate results for compounds of the second and particularly the third TM rows, where relativistic corrections may become more important than correlation energy.[376] Relativistic effects are less important for the first TM row, except for Cu where the neglect of relativity may lead to significant errors.[376,377] The most important relativistic corrections are (i) the Darwin term, (ii) the mass−velocity term which leads to a contraction of the s and p and decontraction of the d and f functions, and (iii) the spin−orbit coupling term. The easiest and most common way of treating relativistic effects is the use of quasi-relativistic ECPs that are parametrized with respect to relativistic all-electron calculations of the atoms. Several authors developed ECPs for TMs which consider by various approximations the relativistic effects i−iii. Test calculations have shown that the use of quasi-relativistic ECPs yields remarkably accurate geometries and energies,[367,378] although the spin−orbit coupling term (iii) is treated only in a spin-averaged way ("scalar relativistic theory"). The accurate calculation of relativistic effects is achieved through approximate solutions of the Dirac equation, which are very complicated because of the four-component Hamiltonian. Full four-component calculations are too time-consuming to become practical for TM compounds that are important for synthetic purposes. Two-component approximations to the full Dirac equations are presently an actively pursued field of quantum chemistry. Several promising methods for all-electron calculations and for pseudopotentials containing two-component approximations have been developed in the last couple of years, but a standard level has not been established yet.[379] Quasi-relativistic ECPs are at present the most commonly used treatment for relativistic effects.[367,378]

Density functional theory has become increasingly popular in the past decade for calculating TM compounds, because the gradient-corrected (nonlocal) exchange and correlation functionals give results which have a comparable and frequently even higher accuracy than ab initio calculations. NL-DFT methods often outperform MP2 while using less computer time. There are also no difficulties for DFT with the calculation of compounds of the first TM row. It seems that already the number of DFT studies about reaction mechanisms of TM compounds is larger than the number of ab initio investigations in this field.

One inherent drawback of DFT methods is the fact that they cannot systematically be improved by going to higher levels of theory like ab initio methods. The most important parameter for a DFT calculation is the choice of the exchange and correlation functionals. The most common functionals which at present appear to give the best results for TM compounds are BP86[380] and B3LYP,[381] although other correlation functionals are also sometimes used. The popularity of these functionals comes from their implementation in widely used commercial software. However, it seems that they have been recently surpassed by other functionals (such as B97,[382] B97-1, and HCTH[383]), which unfortunately are not implemented yet in popular packages. On top of functionals depending on density gradients of first order (commonly referred to as GGAs), a new class of beyond-GGA functionals of second order has recently been reported.[384] These functionals (as well as B97[382]) are 10-parameter fits, and are more precise than "older" functionals such as B3P[381a] or the related B3LYP.[381] Again, their implementation is just in an early stage. These new functionals should be viewed as an exploration of what is the state-of-the-art of gradient-corrected DFT.[385] It may take some time before they are confidently used and spread in the field of TM compounds. Two further parameters which, like in ab initio methods, determine the quality of a DFT calculation are the size of the basis set and the treatment of relativistic effects. The same ECPs and basis sets which have been optimized for ab initio methods can be used for DFT calculations. As a standard, the valence basis sets should have at least DZ+P quality. If possible TZ+2P basis sets should be used in DFT calculations.

Relativistic effects can be considered in DFT calculations in the same way as in ab initio calculations

by using quasi-relativistic ECPs. Approximate treatments of relativistic corrections for all-electron basis sets have also been developed. The recently developed zero-order regular approximation (ZORA), which treats spin−orbit effects through a two-component Hamiltonian, appears to give quite accurate results, but further testing is necessary.[386]

One important parameter of DFT calculations which is often neglected is the grid size of the integral calculation. Since in DFT calculations the integrals are often calculated numerically and not analytically like in most ab initio methods, the number of points which is chosen for the integral calculations strongly determines the numerical values which are given at the end of the calculation. The grid size should be large enough to guarantee that the results do not significantly change when the number of calculated points increases. The programs generally use standard values for the grid size, but in critical cases it is advisable to check whether the grid is dense enough.

An important group of computational methods for calculating large TM complexes with bulky ligands consists of a combination of quantum chemical techniques with molecular mechanics (MM) methods. This is a very promising tool for theoretical studies of real systems which are employed in experimental work. The use of MM methods for the calculation of TM compounds has some drawbacks, however. One of the limitations of modern force fields which clearly affects TM compounds is the neglect of polarization.[387] Only an "average" polarization is included implicitly in the parametrization; atomic charges are often selected to give a dipole moment which is larger than the observed value for an isolated molecule (e.g., the effective dipole moment for H_2O in the solid state is 2.5 D, compared to 1.8 D in the gas phase). This notwithstanding, the most overwhelming problem in using MM for TM compounds is the lack of enough high-quality reference data. Geometrical data for metal compounds are much more scarce than for organic molecules, and vibrational frequencies are often difficult to assign to specific modes because of soft deformation potentials. Deriving parameters from electron structure calculations is troublesome since the presence of multiple ligands means that the number of atoms is quite large, and the metal atom itself contains many electrons. Furthermore, there are often many different low-lying electronic states due to partly occupied d orbitals, indicating that single reference methods are insufficient for even a qualitatively correct wave function. As a result, modern force fields suffer from the lack of good parameters for TM atoms. A word of caution applies here. Many modern force field programs are commercial. Having the program tell the user that his or her favorite organometallic molecule cannot be calculated owing to lack of parameters is against company/business policy. Making the user derive new parameters, and getting the program to accept them, may require more knowledge than the average user possesses, who is just interested in the answer. Many force fields thus have "generic" parameters. This is just a fancy word for the program making more or less educated guesses for the missing parameters. A good force field program should inform the user of the quality of the parameters used in the calculation. This is useful for evaluating the quality of the results. Unfortunately some programs use the necessary number of generic parameters to carry out the calculations *without* notifying the user. In extreme cases, one may perform calculations on TM molecules for which essentially no "good" parameters exist, and get totally useless results out! QM/MM methods can not be considered as standard levels of theory yet, and experts should be consulted before they are used for theoretical studies. The strengths and weaknesses of the QM/MM approach are described in more detail in the contribution by Morokuma in this issue.[388]

V. Concluding Remarks

We have shown in this review that theoretical studies have significantly improved our understanding of many TM-mediated reactions of current importance in industry and contemporary synthetic laboratories. By their very nature, these reactions involve highly reactive intermediates often not amenable to direct observation. Quantum chemical calculations can provide useful information concerning the electronic structure, the energetics, and the relevance of these elusive species. We have seen, for instance, how theoretical calculations have led to the conclusion that the dihydride complex $Fe(CO)_4H_2$ is a likely intermediate in the water−gas shift reaction, while the hydroxycarbene and osmaoxetane species must be rejected as possible intermediates in hydroxymethylation of aldehydes and cis dihydroxylation of alkenes, respectively.

Not only do quantum chemical studies unveil detailed structural information on postulated intermediates, but they also can provide insight otherwise unavailable into *reaction mechanisms*. Using the computed reaction energy and activation energy of each elementary step, it is possible to verify different proposed mechanisms for a certain reaction. For example, the Halpern and Brown mechanisms in alkene hydrogenation, the Dötz and the Casey mechanisms for the Dötz reaction, paths A and B (Scheme 30) in the Pt(0)-catalyzed diboration of unsaturated hydrocarbons, or the [2+2] and [3+2] cycloadditions in the cis dihydroxylation of alkenes have been compared and analyzed through theoretical studies. Remarkably, the prolonged controversy on the mechanism of the cis dihydroxylation of olefins by OsO_4 has been resolved in favor of the [3+2] mechanism with the recent publication of four coinciding theoretical works.[288−291] In addition, quantum mechanical calculations have allowed reaction mechanisms to be reformulated, adding or removing some postulated steps (like in the Halpern mechanism for the hydrogenation of ethylene or in the water−gas shift reaction), and new feasible routes to be proposed, as in the case of the chromahexatriene route in the Dötz reaction or the novel mechanism proposed by Morokuma and co-workers for the Pd(0)-catalyzed alkyne thioboration process.

It should be clear from this review that with the state-of-the-art quantum mechanical calculations the

experimental chemist can obtain mechanistic information that is extremely helpful. The present situation is not any more "a marriage of poor theory with good experiment" as stated by Hoffmann and Woodward in 1968.[389] The studies reviewed herein enlarge the list of examples, showing the respectable size to which theoretical chemistry has grown. There are, however, some aspects that should be improved in forthcoming studies. To date, most of the theoretical studies on homogeneous TM-mediated reactions have been performed without taking into account the effect of the solvent. In few cases, such as in the hydroformylation of ethylene catalyzed by $Rh(CO)(PH_3)_2$ or in the last step of the hydrogenation of CO_2, this effect has been incorporated explicitly by including a solvent molecule in the description of the catalyst. The obtained results indicate that the effect on the kinetics is significant. In addition, the discussion of the chemo-, regio-, and diastereoselectivity of some reactions requires the use of more realistic models of organometallic reactions that include all relevant electronic and steric effects of the ligands. In this sense, the new methodologies that combine the quantum mechanics and molecular mechanics methods (QM/MM) are very promising as has been demonstrated in a recent study that successfully predicts the correct enantioselectivity in the dihydroxylation of styrene catalyzed by OsO_4·$(DHQD)_2PYDZ$.[292−294] As these novel methodologies become more powerful and reliable, the next natural step will be to extend the current computational studies involving TMs to biocatalytic processes. Some chemical companies have already started making choices between chemistry and biology for their corporate growth strategy and R&D emphasis. They know that the best way for them to move forward will be by creating a multidisciplinary environment that combines ideas from combinatorial chemistry, biotechnology, automated synthesis, analytical techniques, informatics, and, last but not least, computational methods. In fact, some theoretical groups have already begun to move into this new hybridic area. Without doubt, this and the above-mentioned aspects are likely to be among the main priorities to focus on at the gate of the new millennium.

VI. Abbreviations

B3P	Becke's 1988 nonlocal exchange correction functional[380a]
B3LYP	Becke's three-parameter nonlocal exchange and Lee−Yang−Parr (1988) nonlocal correlation functional[381]
B97	Becke's 10-parameter nonlocal exchange correlation functional[382]
B97-1	Becke's 10-parameter nonlocal exchange correlation functional[382] reparametrized by Hamprecht−Cohen−Tozer−Handy[383]
BDE	bond dissociation energy
BP86	Perdew's (1986) nonlocal correlation correction and Becke's (1988) nonlocal exchange correction functional[380]
BPR	Berry pseudorotation
CASSCF	complete active space self-consistent field method[390]
CCD	coupled-cluster with double substitutions[374,375]
CCI	contracted configuration interaction method[391]
CCSD	coupled-cluster theory with single and double substitutions[374,375]
CCSD(T)	coupled-cluster theory with singles and doubles and noniterative estimation of triple excitations method[375]
CI	configuration interaction method[392]
CNDO/2	complete neglect of differential overlap/2 method[393]
DFT	density functional theory[394]
ECP	effective core potential[369,395]
EHT	extended-Hückel theory[396]
GGA	generalized gradient approximation[380,381,394]
HCTH	Hamprecht−Cohen−Tozer−Handy (1998) nonlocal exchange correlation functional[383]
HF	Hartree−Fock method[397]
HFS	Hartree−Fock−Slater method[398]
LDA	local density approximation[394,398,399]
MCPF	modified coupled pair functional method[400]
MCSCF	multiconfiguration self-consistent field method[390,401]
Method 1// Method 2	single-point energy calculation by method 1 at the optimized geometry obtained with method 2
MO	molecular orbital
MP2	second-order Møller−Plesset perturbation theory[402]
MP4(SDQ)	fourth-order Møller−Plesset perturbation theory with single, double, and quadruple excitations[402]
NLDA	nonlocal density approximation[380,381,394,403]
PES	potential energy surface
QCISD	singles and doubles quadratic configuration interaction[404]
QCISD(T)	singles and doubles quadratic configuration interaction with an estimation of triple excitations by a perturbation method[404]
QM/MM	quantum mechanics/molecular mechanics[388,405]
SCF	self-consistent field[392]
SD-CI	configuration interaction with single and double substitutions[392]
SPy	square-pyramidal
SPl	square-planar
TBP	trigonal-bipyramidal
TM	transition metal
TS	transition state
ZORA	zero-order regular approximation[386]
ZPE	zero-point energy

VII. Acknowledgment

This work has been funded by the Deutsche Forschungsgemeinschaft and Fonds der Chemischen Industrie, by the Spanish DGICYT Projects No. PB95-0762 and PB98-0457, and by a grant (CHE96-27775) from the National Science Foundation. M.T. and M.S. thank Professor Miquel Duran at the University of Girona for stimulating discussions and collaborations. M.T. also expresses her gratitude to Prof. K. Morokuma and Dr. D. G. Musaev for their support and constructive discussions and acknowledges a Postdoctoral fellowship from the Spanish Ministerio de Educación y Ciencia. Finally, we thank The Royal Society of Chemistry, the National Research Council of Canada, and Wiley-VCH as copyright owners of some pictures that appear in this review.

VIII. References

(1) Herrmann, W. A.; Cornils, B. *Angew. Chem.* **1997**, *109*, 1074; *Angew. Chem., Int. Ed. Engl.* **1997**, *36*, 1048.
(2) For very recent reviews see: (a) Musaev, D. G.; Morokuma, K. *Top. Catal.* **1999**, *7*, 107. (b) Margl, P.; Deng, L.; Ziegler, T. *Top. Catal.* **1999**, *7*, 187.
(3) Hada, M.; Tanaka, Y.; Ito, M.; Murakami, M.; Amii, H.; Ito, Y.; Nakatsuji, H. *J. Am. Chem. Soc.* **1994**, *116*, 8754.
(4) Endo, J.; Koga, N.; Morokuma, K. *Organometallics* **1993**, *12*, 2777.
(5) (a) Margl, P.; Ziegler, T.; Blöchl, P. E. *J. Am. Chem. Soc.* **1995**, *117*, 12625. (b) Margl, P.; Ziegler, T.; Blöchl, P. E. *J. Am. Chem. Soc.* **1996**, *118*, 5412. (c) Frankcombe, K. E.; Cavell, K. J.; Knott, R. B.; Yates, B. F. *Chem. Commun.* **1996**, 781. (d) Frankcombe, K. E.; Cavell, K. J.; Yates, B. F.; Knott, R. B *Organometallics* **1997**, *16*, 6, 3199.
(6) Rathke, J. W.; Klinger, R. J.; Krause, T. R. *Organometallics* **1991**, *10*, 1350.
(7) Süss-Fink, G.; Meister, G. *Adv. Organomet. Chem.* **1993**, *35*, 41.
(8) Roelen, O. (Ruhrchemie AG). D.B.P. 849 458, 1938; *Chem. Zentr.* **1953**, 927.
(9) (a) Cornils, B.; Herrmann, W. A. *Applied Homogeneous Catalysis with Organometallic Compounds*; VCH−Wiley: New York, 1996; Vol. 1, pp 3−25. (b) Papadogianakis, G.; Sheldon, R. A. *New J. Chem.* **1996**, *20*, 175.
(10) (a) Orchin, M. *Acc. Chem. Res.* **1981**, *14*, 259. (b) Orchin, M.; Rupilius, W. *Catal. Rev.* **1972**, *6*, 85. (c) Orchin, M. *Ann. N. Y. Acad. Sci.* **1983**, *415*, 129.
(11) (a) Polo, A.; Claver, C.; Castillón, S.; Ruiz, A.; Bayón, J. C.; Real, J.; Mealli, C.; Masi, D. *Organometallics* **1992**, *11*, 3525. (b) Alvila, L.; Pakkanen, T. A.; Pakkanen, T. T.; Krause, O. *J. Mol. Catal.* **1992**, *73*, 325. (c) Reus, S. I.; Kamalov, G. L.; Golodets, G. I. *Kinet. Catal. (Engl. Transl.)* **1991**, *32*, 694. (d) Crudden, C. M.; Alper, H. *J. Org. Chem.* **1994**, *59*, 3091. (e) van der Veen, L. A.; Kamer, P. C. J.; van Leeuwen, P. W. N. M. *Angew. Chem.* **1999**, 111, 349; *Angew. Chem., Int. Ed. Engl.* **1999**, *38*, 336. (f) Nair, V. S.; Mathew, S. P.; Chaudhari, R. V. *J. Mol. Catal., A* **1999**, *143*, 99. (g) Kiss, G.; Mozeleski, E. J.; Nadler, K. C.; Van-Driessche, E.; DeRoover, C. *J. Mol. Catal., A* **1999**, *138*, 155. (h) Ahn, H. S.; Han, S. H.; Uhm, S. J.; Seok, W. K.; Lee, H. N.; Korneeva, G. A. *J. Mol. Catal., A* **1999**, *144*, 295.
(12) Agbossou, F.; Carpentier, J.-F.; Mortreux, A. *Chem. Rev.* **1995**, *95*, 2485.
(13) (a) Feng, J.; Garland, M. *Organometallics* **1999**, *18*, 417. (b) Paciello, R.; Siggel, L.; Röper, M. *Angew. Chem.* **1999**, 111, 2045; *Angew. Chem., Int. Ed. Engl.* **1999**, *38*, 1920.
(14) (a) Ungváry, F. *Coord. Chem. Rev.* **1999**, *188*, 263. (b) Ungváry, F. *Coord. Chem. Rev.* **1998**, *170*, 245. (c) Ungváry, F. *Coord. Chem. Rev.* **1997**, *167*, 233.
(15) (a) Heck, R. F.; Breslow, D. S. *J. Am. Chem. Soc.* **1961**, *83*, 4023. (b) Heck, R. F.; Breslow, D. S. *J. Am. Chem. Soc.* **1962**, *84*, 2499. (c) Heck, R. F. *Acc. Chem. Res.* **1969**, *2*, 10. (d) Heck, R. F. *Adv. Organomet. Chem.* **1966**, *4*, 243.
(16) (a) Evans, D.; Osborn, J. A.; Wilkinson, G. *J. Chem. Soc. A* **1968**, 3133. (b) Evans, D.; Yagupsky, G.; Wilkinson, G. *J. Chem. Soc. A* **1968**, 2660. (c) Brown, C. K.; Wilkinson, G. *J. Chem. Soc. A* **1970**, 2753.
(17) Ziegler, T.; Versluis, L. *Adv. Chem. Ser.* **1992**, *230*, 75.
(18) Ziegler, T. *NATO ASI Ser.* **1992**, *C367*, 357.
(19) Ziegler, T. *Can. J. Chem.* **1995**, *73*, 743.
(20) Ziegler, T. *Chem. Rev.* **1991**, *91*, 651.
(21) Ziegler, T. *Pure Appl. Chem.* **1991**, *63*, 873.
(22) Koga, N.; Morokuma, K. *Top. Phys. Organomet. Chem.* **1989**, *3*, 1.
(23) Koga, N.; Morokuma, K. *Chem. Rev.* **1991**, *91*, 823.
(24) Koga, N.; Morokuma, K. In *Transition Metal Hydrides*; Dedieu, A., Ed.; VCH: New York, 1992; Chapter 6.
(25) Musaev, D. G.; Matsubara, T.; Mebel, A. M.; Koga, N.; Morokuma, K. *Pure Appl. Chem.* **1995**, *67*, 257.
(26) Musaev, D. G.; Morokuma, K. *Adv. Chem. Phys.* **1996**, *95*, 61.
(27) Siegbahn, P. E. M.; Blomberg, M. R. A. In *Theoretical Aspects of Homogeneous Catalysis*; van Leeuwen, P. W. N. M., Morokuma, K., van Lenthe, J. H., Eds.; Kluwer: Dordrecht, The Netherlands, 1995; pp 15−63.
(28) Koga, N.; Morokuma, K. In *Theoretical Aspects of Homogeneous Catalysis*; van Leeuwen, P. W. N. M., Morokuma, K., van Lenthe, J. H., Eds.; Kluwer: Dordrecht, The Netherlands, 1995; pp 65−91.
(29) Koga, N.; Morokuma, K. In *Theoretical Aspects of Homogeneous Catalysis*; van Leeuwen, P. W. N. M., Morokuma, K., van Lenthe, J. H., Eds.; Kluwer: Dordrecht, The Netherlands, 1995; pp 93−114.
(30) Yoshida, S.; Sakaki, S.; Kobayashi, H. *Electronic Processes in Catalysis;* VCH: New York, 1994.
(31) Folga, E.; Ziegler, T. *J. Am. Chem. Soc.* **1993**, *115*, 5169.
(32) Leung, P. C.; Coppens, C. *Acta Crystallogr.* **1982**, *B39*, 535.
(33) Bellagamba, V.; Ercoli, R.; Gamba, A.; Suffritti, G. B. *J. Organomet. Chem.* **1980**, *190*, 381.
(34) Klinger, R. J.; Rathke, J. W. *Inorg. Chem.* **1992**, *31*, 804.
(35) Tannenbaum, R.; Dietler, U. K.; Bor, G.; Ungváry, F. *J. Organomet. Chem.* **1998**, *570*, 39.
(36) Grima, J. Ph.; Choplin, F.; Kaufmann, G. *J. Organomet. Chem.* **1977**, *129*, 221.
(37) Pensak, D. A.; McKinney, R. J. *Inorg. Chem.* **1979**, *18*, 3407.
(38) Elian, M.; Hoffmann, R. *Inorg. Chem.* **1975**, *14*, 1058.
(39) Antolovic, D., Davidson, E. R. *J. Am. Chem. Soc.* **1987**, *109*, 977.
(40) Antolovic, D., Davidson, E. R. *J. Am. Chem. Soc.* **1987**, *109*, 5828.
(41) Antolovic, D., Davidson, E. R. *J. Chem. Phys.* **1988**, *88*, 4967.
(42) Ziegler, T.; Tschinke, V.; Becke, A. *J. Am. Chem. Soc.* **1987**, *109*, 1351.
(43) Versluis, L.; Ziegler, T.; Baerends, E. J.; Ravenek, W. *J. Am. Chem. Soc.* **1989**, *111*, 2018.
(44) Ziegler, T.; Cavallo, L.; Bérces, A. *Organometallics* **1993**, *12*, 3586.
(45) Jonas, V.; Thiel, W. *J. Chem. Phys.* **1996**, *105*, 3636.
(46) Sosa, C.; Andzelm, J.; Elkin, B. C.; Wimmer, E.; Dobbs, K. D.; Dixon, D. A. *J. Phys. Chem.* **1992**, *96*, 6630.
(47) Veillard, A.; Strich, A. *J. Am. Chem. Soc.* **1988**, *110*, 3793.
(48) Veillard, A.; Daniel, C.; Rohmer, M.-M. *J. Phys. Chem.* **1990**, *94*, 5556.
(49) Daniel, C.; Kolba, E.; Lehr, L.; Manz, J.; Schröder, T. *J. Phys. Chem.* **1994**, *98*, 9823.
(50) Ribbing, C.; Daniel, C. *J. Chem. Phys.* **1994**, *100*, 6591.
(51) Heitz, M.-C.; Ribbing, C.; Daniel, C. *J. Chem. Phys.* **1997**, *106*, 1421.
(52) Daniel, C.; Hyla-Kryspin, I.; Demuynck, J.; Veillard, A. *Nouv. J. Chim.* **1985**, *9*, 582.
(53) Eyermann, C. J.; Chung-Phillips, A. *J. Am. Chem. Soc.* **1984**, *106*, 7437.
(54) Heitz, M.-C.; Finger, K.; Daniel, C. *Coord. Chem. Rev.* **1997**, *159*, 171.
(55) Zhao, Y.; Kühn, O. *Chem. Phys. Lett.* **1999**, *302*, 7.
(56) McNeill, E. A.; Scholer, F. R. *J. Am. Chem. Soc.* **1977**, *99*, 6243.
(57) Torrent, M.; Duran, M.; Solà, M. *Adv. Mol. Sim.* **1996**, *1*, 167.
(58) Baerends, E. J.; Rozendaal, A. In *Quantum Chemistry: The Challenge of Transition Metals and Coordination Chemistry*; Veillard, A., Ed.; Kluwer: Dordrecht, The Netherlands, 1986; pp 159−177.
(59) Jonas, V.; Thiel, W. *J. Chem. Phys.* **1995**, *102*, 8474.
(60) (a) Blomberg, M. R. A.; Karlsson, C. A. M.; Siegbahn, P. E. M. *J. Phys. Chem.* **1993**, *97*, 9341. (b) Siegbahn, P. E. M.; Svensson, M. *Chem. Phys. Lett.* **1993**, *216*, 147.
(61) Aarnts, M.; Stufkens, D. J.; Solà, M.; Baerends, E. J. *Organometallics* **1997**, *16*, 2254.
(62) Wermer, P.; Ault, B. S.; Orchin, M. *J. Organomet. Chem.* **1978**, *162*, 189.
(63) Ungváry, F.; Markó, L. *J. Organomet. Chem.* **1969**, *20*, 205.
(64) Clark, A. C.; Orchin, M. *J. Org. Chem.* **1973**, *38*, 4004.
(65) Feder, H. M.; Rathke, J. W. *Ann. N. Y. Acad. Sci.* **1980**, *333*, 45.
(66) Pidun, U.; Frenking, G. *Chem. Eur. J.* **1998**, *4*, 522.
(67) Berry, R. S. *J. Chem. Phys.* **1960**, *32*, 933.
(68) Vidal, J. L.; Walker, W. E. *Inorg. Chem.* **1981**, *20*, 249.
(69) Schmid, R.; Herrmann, W. A.; Frenking, G. *Organometallics* **1997**, *16*, 701.
(70) *Handbook of Chemistry and Physics*, 78th ed.; Lide D. R., Ed.; CRC Press: Boca Raton, FL, 1996.
(71) Koga, N.; Morokuma, K. *J. Am. Chem. Soc.* **1993**, *115*, 6883.
(72) Solà, M.; Mestres, J.; Carbó, R.; Duran, M. *J. Chem. Phys.* **1996**, *104*, 636.
(73) González-Blanco, O.; Branchadell, V. *Organometallics* **1997**, *16*, 5556.
(74) Matsubara, T.; Koga, N.; Ding, Y.; Musaev, D. G.; Morokuma, K. *Organometallics* **1997**, *16*, 1065.
(75) Van der Veen, L. A.; Boele, M. D. K.; Bregman, F. R.; Kamer, P. C. J.; van Leeuwen, P. W. N. M.; Goubitz, K.; Fraanje, J.; Schenk, H.; Bo, C. *J. Am. Chem. Soc.* **1998**, *120*, 11616.
(76) (a) Brown, J. M.; Kent, A. G. *J. Chem. Soc., Perkin Trans. 2* **1987**, 1597. (b) Kastrup, R. V.; Merola, J. S.; Oswald, A. A. *Adv. Chem. Ser.* **1982**, *No. 196*, 43.
(77) Rossi, A. R.; Hoffmann, R. *Inorg. Chem.* **1975**, *14*, 365.
(78) Versluis, L.; Ziegler, T.; Fan, L. *Inorg. Chem.* **1990**, *29*, 4530.
(79) (a) Dewar, M. J. S. *Bull. Soc. Chim. Fr.* **1951**, *18*, C71. (b) Chatt, J.; Duncanson, L. A. *J. Chem. Soc.* **1953**, 2939.
(80) Ittel, S. D.; Ibers, J. A. *Adv. Organomet. Chem.* **1976**, *14*, 33.
(81) Koga, N.; Jin, S. Q.; Morokuma, K. *J. Am. Chem. Soc.* **1988**, *110*, 3417.
(82) Rocha, W. R.; De Almeida, W. B. *Organometallics* **1998**, *17*, 1961.
(83) Thorn, D. L.; Hoffmann, R. *J. Am. Chem. Soc.* **1978**, *100*, 2079.
(84) Trzeciak, A. M.; Szterenberg, L.; Wolszczak, E.; Ziólkowski, J. J. *J. Mol. Catal., A* **1995**, *99*, 23.
(85) Brookhart, M.; Volpe, A. F., Jr.; Lincoln, D. M.; Horváth, I. T.; Millar, J. M. *J. Am. Chem. Soc.* **1990**, *112*, 5634.
(86) Dedieu, A. *Top. Phys. Organomet. Chem.* **1985**, *1*, 1.
(87) Tsipis, C. A. *Coord. Chem. Rev.* **1991**, *108*, 163.
(88) Koga, N.; Morokuma, K. *NATO ASI Ser.* **1990**, *C176*, 351.

(89) Berke, H.; Hoffmann, R. *J. Am. Chem. Soc.* **1978**, *100*, 7224.
(90) (a) Markó, L. *Transition Met. Chem.* **1992**, *17*, 474. (b) Tam, W.; Wong, W. K.; Gladysz, J. A. *J. Am. Chem. Soc.* **1979**, *101*, 1589. (c) Brown, K. L.; Clark, G. R.; Headford, C. E. L.; Marsden, K.; Roper, W. R. *J. Am. Chem. Soc.* **1979**, *101*, 503.
(91) Demuynck, J.; Strich, A.; Veillard, A. *Nouv. J. Chim.* **1977**, *1*, 217.
(92) Dedieu, A.; Nakamura, S. *NATO ASI Ser.* **1990**, *C176*, 277.
(93) Sweany, R. L.; Rusell, F. N. *Organometallics* **1988**, *7*, 719.
(94) Dombeck, D. *Adv. Catal.* **1983**, *32*, 325.
(95) Versluis, L.; Ziegler, T. *Organometallics* **1990**, *9*, 2985.
(96) Solà, M.; Ziegler, T. *Organometallics* **1996**, *15*, 2611.
(97) Musaev, D. G.; Morokuma, K. *J. Organomet. Chem.* **1995**, *504*, 93.
(98) Heinekey, D. M.; van Roon, M. *J. Am. Chem. Soc.* **1996**, *118*, 12134.
(99) Ungváry, F.; Sisak, A.; Markó, L. *Adv. Chem. Ser.* **1990**, *230*, 297.
(100) Versluis, L.; Ziegler, T. *J. Am. Chem. Soc.* **1990**, *112*, 6763.
(101) (a) Masters, C. *Adv. Organomet. Chem.* **1979**, *17*, 61. (b) Nicholas, K. M. *Organometallics* **1982**, *1*, 1713.
(102) (a) Casey, C. P.; Paulsen, E. L.; Beuttenmueller, E. W.; Proft, B. R.; Petrovich, L. M.; Matter, B. A.; Powell, D. R. *J. Am. Chem. Soc.* **1997**, *119*, 11817. (b) Dierkes, P.; van Leeuwen, P. W. N. M. *J. Chem. Soc., Dalton Trans.* **1999**, 1519.
(103) Castonguay, L. A.; Rappé, A. K.; Casewit, C. J. *J. Am. Chem. Soc.* **1991**, *113*, 7177.
(104) Gleich, D.; Schmid, R.; Herrmann, W. A. *Organometallics* **1998**, *17*, 4828.
(105) Paciello, R.; Siggel, L.; Kneuper, H.-J.; Walker, N.; Röper, M. *J. Mol. Catal., A* **1999**, *143*, 85.
(106) Fischer, E. O.; Maasböl, A. *Angew. Chem*. **1964**, *76*, 645; *Angew. Chem., Int. Ed. Engl*. **1964**, *3*, 580.
(107) For reviews see: (a) Dötz, K. H.; Fischer, H.; Hofmann, P.; Kreissl, F. R.; Schubert, U.; Weiss, K. *Transition Metal Carbene Complexes*; VCH: Weinheim, 1983. (b) Dötz, K. H. *Angew. Chem*. **1984**, *96*, 573; *Angew. Chem., Int. Ed. Engl*. **1984**, *23*, 587. (c) Hegedus, L. S. In *Comprehensive Organometallic Chemistry II*; Abel, E. W., Stone, F. G. A., Wilkinson, G., Eds.; Pergamon Press: Oxford, 1995; Vol. 12, p 549. (d) Wulff, W. D. In *Comprehensive Organic Synthesis*; Trost, B. M., Fleming, I., Eds.; Pergamon Press: Oxford, 1991; Vol. 5, p 1065. (e) Wulff, W. D. In *Comprehensive Organometallic Chemistry II*; Abel, E. W., Stone, F. G. A., Wilkinson, G., Eds.; Pergamon Press: Oxford, 1995; Vol. 12, p 469. (f) Harvey, D. F.; Sigano, D. M. *Chem. Rev*. **1996**, *96*, 271. (g) de Meijere, A. *Pure Appl. Chem*. **1996**, *68*, 61. (h) Barluenga, J. *Pure Appl. Chem*. **1996**, *68*, 543. (i) Aumann, R.; Nienaber, H. *Adv. Organomet. Chem*. **1997**, *41*, 163.
(108) Dötz, K. H. *Angew. Chem*. **1975**, *87*, 672; *Angew. Chem., Int. Ed. Engl*. **1975**, *14*, 644. For a recent review see: Dötz, K. H.; Tomuschat, P. *Chem. Soc. Rev.* **1999**, *28*, 187.
(109) (a) Dötz, K. H.; Dietz, R. *Chem. Ber*. **1978**, *111*, 2517. (b) Dötz, K. H.; Pruskil, I. *Chem. Ber*. **1980**, *113*, 2876. (c) Wulff, W. D.; Tang, P. C.; McCallum, J. S. *J. Am. Chem. Soc*. **1981**, *103*, 7677. (d) Dötz, K. H.; Mühlemeier, J.; Schubert, U.; Orama, O. *J. Organomet. Chem*. **1983**, *247*, 187. (e) Wulff, W. D.; Chan, K. S.; Tang, P. C. *J. Org. Chem*. **1984**, *49*, 2293. (f) Yamashita, A.; Toy, A. *Tetrahedron Lett*. **1986**, *27*, 3471.
(110) Benzannulation with stannylalkynes shows the reversed regioselectivity: Chamberlain, S.; Waters, M. L.; Wulff, W. D. *J. Am. Chem. Soc*. **1994**, *116*, 3113.
(111) (a) Dötz, K. H. *J. Organomet. Chem*. **1977**, *140*, 177. (b) Dötz, K. H.; Pruskil, I. *Chem. Ber*. **1978**, *111*, 2059. (c) Wulff, W. D.; Gilbertson, S. R.; Springer, J. P. *J. Am. Chem. Soc*. **1986**, *107*, 5823. (d) Semmelhack, M. F.; Park, J. *Organometallics* **1986**, *5*, 2550. (e) Garret, K. E.; Sheridan, J. B.; Pourreau, D. B.; Weng, W. C.; Geoffroy, G. L.; Staley, D. L.; Rheingold, A. L. *J. Am. Chem. Soc*. **1989**, *111*, 8383. (f) Yamashita, A. *Tetrahedron Lett*. **1986**, *27*, 5915. (g) Dötz, K. H.; Larbig, H. *J. Organomet. Chem.* **1991**, *405*, C38. (h) Wulff, W. D.; Bax, B. A.; Brandvold, B. A.; Chan, K. S.; Gilbert, A. M.; Hsung, R. P.; Mitchell, J.; Clardy, J. *Organometallics* **1994**, *13*, 102. (i) Aumann, R.; Jasper, B.; Fröhlich, R. *Organometallics* **1995**, *14*, 4, 231. (j) Parlier, A.; Rudler, M.; Rudler, H.; Goumont, R.; Daran, J.-C.; Vaissermann, J. *Organometallics* **1995**, *14*, 2760. (k) Dötz, K. H.; Gerhardt, A. *J. Organomet. Chem.* **1999**, *578*, 223. (l) Tomuschat, P.; Kröner, L.; Steckhan, E.; Nieger, M.; Dötz, K. H. *Chem. Eur. J.* **1999**, *5*, 700.
(112) (a) Hohmann, F.; Siemoneit, S.; Nieger, M.; Kotila, S.; Dötz, K. H. *Chem. Eur. J.* **1997**, *3*, 853. (b) Dötz, K. H.; Stinner, C. *Tetrahedron: Asymmetry* **1997**, *8*, 1751. (c) Gordon, D. M.; Danishefsky, S. H.; Schulte, G. M. *J. Org. Chem*. **1992**, *57*, 7052. (d) King, J.; Quayle, P.; Malone, J. F. *Tetrahedron Lett*. **1990**, *31*, 5221. (e) Parker, K. A.; Coburn, C. A. *J. Org. Chem*. **1991**, *56*, 1666. (f) Boger, D. L.; Jacobson, I. C. *J. Org. Chem*. **1990**, *55*, 1919. (g) Semmelhack, M. F.; Jeong, N. *Tetrahedron Lett*. **1990**, *31*, 650. (h) Semmelhack, M. F.; Jeong, N.; Lee, G. R. *Tetrahedron Lett*. **1990**, *31*, 609. (i) Yamashita, A.; Toy, A.; Scahill, T. A. *J. Org. Chem*. **1989**, *54*, 3625. (j) Wulff, W. D.; McCallum, J. S.; Kung, F. A. *J. Am. Chem. Soc*. **1988**, *110*, 7419.
(113) (a) Dötz, K. H.; Pruskil, I. *J. Organomet. Chem*. **1981**, *209*, C4. (b) Dötz, K. H.; Pruskil, I.; Mühlemeier, J. *Chem. Ber*. **1982**, *115*, 1278. (c) Dötz, K. H.; Kuhn, W. *Angew. Chem*. **1983**, *95*, 755; *Angew. Chem., Int. Ed. Engl*. **1983**, *22*, 732.
(114) (a) Semmelhack, M. F.; Bozell, J. J.; Keller, L.; Sato, T.; Spiess, E. J.; Wulff, W. D.; Zask, A. *Tetrahedron* **1985**, *41*, 5803. (c) Wulff, W. D.; Tang, P. C. *J. Am. Chem. Soc*. **1984**, *106*, 434. (c) Yamashita, A. *J. Am. Chem. Soc*. **1985**, *107*, 5823. (d) Dötz, K. H.; Popall, M. *J. Organomet. Chem*. **1985**, *291*, C1. (e) Dötz, K. H.; Popall, M. *Tetrahedron* **1985**, *41*, 5797. (f) Dötz, K. H.; Popall, M.; Müller, G.; Ackermann, K. *J. Organomet. Chem*. **1990**, *383*, 93. (g) Paetsch, D.; Dötz, K. H. *Tetrahedron Lett.* **1999**, *40*, 487.
(115) (a) Semmelhack, M. F.; Bozell, J. J.; Sato, T.; Wulff, W. D.; Spiess, E.; Zask, A. *J. Am. Chem. Soc*. **1982**, *104*, 5850. (b) Wulff, W.; Su, J.; Tang, P.-C.; Xu, Y.-C. *Synthesis* **1999**, 415. (c) Gilbert, A. M.; Miller, R.; Wulff, W. *Tetrahedron* **1999**, *55*, 1607. (d) Miller, R. A.; Gilbert, A. M.; Xue, S.; Wulff, W. D. *Synthesis* **1999**, 80.
(116) (a) Dötz, K. H.; Popall, M. *Angew. Chem*. **1987**, *99*, 1220; *Angew. Chem., Int. Ed. Engl*. **1987**, *26*, 1158. (b) Wulff, W. D.; Xu, Y.-C. *J. Am. Chem. Soc*. **1988**, *110*, 2312.
(117) (a) Boger, D. L.; Jacobson, I. C. *J. Org. Chem*. **1991**, *56*, 2115. (b) Boger, D. L.; Hüter, O.; Mbiya, K.; Zhang, M. *J. Am. Chem. Soc*. **1995**, *117*, 11839.
(118) Anderson, B. A.; Bao, J.; Brandvold, T. A.; Challener, C. A.; Wulff, W. D.; Xu, Y.-C.; Rheingold, A. L. *J. Am. Chem. Soc*. **1993**, *115*, 10671.
(119) Harrity, J. P. A.; Kerr, W. J. *Tetrahedron Lett*. **1993**, *34*, 2995.
(120) Harrity, J. P. A.; Kerr, W. J. *Tetrahedron* **1993**, *49*, 5565.
(121) (a) Choi, Y. H.; Rhee, K. S.; Kim, K. S.; Shin, G. C.; Shin, S. C. *Tetrahedron Lett*. **1995**, *36*, 1871. (b) Weyershausen, B.; Dötz, K. H. *Synlett* **1999**, 231.
(122) (a) Dötz, K. H.; Fügen-Köster, B. *Chem. Ber*. **1980**, *113*, 1449. (b) Harvey, D. F.; Grenzer, E. M.; Gantzel, P. K. *J. Am. Chem. Soc*. **1994**, *116*, 6719.
(123) (a) Strain, M. C.; Scuseria, G. E.; Frisch, M. J. *Science* **1996**, *271*, 51. (b) Taubes, G. *Science* **1996**, *273*, 1655. (c) van Leeuwen, P. W. N. M., Morokuma, K., van Lenthe, J. H., Eds. *Theoretical Aspects of Homogeneous Catalysis*; Kluwer: Dordrecht, The Netherlands, 1995. (d) Broer, R., Aerts, P. J. C., Bagus, P. S., Eds. *New Challenges in Computational Quantum Chemistry*; University of Groningen: Groningen, The Netherlands, 1994.
(124) Hofmann, P.; Hämmerle, M. *Angew. Chem*. **1989**, *101*, 940; *Angew. Chem., Int. Ed. Engl*. **1989**, *28*, 908.
(125) Hofmann, P.; Hämmerle, M.; Unfried, G. *New J. Chem*. **1991**, *15*, 769.
(126) Casey, C. P. In *Reactive Intermediates*; Jones, M., Jr., Moss, R. A., Eds.; Wiley: New York, 1981; Vol. 2, p 155.
(127) Fischer, H.; Mühlemeier, J.; Märkl, R.; Dötz, K. H. *Chem. Ber*. **1982**, *115*, 1355.
(128) For complex **34** see: (a) Tang, P.-C.; Wulff, W. D. *J. Am. Chem. Soc*. **1984**, *106*, 1132. (b) Wulff, W. D.; Bax, B. M.; Brandvold, T. A.; Chan, K. S.; Gilbert, A. M.; Hsung, R. P. *Organometallics* **1994**, *13*, 102.
(129) (a) Mitsudo, T.-A.; Ishihara, A.; Kadokura, M.; Watanabe, Y. *Organometallics* **1986**, *5*, 238. (b) Casey, C. P.; O'Connor, J. M.; Haller, K. J. *J. Am. Chem. Soc*. **1985**, *107*, 3172.
(130) (a) Mitsudo, T.-A.; Sakaki, T.; Watanabe, Y.; Takegami, Y.; Nishigaki, S.; Nakatsu, K. *J. Chem. Soc., Chem. Commun.* **1978**, 252. (b) Wood, C. D.; McLain, S. J.; Schrock, R. R. *J. Am. Chem. Soc*. **1979**, *101*, 3210. (c) Dötz, K. H. *Angew. Chem*. **1979**, *91*, 1021; *Angew. Chem., Int. Ed. Engl*. **1979**, *18*, 954. (d) Dötz, K. H.; Sturm, W. *J. Organomet. Chem*. **1985**, *285*, 205. (e) O'Connor, J. M.; Ji, H.-L.; Rheingold, A. L. *J. Am. Chem. Soc*. **1993**, *115*, 9846.
(131) Synthesis of η^4-vinylketene complexes by insertion of Rh(I) and Co(I) reagents into cyclobutenones has been reported, together with the reaction of η^4-vinylketene cobalt complexes with alkynes to form phenols: Huffman, M. A.; Liebeskind, L. S.; Pennington, W. T. *Organometallics* **1992**, *11*, 255.
(132) Garret, K. E.; Sheridan, J. B.; Pourreau, D. B.; Feng, W. C.; Geoffroy, G. L.; Staley, D. L.; Rheingold, A. L. *J. Am. Chem. Soc*. **1989**, *111*, 8383.
(133) (a) Chan, K. S.; Petersen, G. A.; Brandvold, T. A.; Faron, K. L.; Challener, C. A.; Hydahl, C.; Wulff, W. D. *J. Organomet. Chem*. **1987**, *334*, 9. (b) Bos, M. E.; Wulff, W. D.; Miller, R. A.; Chamberlin, S.; Brandvold, T. A. *J. Am. Chem. Soc*. **1991**, *113*, 9293.
(134) McCallum, J. S.; Kung, F.-A.; Gilbertson, S. R.; Wulff, W. D. *Organometallics* **1988**, *7*, 2346.
(135) Torrent, M. Ph.D. Thesis, Universitat de Girona, Girona, Spain, 1998; Chapters 9 and 10.
(136) Torrent, M. Duran, M.; Solà, M. *Organometallics* **1998**, *17*, 1492.
(137) Torrent, M.; Duran, M.; Solà, M. *Chem. Commun*. **1998**, 999.
(138) Torrent, M.; Duran, M.; Solà, M. *J. Am. Chem. Soc*. **1999**, 121, 1309.

(139) Gleichmann, M. M.; Dötz, K. H.; Hess, B. A. *J. Am. Chem. Soc.* **1996**, *118*, 10551.
(140) Dötz, K. H.; Dietz, R. *Chem. Ber.* **1977**, *110*, 1555.
(141) Barluenga, J.; Aznar, F.; Martín, A.; García-Granda, S.; Pérez-Carreño, E. *J. Am. Chem. Soc.* **1994**, *116*, 11191.
(142) Fischer, H.; Hofmann, P. *Organometallics* **1999**, *18*, 2590.
(143) Waters, M. L.; Bos, M. E.; Wulff, W. D. *J. Am. Chem. Soc.* **1999**, *121*, 6403.
(144) Hughes, R. P.; Trujillo, J. A.; Gauri, A. J. *Organometallics* **1995**, *14*, 4319.
(145) (a) Lukehart, C. M. In *Fundamental Transition Metal Organometallic Chemistry*; Geoffroy, G. L., Ed.; Brooks/Cole Publishing: Pacific Grove, California, 1985; Chapter 13. (b) Collman, J. P., Hegedus, L. S., Norton, J. R., Finke, R. G., Eds. *Principles and Applications of Organotransition Metal Chemistry*; 2nd Ed., University Science Books: Sausalito, California, 1987. (c) Wilkinson, S. G., Gillard, R. D., McCleverty, J. A., Eds. *Comprehensive Coordination Chemistry: The Synthesis, Reactions, Properties & Applications of Coordination Compounds*; Vol. 6, Pergamon: Oxford, 1987; pp 269−292.
(146) (a) Storch, H. H.; Golumbic, N.; Anderson, R. B. *The Fischer−Tropsch and Related Syntheses*; Wiley: New York, 1951. (b) *Catalyst Handbook*; Springer-Verlag: London, 1970; Chapters 5 and 6. (c) Keim, W., Ed. *Catalysis in C_1 Chemistry*; D. Reidel Publishing Co.: Dordrecht, The Netherlands, 1983; pp 50 and 136. (d) Shelef, M.; Gandhi, H. S. *Ind. Eng. Chem. Prod. Res. Dev.* **1975**, *13*, 80. (e) Querido, R.; Short, W. L. *Ind. Eng. Chem. Process Des. Dev.* **1973**, *12*, 10. (f) Lin, G. I.; Samokhin, P. V.; Kaloshkin, S. D.; Rozovskii, A. Y. *Kinet. Catal. (Engl. Transl.)* **1998**, *39*, 577.
(147) Herrmann, W. A. In *Applied Homogeneous Catalysis with Organometallic Compounds*; Cornils, B., Herrmann, W. A., Eds.; VCH: Weinheim, 1996; Vol. 2, pp 957−963.
(148) Ford, P. C. *Acc. Chem. Res.* **1981**, *14*, 31.
(149) (a) Yoshida, T.; Ueda, Y.; Otsuka, S. *J. Am. Chem. Soc.* **1978**, *100*, 3942. (b) Laine, R. M.; Thomas, D. W.; Carry, L. W.; Buttrill, S. E. *J. Am. Chem. Soc.* **1978**, *100*, 6527. (c) Ford, P. C.; Rinker, R. G.; Laine, R. M.; Ungermann, C.; Landis, V.; Moya, S. A. *Adv. Chem. Ser.* **1979**, *173*, 81. (d) Ungermann, C.; Landis, V.; Moya, S. A.; Cohen, H.; Walker, H.; Pearson, R. G.; Ford, P. C. *J. Am. Chem. Soc.* **1979**, *101*, 5922. (e) Baker, E. C.; Hendriksen, D. E.; Eisenberg, R. *J. Am. Chem. Soc.* **1980**, *102*, 1020. (f) King, A. D.; King, R. B.; Yang, D. B. *Chem. Commun.* **1980**, 529. (g) Yoshida, T.; Okano, T.; Ueda, Y.; Otsuka, S. *J. Am. Chem. Soc.* **1981**, *103*, 3411. (h) Ford, P. C.; Rokocki, A. *Adv. Organomet. Chem.* **1988**, *28*, 139.
(150) (a) Reppe, J. W.; Reindl, E. *Liebigs Ann. Chem.* **1953**, *582*, 121. (b) Frazier, C. C.; Hanes, R. M.; King, A. D.; King, R. B. *Adv. Chem. Ser.* **1979**, *173*, 94. (c) Darensbourg, D. J.; Darensbourg, M. Y.; Burch, R. R.; Froelich, J. A.; Incorvia, M. J. *Adv. Chem. Ser.* **1979**, *173*, 106. (d) Yoshida, T.; Thorn, D. L.; Okano, T.; Ibers, J. A.; Otsuka, S. *J. Am. Chem. Soc.* **1979**, *101*, 4212. (e) King, R. B.; Frazier, C. C.; Hanes, R. M.; King, A. D. *J. Am. Chem. Soc.* **1978**, *100*, 2925.
(151) (a) Laine, R. M.; Rinker, R. S.; Ford, P. C. *J. Am. Chem. Soc.* **1977**, *99*, 253. (b) Luukkanen, S.; Homanen, P.; Haukka, M.; Pakkanen, T. A.; Deronzier, A.; Chardon-Noblat, S.; Zsoldos, D.; Ziessel, R. *Appl. Catal., A* **1999**, *185*, 157. (c) Haukka, M.; Hirva, P.; Luukkanen, S.; Kallinen, M.; Ahlgrén, M.; Pakkanen, T. A. *Inorg. Chem.* **1999**, *38*, 3182. (d) Zhang, S.-W.; Sugioka, T.; Takahashi, S. *J. Mol. Catal., A* **1999**, *143*, 211.
(152) (a) Cheng, C.-H.; Hendricksen, D. E.; Eisenberg, R. *J. Am. Chem. Soc.* **1977**, *99*, 2791. (b) Kubiak, C. P.; Eisenberg, R. *J. Am. Chem. Soc.* **1980**, *102*, 3637. (c) Kubiak, C. P.; Woodcock, C.; Eisenberg, R. *Inorg. Chem.* **1982**, *21*, 2119. (d) Tominaga, K.; Sasaki, Y.; Hagihara, K.; Watanabe, T.; Saito, M. *Chem. Lett.* **1994**, 1391. (e) Kallinen, K. O.; Pakkanen, T. T.; Pakkanen, T. A. *J. Organomet. Chem.* **1997**, *547*, 319. (f) Bryce, D. J. F.; Dyson, P. J.; Nicholson, B. K.; Parker, D. G. *Polyhedron* **1998**, *17*, 2899. (g) Clark, R. J. H.; Dyson, P. J.; Humphrey, D. G.; Johnson, B. F. G. *Polyhedron* **1998**, *17*, 2985.
(153) Gross, D. C.; Ford, P. C. *Inorg. Chem.* **1982**, *21*, 1704.
(154) Laine, R. M.; Wilson, R. B. In *Aspects of Homogeneous Catalysis*; Ugo, R., Ed.; Reidel (Kluwer): Dordrecht, The Netherlands, 1984; Vol. 5.
(155) Kang, H.; Mauldin, C.; Cole, T.; Slegeir, W.; Pettit, R. *J. Am. Chem. Soc.* **1977**, *99*, 8323.
(156) Grice, N.; Kao, S. C.; Pettit, R. *J. Am. Chem. Soc.* **1979**, *101*, 1627.
(157) Lane, K. R.; Lee, R. E.; Sallans, L.; Squires, R. R. *J. Am. Chem. Soc.* **1984**, *106*, 5767.
(158) Kruck, T.; Noack, M. *Chem. Ber.* **1964**, *97*, 1693.
(159) Darensbourg, D. J.; Froelich, J. A. *J. Am. Chem. Soc.* **1977**, *99*, 4726.
(160) (a) Hieber, W.; Kruck, T. *Z. Naturforsch., B* **1961**, *16*, 709. (b) Clark, H. C.; Dixon, K. R.; Jacobs, W. J. *Chem. Commun.* **1968**, 548.
(161) Krumholz, P.; Stettiner, H. M. A. *J. Am. Chem. Soc.* **1949**, *71*, 3035.
(162) Sternberg, H. W.; Markby, R.; Wender, I. *J. Am. Chem. Soc.* **1957**, *79*, 6116.
(163) Hieber, W.; Vetter, H. *Z. Anorg. Allg. Chem.* **1933**, *212*, 145.
(164) Nakamura, S.; Dedieu, A. *Theor. Chim. Acta* **1982**, *61*, 587.
(165) Dedieu, A.; Nakamura, S. *Nouv. J. Chim.* **1984**, *8*, 317.
(166) (a) Ehlers, A. W.; Frenking, G. *Organometallics* **1995**, *14*, 423. (b) Lionel, T.; Morton, J. R.; Preston, K. F. *J. Chem. Phys.* **1982**, *76*, 234. (c) Bogdan, P.; Weitz, E. *J. Am. Chem. Soc.* **1989**, *111*, 3163. (d) Bogdan, P.; Weitz, E. *J. Am. Chem. Soc.* **1990**, *112*, 639. (e) Lyne, P. D.; Mingos, D. M. P.; Ziegler, T.; Downs, A. J. *Inorg. Chem.* **1993**, *32*, 4785. (f) Radius, U.; Bickelhaupt, F. M.; Ehlers, A. W.; Goldberg, N.; Hoffmann, R. *Inorg. Chem.* **1998**, *37*, 1080. (g) González-Blanco, O.; Branchadell, V. *J. Chem. Phys.* **1999**, *110*, 778. (g) Rubner, O.; Engel, V.; Hachey, M. R.; Daniel, C. *Chem. Phys. Lett.* **1999**, *302*, 489.
(167) Sunderlin, L. S.; Squires, R. R. *J. Am. Chem. Soc.* **1993**, *115*, 337.
(168) Torrent, M.; Solà, M.; Frenking, G. *Organometallics* **1999**, *18*, 2801.
(169) King, A. D.; King, R. B.; Yang, D. B. *J. Am. Chem. Soc.* **1981**, *103*, 2699.
(170) Slegeir, W. A. R.; Sapienza, R. S.; Rayford, R.; Lam, L. *Organometallics* **1982**, *1*, 1728.
(171) Weiller, B. H.; Liu, J.-P.; Grant, E. R. *J. Am. Chem. Soc.* **1985**, *107*, 1595.
(172) Ungváry, F. *Coord. Chem. Rev.* **1997**, *160*, 129.
(173) (a) Rubene, N. A.; Davydon, A. A.; Kravstov, A. V.; Ursheva, N. V.; Smol'yaninov, S. I. *Kinet. Catal. (Engl. Transl.)* **1976**, *17*, 400. (b) Tamaru, K. *Dynamic Heterogeneous Catalysis*; Academic Press: New York, 1978; p 121.
(174) Darensbourg, D. J.; Rokicki, A.; Darensbourg, M. Y. *J. Am. Chem. Soc.* **1981**, *103*, 3223.
(175) (a) Haynes, P.; Slaugh, L. H.; Kohnle, J. F. *Tetrahedron Lett.* **1970**, 365. (b) Hofman, K.; Schibsted, H. *Chem. Ber.* **1918**, *51*, 1389, 1398.
(176) Darensbourg, D. J.; Rokicki, A. *Organometallics* **1982**, *1*, 1685.
(177) Trautman, R. J.; Gross, D. C.; Ford, P. C. *J. Am. Chem. Soc.* **1985**, *107*, 2355.
(178) Pearson, R. G.; Mauermann, H. *J. Am. Chem. Soc.* **1982**, *104*, 500.
(179) (a) Bercaw, J. E.; Goh, L. Y.; Halpern, J. *J. Am. Chem. Soc.* **1972**, *94*, 6534. (b) Darensbourg, D. J.; Froelich, J. A. *Inorg. Chem.* **1978**, *17*, 3300. (c) Sweet, J. R.; Graham, W. A. G. *Organometallics* **1982**, *1*, 982.
(180) Catellani, M.; Halpern, J. *Inorg. Chem.* **1980**, *19*, 566.
(181) Clark, H. C.; Jacobs, W. J. *Inorg. Chem.* **1970**, *9*, 1229.
(182) (a) Kruck, T.; Hofler, M.; Noack, M. *Chem. Ber.* **1966**, *99*, 1153. (b) Clark, H. C.; Dixon, K. R.; Jacobs, W. J. *J. Am. Chem. Soc.* **1969**, *91*, 1346.
(183) (a) Ruelle, P.; Kesselring, U. W.; Nam-Tran, H. *J. Am. Chem. Soc.* **1986**, *108*, 371. (b) Ruelle, P. *J. Am. Chem. Soc.* **1987**, *109*, 1722.
(184) Hoffmann, R. *Angew. Chem.* **1982**, *94*, 725; *Angew. Chem., Int. Ed. Engl.* **1982**, *21*, 711.
(185) Lane, K. R.; Squires, R. R. *J. Am. Chem. Soc.* **1986**, *108*, 7187.
(186) Lane, K. R.; Sallans, L.; Squires, R. R. *J. Am. Chem. Soc.* **1986**, *108*, 4368.
(187) Eisenstein, O.; Maseras, F.; Lledós, A. *Chem. Rev.* **2000**, *100*, 601 (in this issue) and references therein.
(188) (a) Haynes, G. R.; Martin, R. L.; Hay, P. J. *J. Am. Chem. Soc.* **1992**, *114*, 28. (b) Maseras, F.; Koga, N.; Morokuma, K. *J. Am. Chem. Soc.* **1993**, *115*, 8313. (c) Maseras, F.; Li, X. K.; Koga, N.; Morokuma, K. *J. Am. Chem. Soc.* **1993**, *115*, 10974. (d) Maseras, F.; Koga, N.; Morokuma, K. *Organometallics* **1994**, *13*, 4003. (e) Maseras, F.; Duran, M.; Lledós, A.; Bertrán, J. *J. Am. Chem. Soc.* **1992**, *114*, 2922. (f) Maseras, F.; Lledós, A.; Costas, M.; Poblet, J. M. *Organometallics* **1996**, *15*, 2947. (g) Antinolo, A.; Carrillo-Hermosilla, F.; Fajardo, M.; Garcia-Yuste, S.; Otero, A.; Camanyes, S.; Maseras, F.; Moreno, M.; Lledós, A.; Lluch, J. M. *J. Am. Chem. Soc.* **1997**, *119*, 6107.
(189) Drouin, B. J.; Kukolich, S. G. *J. Am. Chem. Soc.* **1998**, *120*, 6774.
(190) (a) Brandes, K. H.; Jonassen, H. B. *Z. Anorg. Allg. Chem.* **1966**, *343*, 215. (b) Muetterties, E. L.; Watson, P. L. *J. Am. Chem. Soc.* **1978**, *100*, 6978.
(191) Sweaney, R. L. *J. Am. Chem. Soc.* **1981**, *103*, 2410.
(192) Pearson, R. G. *Trans. Am. Crystallogr. Assoc.* **1978**, *14*, 89.
(193) Ford, P. C.; Rinker, R. G.; Ungermann, C.; Laine, R. M.; Landis, V.; Moya, S. A. *J. Am. Chem. Soc.* **1978**, *100*, 4595.
(194) Bickelhaupt, F. M.; Ziegler, T.; Schleyer, P. v. R. *Organometallics* **1995**, *14*, 2288.
(195) King, A. D. Jr.; King, R. B.; Yang, D. B. *J. Am. Chem. Soc.* **1980**, *102*, 1028.
(196) Lewis, K. E.; Golden, D. M.; Smith, G. P. *J. Am. Chem. Soc.* **1984**, *106*, 3905.
(197) Yin, X.; Moss, J. R. *Coord. Chem. Rev.* **1999**, *181*, 27.
(198) Leitner, W. *Angew. Chem.* **1995**, *107*, 2391; *Angew. Chem., Int., Ed. Engl.* **1995**, *34*, 2207.

(199) (a) Jessop, P. G.; Ikariya, T.; Noyori, R. *Chem. Rev.* **1995**, *95*, 259. (b) Jessop, P. G.; Ikariya, T.; Noyori, R. *Nature* **1994**, *368*, 231.
(200) Leitner, W. *Coord. Chem. Rev.* **1996**, *153*, 257.
(201) Burgemeister, T.; Kastner, F.; Leitner, W. *Angew. Chem.* **1993**, *105*, 781; *Angew. Chem., Int. Ed. Engl.* **1993**, *32*, 739.
(202) Tsai, J.-C.; Nicholas, K. M. *J. Am. Chem. Soc.* **1992**, *114*, 5117.
(203) Graf. E.; Leitner, W. *J. Chem. Soc., Chem. Commun.* **1992**, 623.
(204) Fornika, R.; Görls, H.; Seeman, B.; Leitner, W. *J. Chem. Soc., Chem. Commun.* **1995**, 1479.
(205) Noyori, R.; Hashiguchi, S. *Acc. Chem. Res.* **1997**, *30*, 97.
(206) Leitner, W.; Dinjus, E.; Gassner, F. *J. Organomet. Chem.* **1994**, *475*, 257.
(207) Lindner, E.; Keppeler, B.; Wegner, P. *Inorg. Chim. Acta* **1997**, *258*, 97.
(208) Angermund, K.; Baumann, W.; Dinjus, E.; Fornika, R.; Görls, H.; Kessler, M.; Krüger, C.; Leitner, W.; Lutz, F. *Chem. Eur. J.* **1997**, *3*, 755.
(209) Vigalok, A.; Ben-David, Y.; Milstein, D. *Organometallics* **1996**, *15*, 1839.
(210) Kainz, S.; Koch, D.; Baumann, W.; Leitner, W. *Angew. Chem.* **1997**, *109*, 1699; *Angew. Chem., Int. Ed. Engl.* **1997**, *36*, 1628.
(211) Graf, E.; Leitner, W. *Chem. Ber.* **1996**, *129*, 91.
(212) Gassner, F.; Dinjus, E.; Görls, H.; Leitner, W. *Organometallics* **1996**, *15*, 2078.
(213) Gassner, F.; Leitner, W. *J. Chem. Soc., Chem. Commun.* **1993**, 1465.
(214) Fryzuk, M. D.; Piers, W. E.; Einstein, F. W. B.; Jones, T. *Can. J. Chem.* **1989**, *67*, 883.
(215) Hutschka, F.; Dedieu, A.; Eichberger, M.; Fornika, R.; Leitner, W. *J. Am. Chem. Soc.* **1997**, *119*, 4432.
(216) For recent reviews on the different coordination modes of CO_2 to TMs see ref 200 and Gibson, D. H. *Chem. Rev.* **1996**, *96*, 2063.
(217) (a) Calabrese, J. C.; Herskovitz, T.; Kinney, J. B. *J. Am. Chem. Soc.* **1983**, *105*, 5914. (b) Gambarotta, S.; Floriani, C.; Chiesi-Villa, A.; Guastini, C. *J. Am. Chem. Soc.* **1985**, *107*, 2985. (c) Aresta, M.; Nobile, C. F.; Albano, V. G.; Forni, E.; Manassero, M. *J. Chem. Soc., Chem. Commun.* **1975**, 636. (d) Gambarotta, S.; Arena, F.; Floriani, C.; Zanazzi, P. F. *J. Am. Chem. Soc.* **1982**, *104*, 5082. (e) Bristow, G. S.; Hitchcock, P. B.; Lappert, M. F. *J. Chem. Soc., Chem. Comunn.* **1981**, 1145.
(218) Sakaki, S.; Dedieu, A. *Inorg. Chem.* **1987**, *26*, 3278.
(219) Sakaki, S.; Aizawa, T.; Koga, N.; Morokuma, K.; Ohkubo, K. *Inorg. Chem.* **1989**, *28*, 103.
(220) Jegat, C.; Fouassier, M.; Tranquille, M.; Mascetti, J.; Tommasi, I.; Aresta, M.; Ingold, F.; Dedieu, A. *Inorg. Chem.* **1993**, *32*, 1279.
(221) Rosi, M.; Sgamellotti, A.; Tarantelli, F.; Floriani, C. *J. Organomet. Chem.* **1987**, *332*, 153.
(222) Sakaki, S.; Musashi, Y. *J. Chem. Soc., Dalton Trans.* **1994**, 3047.
(223) Sakaki, S.; Musashi, Y. *Int. J. Quantum Chem.* **1996**, *57*, 481.
(224) Musashi, Y.; Sakaki, S. *J. Chem. Soc., Dalton Trans.* **1998**, 577.
(225) Albright, T. A.; Burdett, J. K.; Whangbo, M.-H. *Orbital Interactions in Chemistry*; Wiley: New York, 1985.
(226) Sakaki, S.; Okhubo, K. *Inorg. Chem.* **1988**, *27*, 2020.
(227) Sakaki, S.; Okhubo, K. *Inorg. Chem.* **1989**, *28*, 2583.
(228) Sakaki, S.; Okhubo, K. *Organometallics* **1989**, *8*, 2970.
(229) Sakaki, S.; Musashi, Y. *Inorg. Chem.* **1995**, *34*, 1914.
(230) Koga, N.; Morokuma, K. *J. Phys. Chem.* **1990**, *94*, 5454.
(231) Hutschka, F.; Dedieu, A.; Leitner, W. *Angew. Chem.* **1995**, 107, 1905; *Angew. Chem., Int. Ed. Engl.* **1995**, *34*, 1742.
(232) (a) Ziegler, T.; Folga, E.; Bérces, A. *J. Am. Chem. Soc.* **1993**, *115*, 636. (b) Burger, B. J.; Thompson, M. E.; Cotter, W. D.; Bercaw, J. E. *J. Am. Chem. Soc.* **1990**, *112*, 1566 (c) Thompson, M. E.; Buxter, S. M.; Bulls, A. R.; Burger, B. J.; Nolan, M. C.; Santarsiero, B. D.; Schaefer, W. P.; Bercaw, J. E. *J. Am. Chem. Soc.* **1987**, *109*, 203. (d) Watson, P. L.; Parshall, G. W. *Acc. Chem. Res.* **1985**, *18*, 51. (e) Davis, J. A., Watson, P. L., Liebman, J. F., Greenberg, A., Eds. *Selective Hydrocarbon Activation*; VCH Publishers: New York, 1990.
(233) Hutschka, F.; Dedieu, A. *J. Chem. Soc., Dalton Trans.* **1997**, 1899.
(234) Pomelli, C. S.; Tomasi, J.; Solà, M. *Organometallics* **1998**, *17*, 3164.
(235) Bo, C.; Dedieu, A. *Inorg. Chem.* **1989**, *28*, 304.
(236) (a) Jessop, P. G.; Hisao, Y.; Ikariya, T.; Noyori, R. *J. Am. Chem. Soc.* **1996**, *118*, 344. (b) Jessop, P. G.; Ikariya, T.; Noyori, R. *Science* **1995**, *269*, 1065. (c) Hitzler, M. G.; Poliakoff, M. *Chem. Commun.* **1997**, 1667. (c) Koch, D.; Leitner, W. *J. Am. Chem. Soc.* **1998**, *120*, 13398. (d) Jessop, P. G.; Ikariya, T.; Noyori, R. *Chem. Rev.* **1999**, *99*, 475.
(237) Fischer, F.; Tropsch, H. *Brennst.-Chem.* **1926**, *7*, 97. Fischer, F.; Tropsch, H. *Ber. Dtsch. Chem. Ges.* **1926**, *59*, 830.
(238) (a) Dry, M. E. *Appl. Catal., A* **1996**, *138*, 319. (b) Adesina, A. A. *Appl. Catal., A* **1996**, *138*, 345. (c) Adesina, A. A.; Hudgins, R. R.; Silveston, P. L. *Catal. Today* **1995**, *25*, 127.
(239) Herrmann, W. A. In *Applied Homogeneous Catalysis with Organometallic Compounds;* Cornils, B., Herrmann, W. A., Eds.; VCH: Weinheim, 1996; Vol. 2, p 747 f.
(240) Markó, L. *Transition Met. Chem.* **1992**, *17*, 587.
(241) Pruett, R. L. *Ann. N. Y. Acad. Sci.* **1977**, *295*, 239.
(242) Herrmann, W. A. *Angew. Chem.* **1982**, *94*, 118; *Angew. Chem., Int. Ed. Engl.* **1982**, *21*, 117.
(243) Knifton, J. F. *J. Am. Chem. Soc.* **1981**, *103*, 3959.
(244) (a) Nakamura, S.; Dedieu, A. *Chem. Phys. Lett.* **1984**, *111*, 243. (b) Dedieu, A.; Nakamura, S. In *Quantum Chemistry: The Challenge of Transition Metals and Coordination Chemistry*; Veillard, A., Ed.; NATO ASI Series; Reidel: Dordrecht, The Netherlands, 1986; Vol. 176, p 277. (c) Dedieu, A.; Sakaki, S.; Strich, A.; Siegbahn, P. E. M. *Chem. Phys. Lett.* **1987**, *133*, 317. (d) Axe, F. U.; Marynick, D. S. *Chem. Phys. Lett.* **1987**, *141*, 455. (e) Dedieu, A. In *The Challenge of d and f Electrons: Theory and Computation*; Salahub, D. R., Zerner, M. C., Eds.; ACS Symposium Series 384; American Chemical Society: Washington, DC, 1989; p 58. (f) Ziegler, T.; Versluis, L.; Tschinke, V. *J. Am. Chem. Soc.* **1986**, *108*, 612. (g) Rappé, A. K. *J. Am. Chem. Soc.* **1987**, *109*, 5605. (h) Tatsumi, K.; Nakamura, A.; Hofmann, P.; Stauffert, P.; Hoffmann, R. *J. Am. Chem. Soc.* **1985**, *107*, 4440. (i) Axe, F. U.; Marynick, D. S. *J. Am. Chem. Soc.* **1988**, *110*, 3728. (j) McKee, M. L.; Dai, C. H.; Worley, S. D. *J. Phys. Chem.* **1988**, *92*, 1056. (k) Pacchioni, G.; Fantucci, P.; Koutecky, J.; Ponec, V. *J. Catal.* **1988**, *112*, 34. (l) Henderson, M. A.; Worley, S. D. *J. Phys. Chem.* **1985**, *89*, 392.
(245) Rosi, M.; Sgamellotti, A.; Tarantelli, F.; Floriani, C. *J. Chem. Soc., Dalton Trans.* **1988**, 249.
(246) Koga, N.; Morokuma, K. *Organometallics* **1991**, *10*, 946.
(247) (a) Isobe, K.; Andrews, D. G.; Mann, B. E.; Maitlis, P. M. *J. Chem. Soc., Chem. Commun.* **1981**, 809. (b) Isobe, K.; Vazquez de Miguel, A.; Bailey, P. M.; Okeya, S.; Maitlis, P. M. *J. Chem. Soc., Dalton Trans.* **1983**, 1441. (c) Saez, I. M.; Meanwell, N. J.; Nutton, A.; Isobe, K.; Vazquez de Miguel, A.; Bruce, D. W.; Okeya, S.; Andrews, D. G.; Ashton, P. R.; Johnstone, I. R.; Maitlis, P. M. *J. Chem. Soc., Dalton Trans.* **1986**, 1565.
(248) (a) Ren-Hu, W.; Yin-Sheng, X. *J. Mol. Catal.* **1989**, *54*, 478. (b) Xiao-Guang, Z.; Yin-Sheng, X.; Xie-Xian, G. *J. Mol. Catal.* **1988**, *43*, 381. (c) Zheng Ping, H.; Tian Wei, Z.; Li Dun, A. *Chin. Chem. Lett.* **1994**, *5*, 511.
(249) Parshall, G. W.; Steven, D. I. In *Homogeneous Catalysis. The applications and Chemistry of Catalysis by Soluble Transition Metal Complexes;* Wiley: New York, 1992; pp 25−50.
(250) (a) Osborn, J. A.; Jardine, F. H.; Young, J. F.; Wilkinson, G. *J. Chem. Soc. A* **1966**, 1711. (b) Montelatici, S.; van der Ent, A.; Osborn, J. A.; Wilkinson, G. *J. Chem. Soc. A* **1968**, 1054. (c) O'Connor, C.; Wilkinson, G. *J. Chem. Soc. A* **1968**, 2665. (d) Jardine, F. H.; Osborn, J. A.; Wilkinson, G. *J. Chem. Soc. A* **1967**, 1574.
(251) Young, J. F.; Osborn, J. A.; Jardine, F. H.; Wilkinson, G. *Chem. Commun.* **1965**, 131.
(252) Brown, J. M. *Chem. Soc. Rev.* **1993**, 25.
(253) Chan, A. S. C.; Halpern, J. *J. Am. Chem. Soc.* **1980**, *102*, 838.
(254) Halpern, J. *Inorg. Chim. Acta* **1981**, *50*, 11.
(255) Landis, C. R.; Halpern, J. *J. Am. Chem. Soc.* **1987**, *109*, 1746.
(256) Halpern, J. In *Asymmetric Synthesis*; Morrison, J. D., Ed.; Academic Press: New York, 1985; Vol. 5, p 41.
(257) (a) Halpern, J.; Wong, C. S. *J. Chem. Soc., Chem. Commun.* **1973**, 629. (b) Halpern, In J. *Organotransition Metal Chemistry*; Ishii, Y., Tsutsui, M., Eds.; Plenum: New York, 1975; p 109. (c) Halpern, J.; Okamoto, T.; Zakhariev, A. *J. Mol. Catal.* **1976**, *2*, 65.
(258) Tolman, C. A.; Meakin, P. Z.; Lindner, D. L.; Jesson, J. P. *J. Am. Chem. Soc.* **1974**, *96*, 2762.
(259) (a) Koga, N.; Daniel, C.; Han, J.; Fu, X. Y.; Morokuma, K. *J. Am. Chem. Soc.* **1987**, *109*, 3455. (b) Daniel, C.; Koga, N.; Han, J.; Fu, X. Y.; Morokuma, K. *J. Am. Chem. Soc.* **1988**, *110*, 3773.
(260) (a) Brown, J. M.; Chaloner, P. A.; Morris, G. A. *J. Chem. Soc., Perkin Trans. 2* **1987**, 1583. (b) Brown, J. M.; Evans, P. L.; Lucy, A. R. *J. Chem. Soc., Perkin Trans. 2* **1987**, 1589. (c) Brown, J. M.; Evans, P. L. *Tetrahedron* **1988**, *44*, 4905.
(261) Duckett, S. B.; Newell, C. L.; Eisenberg, R. *J. Am. Chem. Soc.* **1994**, *116*, 10548.
(262) Strauss, S. H.; Shriver, D. F. *Inorg. Chem.* **1978**, *17*, 3069.
(263) Wink, D. A.; Ford, P. C. *J. Am. Chem. Soc.* **1987**, *109*, 436.
(264) Esteruelas, M. A.; Oro, L. A. *Chem. Rev.* **1998**, *98*, 577.
(265) (a) Dedieu. A.; Strich, A. *Inorg. Chem.* **1979**, *18*, 2941. (b) Dedieu, A. *Inorg. Chem.* **1980**, *19*, 375. (c) Dedieu, A. *Inorg. Chem.* **1981**, *20*, 2803. (d) Dedieu, A.; Hyla-Krispin, I. *J. Organomet. Chem.* **1981**, *220*, 115.
(266) For more detailed reviews on these works see: (a) Reference 86. (b) Dedieu, A.; Strich, A.; Rossi, A. In *Quantum Theory of Chemical Reactivity*; Daudel, R., Pullman, A., Salem, A., Veillard, A., Eds.; Reidel: Dordrecht, The Netherlands, 1981; Vol. 2, p 193.
(267) Roe, R. C. *J. Am. Chem. Soc.* **1983**, *105*, 7770.
(268) Koga, N.; Morokuma, K. In *The Challenge of d and f Electrons: Theory and Computation*; Salahub, D. R., Zerner, M. C., Eds.; ACS Symposium Series 394; American Chemical Society: Washington, DC, 1989; pp 77−91.
(269) Koga, N.; Obara, S.; Kitaura, K.; Morokuma, K. *J. Am. Chem. Soc.* **1985**, *107*, 7109.

(270) (a) Siegbahn, P. E. M. *J. Am. Chem. Soc.* **1993**, *115*, 5803. (b) Siegbahn, P. E. M. *Chem. Phys. Lett.* **1993**, *205*, 290 (c) Siegbahn, P. E. M. *J. Organomet. Chem.* **1994**, *478*, 83.
(271) Demortier, Y.; de Aguirre, I. *Bull. Soc. Chim. Fr.* **1974**, 1619.
(272) (a) Maienza, F.; Wörle, M.; Steffanut, P.; Mezzetti, A.; Spindler, F. *Organometallics* **1999**, *18*, 1041. (b) Lightfoot, A.; Schnider, P.; Pfaltz, A. *Angew. Chem.* **1999**, *110*, 3047; *Angew. Chem., Int. Ed. Engl*. **1999**, *37*, 2897.
(273) Bogdan, P. L.; Irwin, J. J.; Bosnich, B. *Organometallics* **1989**, *8*, 1450.
(274) Brown, J. M.; Evans, P. L. *Tetrahedron* **1988**, *44*, 4905.
(275) Margl, P.; Ziegler, T.; Blöchl, P. E. *J. Am. Chem. Soc.* **1995**, *117*, 12625.
(276) Musaev, D. G.; Mebel, A. M.; Morokuma, K. *J. Am. Chem. Soc.* **1994**, *116*, 10693.
(277) Dorigo, A. E.; Schleyer, P. v. R. *Angew. Chem.* **1995**, *107*, 108; *Angew. Chem., Int. Ed. Engl*. **1995**, *34*, 115.
(278) Poli, R. *Chem. Rev.* **1996**, *96*, 2135.
(279) Benson, M. T.; Cundari, T. R. *Inorg. Chim. Acta* **1997**, *259*, 91.
(280) (a) Duca, D.; Baranyai, P.; Vidóczy, T. *J. Comput. Chem.* **1998**, *19*, 396. (b) Duca, D.; La Manna, G.; Russo, M. R. *Phys. Chem. Chem. Phys.* **1999**, *1*, 1375.
(281) Criegee, R.; Marchand, B.; Wannowius, H. *Liebigs Ann. Chem.* **1942**, *550*, 99.
(282) (a) Sharpless, K. B.; Teranishi, A. Y.; Bäckvall, J.-E. *J. Am. Chem. Soc*. **1977**, *99*, 3120. (b) Hentges, S. G.; Sharpless, K. B. *J. Am. Chem. Soc*. **1980**, *102*, 4263. (c) Jacobsen, E. N.; Markó, I.; Mungall, W. S.; Schröder, G.; Sharpless, K. B. *J. Am. Chem. Soc*. **1988**, *110*, 1968. (d) Norrby, P. O.; Becker. H.; Sharpless, K. B.. *J. Am. Chem. Soc*. **1996**, *118*, 35.
(283) Göbel, T.; Sharpless, K. B. *Angew. Chem*. **1993**, *105*, 1417; *Angew. Chem., Int. Ed. Engl.* **1993**, *32*, 1329.
(284) (a) Corey, E. J.; Jardine, P. D.; Virgil, S.; Yuen, P.-W.; Connell, R. D. *J. Am. Chem. Soc.* **1989**, *111*, 9243. (b) Corey, E. J.; Lotto, G. I. *Tetrahedron Lett*. **1990**, *31*, 2665. (c) Corey, E. J.; Noe, M. C.; Sarshar, S. *J. Am. Chem. Soc*. **1993**, *115*, 3828. (d) Corey, E. J.; Noe, M. C. *J. Am. Chem. Soc.* **1996**, *118*, 319. (e) Corey, E. J.; Noe, M. C.; Grogan M. J. *Tetrahedron Lett.* **1996**, *37*, 4899. (f) Corey, E. J.; Noe, M. C. *J. Am. Chem. Soc*. **1996**, *118*, 11038.
(285) Jørgensen, K. A.; Hoffmann, R. *J. Am. Chem. Soc*. **1986**, *108*, 1867.
(286) Veldkamp, A.; Frenking, G. *J. Am. Chem. Soc*. **1994**, *116*, 4937.
(287) (a) Norrby, P.-O.; Kolb, H. C.; Sharpless, K. B. *Organometallics* **1994**, *13*, 344. (b) Norrby, P.-O.; Kolb, H. C.; Sharpless, K. B. *J. Am. Chem. Soc*. **1994**, *116*, 8470.
(288) Pidun, U.; Boehme, C.; Frenking, G. *Angew. Chem*. **1996**, *108*, 3008; *Angew. Chem., Int. Ed. Engl.* **1996**, *35*, 2817.
(289) Dapprich, S.; Ujaque, G.; Maseras, F.; Lledós, A.; Musaev, D. G.; Morokuma, K. *J. Am. Chem. Soc*. **1996**, *118*, 11660.
(290) Torrent, M.; Deng, L.; Duran, M.; Solà, M.; Ziegler, T. *Organometallics* **1997**, *16*, 13.
(291) Del Monte, A. J.; Haller, J.; Houk, K. N.; Sharpless, K. B.; Singleton, D. A.; Straβner, T.; Thomas, A. A. *J. Am. Chem. Soc*. **1997**, *119*, 9907.
(292) Ujaque, G.; Maseras, F.; Lledós, A. *J. Am. Chem. Soc*. **1999**, *121*, 1317.
(293) Ujaque, G.; Maseras, F.; Lledós, A. *J. Org. Chem*. **1997**, *62*, 7892.
(294) Ujaque, G. Ph.D. Thesis, Universitat Autònoma de Barcelona, Barcelona, Spain, 1999, Chapter 2.
(295) (a) Gable, K. P.; Phan, T. N. *J. Am. Chem. Soc*. **1994**, *116*, 833. (b) Gable, K. P.; Juliette, J. J. J. *J. Am. Chem. Soc.* **1995**, *117*, 955. (c) Gable, K. P.; Juliette, J. J. J. *J. Am. Chem. Soc*. **1996**, *118*, 2625. (d) Gable, K. P. *Adv. Organomet. Chem*. **1997**, *41*, 127. (e) Gable, K. P.; AbuBaker, A.; Zientara, K.; Wainwright, A. M. *Organometallics* **1999**, *18*, 173.
(296) (a) Romão, C. C.; Kühn, F. E.; Herrmann W. A. *Chem. Rev*. **1997**, *97*, 3197. (b) Herrmann, W. A.; Kühn, F. E. *Acc. Chem. Res*. **1997**, *30*, 169. (c) Herrmann, W. A. *J. Organomet. Chem*. **1995**, *500*, 149. (c) Herrmann, W. A.; Fischer, R W.; Marz, D. W. *Angew. Chem*. **1991**, *103*, 1706; *Angew. Chem., Int. Ed. Engl*. **1991**, *30*, 1638. (d) Herrmann, W. A.; Fischer, R. W.; Scherer, W.; Rauch, M. U. *Angew. Chem*. **1993**, *105*, 1209; *Angew. Chem., Int. Ed. Engl*. **1993**, *32*, 1157.
(297) Commereuc, D. *J. Chem. Soc., Chem. Commun*. **1995**, 791.
(298) Sharpless, K. B.; Teranishi, A. Y.; Bäckvall, J.-E. *J. Am. Chem. Soc*. **1977**, *99*, 3120.
(299) Pietsch, M. A.; Russo, T. V.; Murphy, R. B.; Martin, R. L.; Rappé, A. K. *Organometallics* **1998**, *17*, 2716.
(300) Deubel, D. V.; Frenking, G. *J. Am. Chem. Soc*. **1999**, *121*, 2021.
(301) Schlecht, S.; Deubel, D. V.; Dehnicke, K.; Frenking, G., to be published.
(302) (a) Herrmann, W. A.; Küsthardt, U.; Ziegler, M. L.; Zahn, T. *Angew. Chem*. **1985**, *97*, 857; *Angew. Chem., Int. Ed. Engl*. **1985**, *24*, 860. (b) Küsthardt, U.; Herrmann, W. A.; Ziegler, M. L.; Zahn, T.; Nuber, B. *J. Organomet. Chem*. **1986**, *311*, 163. (c) Herrmann, W. A.; Poesky, P. W.; Scherer, W.; Kleine, M. *Organometallics* **1994**, *13*, 4536.
(303) Sheldon, R. A. In *Applied Homogeneous Catalysis with Organometallic Compounds*; Cornils, B., Herrmann, W. A., Eds.; VCH: Weinheim, 1996; Vol. 1, p 411 f.
(304) Sheldon, R. A. *Recl. Trav. Chim. Pays-Bas* **1973**, *253*, 367.
(305) Chong, A. O.; Sharpless, K. B. *J. Org. Chem*. **1977**, *42*, 1587.
(306) (a) Mimoun, H. *J. Mol. Catal*. **1980**, *7*, 1. (b) Mimoun, H. *Angew. Chem., Int. Ed. Engl.* **1982**, *2*, 734. (c) Mimoun, H.; Mignard, M.; Brechot, P.; Saussine, L. *J. Am. Chem. Soc*. **1986**, *108*, 3711. (d) Mimoun, H. *Catal. Today* **1987**, *1*, 297.
(307) Jørgensen, K. A.; Schiøtt, B. *Chem. Rev*. **1990**, *90*, 1483.
(308) Bäckvall, J.-E.; Bökman, F.; Blomberg, M. R. A. *J. Am. Chem. Soc*. **1992**, *114*, 534.
(309) Bach, R. D.; Wolber, G. J.; Coddens, B. A. *J. Am. Chem. Soc*. **1984**, *106*, 6098.
(310) Jørgensen, K. A.; Hoffmann, R. *Acta Chem. Scand*. **1986**, *B40*, 411.
(311) Filotov, M. J.; Shalyaev, K. V.; Talsi, E. P. *J. Mol. Catal*. **1994**, *87*, L5.
(312) Salles, L.; Piquemal, J.-Y.; Thouvenot, R.; Minot, C.; Brégeault, J.-M. *J. Mol. Catal.* **1997**, *117*, 375.
(313) Gisdakis, P.; Antonczak, S.; Köstlmeier, S.; Herrmann, W. A.; Rösch, N. *Angew. Chem*. **1998**, 110, 2333; *Angew. Chem., Int. Ed. Engl*. **1998**, *37*, 2211.
(314) Fantucci, P.; Lolli, S.; Pizzotti, M.; Ugo, R. *Inorg. Chim. Acta* **1998**, *270*, 479.
(315) (a) Ishii, Y.; Yamawaiki, K.; Yoshida, T.; Ura, T.; Ogawa, M. *J. Org. Chem*. **1987**, 52, 1868. (b) Carey, F. A.; Sundberg, R. J. *Advanced Organic Chemistry*; Plenum: New York, 1977. (c) Lee, D. G. In *Oxidation in Organic Chemistry*; Trahanovsky, W. S., Ed.; Academic Press: New York, 1973; Part B. (d) Lee, D. G.; van den Engh, M. *Can. J. Chem*. **1972**, *50*, 3129. (e) Singh, H. K. In *Cytochrome P-450: Structure, Mechanism, and Biochemistry*; Ortiz de Montellano, P. R., Ed.; Plenum: New York, 1986. (f) Stewart, R. In *Oxidation in Organic Chemistry*; Wiberg, K. B., Ed.; Academic Press: New York, 1965; Part A, pp 1−68. (g) House, H. O. In *Modern Synthetic Reactions*; Benjamin: Menlo Park, CA, 1972; pp 257−291. (h) Walba, D. M.; Wand, M. D.; Wilkes, M. C. *J. Am. Chem. Soc*. **1979**, *101*, 4398. (i) Baldwin, J. E.; Crossley, M. L.; Lehtonen, E. M. *J. Chem. Soc., Chem. Commun*. **1979**, 918. (j) Klein, E.; Rojahn, W. *Tetrahedron* **1965**, *21*, 2353. (k) Schröder, M. *Chem. Rev*. **1980**, *80*, 107. (l) Sharpless, K. B.; Chong, C. A.; Oshima, K. J. *J. Org. Chem*. **1976**, *41*, 177. (m) Herranz, E.; Sharpless, K. B. *J. Org. Chem*. **1978**, *43*, 2544. (n) Herranz, E.; Biller, S. A.; Sharpless, K. B. *J. Am. Chem. Soc*. **1978**, *100*, 3596. (o) Herranz, E.; Sharpless, K. B. *J. Org. Chem*. **1980**, *45*, 2710.
(316) (a) Limberg, C.; Köppe, R. *Inorg. Chem.* **1999**, *38*, 2106. (b) Limberg, C.; Cunskis, S.; Frick, A. *Chem. Commun*. **1998**, 225.
(317) (a) Étard, M. A.; Moissan, H. M. *C. R. Hebd. Seances Acad. Sci*. **1893**, *116*, 434. (b) Cristol, S. J.; Eilar, K. R. *J. Am. Chem. Soc*. **1950**, *72*, 4353. (c) Stairs, R. A.; Diaper, D. G. M.; Gatzke, A. L. *Can. J. Chem*. **1963**, *41*, 1059. (d) Freeman, F.; Cameron, P. J.; DuBois, R. H. *J. Org. Chem*. **1968**, *33*, 3970. (e) Gatzke, A. L.; Stairs, R. A.; Diaper, D. G. M. *Can. J. Chem*. **1968**, *46*, 3695. (f) Freeman, F.; DuBois, R. H.; Yamachika, N. J. *Tetrahedron* **1969**, *25*, 3441. (g) Bachelor, F. W.; Cheriyan, U. O. *Can. J. Chem*. **1972**, *50*, 4022. (h) Freeman, F. *Chem. Rev*. **1975**, *75*, 439. (i) Freeman, F. In *Organic Synthesis by Oxidation with Metal Compounds*; Mijs, W. J., de Jonge, C. R. H. I., Eds.; Plenum: New York, 1986; Chapter 2, pp 41−118.
(318) (a) Torrent, M. Ph.D. Thesis, Universitat de Girona, Girona, Spain, 1998, Chapter 8. (b) Torrent, M.; Deng, L.; Duran, M.; Solà, M.; Ziegler, T. *Can. J. Chem*. **1999**, *77*, 1476. (c) Limberg, C.; Witsuba, T. *J. Org. Chem.* **1999**, *64*, 6169.
(319) (a) Bäckvall, J.-E.; Young, M. W.; Sharpless, K. B. *Tetrahedron Lett*. **1977**, *40*, 3523. (b) Schlecht, M. F.; Kim, H.-J. *Tetrahedron Lett*. **1986**, *27*, 4889. (c) Schlecht, M. F.; Kim, H.-J. *J. Org. Chem*. **1989**, *54*, 583.
(320) (a) Mansuy, D.; Leclaire, J.; Fontecave, M.; Dausette, P. *Tetrahedron* **1984**, *40*, 2847. (b) Collman, J. P.; Brauman, J. I.; Meunier, B.; Raybuck, S. A.; Kodadek, T. *Proc. Natl. Acad. Sci. U.S.A.* **1984**, *81*, 3245. (c) Ortiz de Montellano, P. R.; Komives, E. A. *J. Biol. Chem*. **1985**, *260*, 3330. (d) Collman, J. P.; Brauman, J. I.; Meunier, B.; Hayashi, T.; Kodadek, T.; Raybuck, S. A. *J. Am. Chem. Soc*. **1985**, *107*, 2000. (e) Groves, J. T.; Watanabe, Y. *J. Am. Chem. Soc*. **1986**, *108*, 507. (f) Komives, E. A.; Ortiz de Montellano, P. R. *J. Biol. Chem*. **1987**, *262*, 9793.
(321) Samsel, E. G.; Srinivasan, K.; Kochi, J. K. *J. Am. Chem. Soc*. **1985**, *107*, 7606.
(322) Barrett, A. G. M.; Barton, D. H. R.; Tsushima, T. *J. Chem. Soc., Perkin Trans*. **1980**, *1*, 639.
(323) Groves, J. T.; Nemo, T. E. *J. Am. Chem. Soc*. **1983**, *105*, 5786.
(324) (a) Rappé, A. K.; Goddard, W. A. *J. Am. Chem. Soc*. **1980**, *102*, 5114. (b) *ibid*. **1982**, *104*, 3287. (c) Upton, T. H.; Rappé, A. K. *J. Am. Chem. Soc*. **1985**, *107*, 1206.
(325) Rappé, A. K.; Goddard, W. A. *Nature* **1980**, *285*, 311.
(326) Yamaguchi, K.; Tekahara, Y.; Fueno, T. In *Applied Quantum Chemistry*; Smith, V. H., Schaefer, H. F., Morokuma, K., Eds.; D. Reidel: Dordrecht, The Netherlands, 1986.

(327) (a) Walba, D. M.; DePuy, C. H.; Grabowski, J. J.; Bierbaum, V. M. *Organometallics* **1984**, *3*, 498. (b) Kang, H.; Beauchamp, J. L. *J. Am. Chem. Soc.* **1979**, *101*, 6449.
(328) (a) Calhorda, M. J.; Galvão, A. M.; Ünaleroglu, C.; Zlota, A. A.; Frolow, F.; Milstein, D. *Organometallics* **1993**, *12*, 3316. (b) Bakos, J.; Orosz, Á.; Cserépi, S.; Tóth, I.; Sinou, D. *J. Mol. Catal., A* **1997**, *116*, 85. (c) de Bruin, B.; Boerakker, M. J.; Donners, J. J. J. M.; Christiaans, B. E. C.; Schlebos, P. P. J.; de Gelder, R.; Smits, J. M. M.; Spek, A. L.; Gal, A. W. *Angew. Chem.* **1997**, *109*, 2153; *Angew. Chem., Int. Ed. Engl.* **1997**, *36*, 2064.
(329) Day, V. W.; Klemperer, W. G.; Lockledge, S. P.; Main, D. J. *J. Am. Chem. Soc.* **1990**, *112*, 2031.
(330) Baba, S.; Ogura, T.; Kawaguchi, S. *J. Chem. Soc., Chem. Commun.* **1972**, 910.
(331) Lenarda, M.; Pahor, N. B.; Calligaris, M.; Graziani, M.; Randaccio, L. *J. Chem. Soc., Dalton Trans.* **1978**, 279.
(332) (a) Ebbinghaus, B. B. *Combust. Flame* **1995**, *101*, 311. (b) Limberg, C.; Köppe, R.; Schnöckel, H. *Angew. Chem.* **1998**, *110*, 512; *Angew. Chem., Int. Ed. Engl.* **1998**, *37*, 496.
(333) Torrent, M.; Deng, L.; Ziegler, T. *Inorg. Chem.* **1998**, *37*, 1307.
(334) For recent reviews see: (a) Irvine, G. J.; Lesley, M. J. G.; Marder, T. B.; Norman, N. C.; Rice, C. R.; Robins, E. G.; Roper, W. R.; Whittell, G. R.; Wright, L. J. *Chem. Rev.* **1998**, *98*, 2685. (b) Braunscheig, H. *Angew. Chem.* **1998**, *110*, 1882; *Angew. Chem., Int. Ed. Engl.* **1998**, *37*, 1786. (c) Wadepohl, H. *Angew. Chem.* **1997**, *109*, 2547; *Angew. Chem., Int. Ed. Engl.* **1997**, *36*, 2441.
(335) (a) Kerr, A.; Marder, T. B.; Norman, N. C.; Orpen, A. G.; Quayle, M. J.; Rice, C. R.; Timms, P. L.; Whittell, G. R. *Chem. Commun.* **1998**, 319. (b) Braunscheig, H.; Kollman, C.; Müller, M. *Eur. J. Inorg. Chem.* **1998**, 291. (c) Muhoro, C. N.; Hartwig, J. F. *Angew. Chem* **1997**, *109*, 1536; *Angew. Chem., Int. Ed. Engl.* **1997**, *36*, 1510. (d) Cowley, A. H.; Lomelí, V.; Voigt, A. *J. Am. Chem. Soc.* **1998**, *120*, 6401. (e) Braunscheig, H.; Ganter, B. *J. Organomet. Chem.* **1997**, 163. (f) Braunscheig, H.; Müller, M. *Chem. Ber.* **1997**, *130*, 1295. (g) Braunscheig, H.; Kollman, C.; Englert, U. *Eur. J. Inorg. Chem.* **1998**, 465.
(336) (a) Brown, H. C. *Boranes in Organic Chemistry*; Cornell University Press: London, 1972. (b) Brown, H. C. *Organic Synthesis via Organoboranes*; Wiley-Interscience: New York, 1975. (c) Pelter, A.; Smith, K.; Brown, H. C. *Borane Reagents*; Academic Press: New York, 1988. (d) Evans, D. A.; Fu, G. C. *J. Org. Chem.* **1990**, *55*, 2280. (e) Evans, D. A.; Fu, G. C. *J. Am. Chem. Soc.* **1991**, *113*, 4042. (f) Evans, D. A.; Fu, G. C.; Hoveyda, A. H. *J. Am. Chem. Soc.* **1992**, *114*, 6671. (g) Evans, D. A.; Fu, G. C.; Anderson, B. A. *J. Am. Chem. Soc.* **1992**, *114*, 6679. (h) Burgess, K.; Cassidy, J.; Ohlmeyer, M. J. *J. Org. Chem.* **1991**, *56*, 1020. (i) Burgess, K.; Ohlmeyer, M. J. *J. Org. Chem.* **1991**, *56*, 1027. (j) Burgess, K.; Ohlmeyer, M. J. *Tetrahedron Lett.* **1989**, *30*, 395. (k) Burgess, K.; Ohlmeyer, M. J. *Tetrahedron Lett.* **1989**, *30*, 5857. (l) Burgess, K.; Ohlmeyer, M. J. *Tetrahedron Lett.* **1989**, *30*, 5861. (m) Burgess, K.; van der Donk, W. A.; Jarstfer, M. B.; Ohlmeyer, M. J. *J. Am. Chem. Soc.* **1991**, *113*, 6139. (n) Satoh, M.; Nomoto, Y.; Miyaura, N.; Suzuki, A. *Tetrahedron Lett.* **1989**, *30*, 3789. (o) Satoh, M.; Miyaura, N. Suzuki, A. *Tetrahedron Lett.* **1990**, *31*, 231. (p) Brown, J. M.; Lloyd-Jones, G. C. *Tetrahedron: Asymmetry* **1990**, *1*, 869. (q) Hayashi, T.; Matsumoto, Y.; Ito, Y. *J. Am. Chem. Soc.* **1989**, *111*, 3426. (r) Hayashi, T.; Matsumoto, Y.; Ito, Y. *Tetrahedron: Asymmetry* **1991**, *2*, 601. (s) Matsumoto, Y.; Hayashi, T. *Tetrahedron Lett.* **1991**, *32*, 3387. (t) Burgess, K.; Ohlmeyer, M. J. *J. Org. Chem.* **1988**, *53*, 5178. (u) Burgess, K.; van der Donk, W. A.; Ohlmeyer, M. J. *Tetrahedron: Asymmetry* **1991**, *2*, 613. (v) Zhang, J.; Lou, B.; Guo, G.; Dai, L. *J. Org. Chem.* **1991**, *56*, 1670. (w) Baker, R. T.; Ovenall, D. W.; Calabrese, J. C.; Westcott, S. A.; Taylor, N. J.; Williams, I. D.; Marder, T. B. *J. Am. Chem. Soc.* **1990**, *112*, 9399. (x) Baker, R. T.; Ovenall, D. W.; Harlow, R. L.; Westcott, S. A.; Taylor, N. J.; Marder, T. B. *Organometallics* **1990**, *9*, 3028. (y) Westcott, S. A.; Blom, H. P.; Marder, T. B.; Baker, R. T.; Calabrese, J. C. *Inorg. Chem.* **1993**, *32*, 2175. (z) Burgess, K.; Jaspars, M. *Organometallics* **1993**, *12*, 497. (aa) Burgess, K.; van der Donk, W. A.; Kook, A. M. *J. Org. Chem.* **1991**, *5*, 2949. (bb) Knorr, J. R.; Merola, J. S. *Organometallics* **1990**, *9*, 3008. (cc) Burgess, K.; van der Donk, W. A.; Wescott, S. A.; Marder, T. B.; Baker, R. T.; Calabrese, J. C. *J. Am. Chem. Soc.* **1992**, *114*, 9350. (dd) Crabtree, R. H.; Davis, M. W. *J. Org. Chem.* **1986**, *51*, 2655. (ee) Wescott, S. A.; Marder, T. B.; Baker, R. T. *Organometallics* **1993**, *12*, 975. (ff) Baker, R. T.; Calabrese, J. C.; Wescott, S. A.; Nguyen, P.; Marder, T. B. *J. Am. Chem. Soc.* **1993**, *115*, 4367. (gg) Hartwing, J. F.; Bhandari, S.; Rablen, P. R. *J. Am. Chem. Soc.* **1994**, *116*, 1839. (hh) He, X.; Hartwig, J. F. *J. Am. Chem. Soc.* **1996**, *118*, 1696. (ii) Bijpost, E. A.; Duchateau, R.; Teuben, J. H. *J. Mol. Catal., A* **1995**, *95*, 121. (jj) Gridnev, I. D.; Miyaura, N.; Suzuki, A. *Organometallics* **1993**, *12*, 589. (kk) Hewes, J. D.; Kreimendahl, C. W.; Marder, T. B.; Hawthorne, M. F. *J. Am. Chem. Soc.* **1984**, *106*, 5757.
(337) (a) Evans, D. A.; Fu, G. C.; Hoveyda, A. H. *J. Am. Chem. Soc.* **1988**, *110*, 6917. (b) Harrison, K. N.; Marks, T. J. *J. Am. Chem. Soc.* **1992**, *114*, 9221. (c) Männig, D.; Nöth, H. *Angew. Chem.* **1985**, *97*, 854; *Angew. Chem., Int. Ed. Engl.* **1985**, *24*, 878. (d) Westcott, S. A.; Taylor, N. J.; Marder, T. B.; Baker, R. T.; Jones, N. J.; Calabrese, J. C. *J. Chem. Soc., Chem. Commun.* **1991**, 304. (e) Westcott, S. A.; Blom, H. P.; Marder, T. B.; Baker, R. T. *J. Am. Chem. Soc.* **1992**, *114*, 8863. (f) Doucet, H.; Fernandez, E.; Layzell, T. P.; Brown, J. M. *Chem. Eur. J.* **1999**, *5*, 1320.
(338) (a) Pender, M. J.; Wideman, T.; Carroll, P. J.; Sneddon, L. G. *J. Am. Chem. Soc.* **1998**, *120*, 9108. (b) Garrett, C. E.; Fu, G. C. *J. Org. Chem.* **1998**, *63*, 1370. (c) Hou, X.-L.; Xie, Q.-C.; Dai, L.-X. *J. Chem. Res., Synop.* **1997**, 436. (d) Clark, G. R.; Irvine, G. J.; Roper, W. R.; Wright, L. J. *Organometallics* **1997**, *16*, 5499. (e) Lantero, D. R.; Ward, D. L.; Smith, M. R., III. *J. Am. Chem. Soc.* **1997**, *119*, 9699. (f) Juliette, J. J. J.; Horvath, I. T.; Gladysz, J. A. *Angew. Chem.* **1997**, *109*, 1682; *Angew. Chem., Int. Ed. Engl.* **1997**, *36*, 1610. (g) Pereira, S.; Srebnik, M. *Tetrahedron Lett.* **1996**, *37*, 3283. (h) Pereira, S.; Srebnik, M. *J. Am. Chem. Soc.* **1996**, *118*, 909. (i) Villiers, C.; Ephritikhine, M. *J. Chem. Soc., Chem. Commun.* **1995**, 979. (j) Fazen, P. J.; Sneddon, L. G. *Organometallics* **1994**, *13*, 2867.
(339) Musaev, D. G.; Morokuma, K. *J. Phys. Chem.* **1996**, *100*, 6509.
(340) Kulkarni, S. A.; Koga, N. *J. Mol. Struct.: THEOCHEM* **1999**, *461*−*462*, 297.
(341) (a) Ishiyama, T.; Matsuda, N.; Murata, M.; Ozawa, F.; Suzuki, A.; Miyaura, N. *Organometallics* **1996**, *15*, 713. (b) Ishiyama, T.; Yamamoto, M.; Miyaura, N. *Chem. Lett.* **1996**, 1117. (c) Ishiyama, T.; Yamamoto, M.; Miyaura, N. *Chem. Commun.* **1996**, 2073. (d) Iverson, C. N.; Smith, M. R., III. *Organometallics* **1997**, *16*, 2757. (e) Ishiyama, T.; Yamamoto, M.; Miyaura, N. *Chem. Commun.* **1997**, 689. (f) Clegg, W.; Johann, T.; Marder, T. B.; Norman, N. C.; Orpen, A. G.; Peakman, T.; Quayle, M. J.; Rice, C. R.; Scott, A. J. *J. Chem. Soc., Dalton Trans.* **1998**, 1431. (g) Lawson, Y. G.; Lesley, M. J. G.; Marder, T. B.; Norman, N. C.; Rice, C. R. *Chem. Commun.* **1997**, 2051. (h) Marder, T. B.; Norman, N. C.; Rice, C. R. *Tetrahedron Lett.* **1998**, *39*, 155. (i) Ishiyama, T.; Kitano, T.; Miyaura, N. *Tetrahedron Lett.* **1998**, *39*, 2357. (j) Maderna, A.; Pritzkow, H.; Siebert, W. *Angew. Chem.*, **1996**, *108*, 1664; *Angew. Chem., Int. Ed. Engl.* **1996**, *35*, 1501.
(342) (a) Ishiyama, T.; Matsuda, N.; Miyaura, N.; Suzuki, A. *J. Am. Chem. Soc.* **1993**, *115*, 11018. (b) Iverson, C. N.; Smith, M. R., III. *J. Am. Chem. Soc.* **1995**, *117*, 4403. (c) Suzuki, A. *Pure Appl. Chem.* **1994**, *66*, 213. (d) Gridnev, I. D.; Miyaura, N.; Suzuki, A. *Organometallics* **1993**, *12*, 589. (e) Lesley, G.; Nguyen, P.; Taylor, N. J.; Marder, T. B.; Scott, A. J.; Clegg, W.; Norman, N. C. *Organometallics* **1996**, *15*, 5137 and references therein. (f) Iverson, C. N.; Smith, M. R., III. *Organometallics* **1996**, *15*, 5155.
(343) (a) Chenard, B. L.; Van Zyl, C. M. *J. Org. Chem.* **1986**, *51*, 3561. (b) Murakami, M.; Amii, H.; Takizawa, N.; Ito, Y. *Organometallics* **1993**, *12*, 4223.
(344) Cui, Q.; Musaev, D. G.; Morokuma, K. *Organometallics* **1997**, *16*, 1355.
(345) Cui, Q.; Musaev, D. G.; Morokuma, K. *Organometallics* **1998**, *17*, 742.
(346) Cui, Q.; Musaev, D. G.; Morokuma, K. *Organometallics* **1998**, *17*, 1383.
(347) (a) Houk, K. N.; Rondan, N. G.; Wu, Y. D.; Metz, J. T.; Paddon-Row, M. N. *Tetrahedron* **1984**, *40*, 2257. (b) Van Eikema Hommes, N. J.; Schleyer, P. v. R. *J. Org. Chem.* **1991**, *56*, 4074.
(348) (a) Evans, D. A.; Fu, G. C.; Hoveyda, A. H. *J. Am. Chem. Soc.* **1992**, *114*, 6671. (b) Evans, D. A.; Fu, G. C.; Anderson, B. A. *J. Am. Chem. Soc.* **1992**, *114*, 6679.
(349) For reviews of metal-catalyzed hydroboration reactions see: (a) Burgess, K.; Ohlmeyer, M. J. *Chem. Rev.* **1991**, *91*, 1179. (b) Westcott, S. A.; Nguyen, P.; Blom, H. Taylor, N.; Marder, T. B.; Baker, R. T.; Calabrese, J. C. *Can. Spec. Publ.*−*R. Soc. Chem.* **1994**, *143*, 68. (c) Fu, G. C.; Evans, D. A.; Muci, A. R. *Adv. Catal. Processes* **1995**, *1*, 95. (d) Beletskaya, I.; Pelter, A. *Tetrahedron* **1997**, *53*, 4957. (e) Fu, G. C. In *Transition Metals in Organic Synthesis*; Beller, M., Bolm, C., Eds.; Wiley-VCH Verlag: Weinheim, 1998; Vol. 2, pp 141−146.
(350) Rablen, P. R.; Hartwig, J. F.; Nolan, S. P. *J. Am. Chem. Soc.* **1994**, *116*, 4121.
(351) Simões, J. A. M.; Beauchamp, J. L. *Chem. Rev.* **1990**, *90*, 629.
(352) (a) Skinner, H. *Adv. Organomet. Chem.* **1964**, *2*, 49. (b) McCoy, R. E.; Bauer, S. H. *J. Am. Chem. Soc.* **1956**, *78*, 2061. (c) Odom, J. D. In *Comprehensive Organometallic Chemistry*; Wilkinson, G., Stone, F. G. A., Abel, E. W., Eds.; Pergamon Press: Oxford, 1982; Vol. 1, p 257.
(353) Massey, A. G. *Adv. Inorg. Chem. Radiochem.* **1983**, *26*, 1.
(354) For a review of metal-catalyzed diboration see: Marder, T. B.; Norman, N. C. In *Topics in Catalysis*; Leitner, W., Blackmond, D. G., Eds.; Baltzer Science Publishers: Amsterdam, The Netherlands, 1998; Vol. 5, pp 63−73.
(355) (a) Clegg, W.; Dai, C.; Lawlor, F. J.; Lesley, G.; Marder, T. B.; Nguyen, P.; Norman, N. C.; Pickett, N. L.; Rice, C. R.; Robins, E. G.; Scott, A. J.; Taylor, N. J. *U.K. Spec. Publ.*−*R. Soc. Chem.* **1997**, *201*, 389. (b) Baker, R. T.; Nguyen, P.; Marder, T. B.; Wescott, S. A. *Angew. Chem.* **1995**, *107*, 1451; *Angew. Chem., Int. Ed. Engl.* **1995**, *34*, 1336. (c) Corcoran, E. W., Jr.; Sneddon, L. G. *J. Am. Chem. Soc.* **1985**, *107*, 7446.

(356) Sakaki, S.; Kikuno, T. *Inorg. Chem*. **1997**, *36*, 226.
(357) (a) Onozawa, S.-Y.; Hatanaka, Y.; Sakakura, T.; Shimada, S.; Tanaka, M. *Organometallics* **1996**, *15*, 5450. (b) Suginome, M.; Nakamura, H.; Ito, Y. *J. Chem. Soc., Chem. Commun*. **1996**, 2777. (c) Onozawa, S.-Y.; Hatanaka, Y.; Tanaka, M. *J. Chem. Soc., Chem. Commun*. **1997**, 1229. (d) Suginome, M.; Nakamura, H.; Ito, Y. *Angew. Chem.* **1997**, *109*, 2627; *Angew. Chem., Int. Ed. Engl*. **1997**, *36*, 2516. (e) Suzuki, A. *Jpn. Spec. Publ.—R. Soc. Chem*. **197**, *201*, 163. (f) Suzuki, A. *Jpn. Organomet. News* **1995**, 77.
(358) Howarth, J.; Helmchen, G.; Kiefer, M. *Tetrahedron Lett*. **1993**, *34*, 4095.
(359) Ishiyama, T.; Nishijima, K.; Miyaura, N.; Suzuki, A. *J. Am. Chem. Soc*. **1993**, *115*, 7219.
(360) (a) Weidenbruch, M. *Coord. Chem. Rev*. **1994**, *130*, 275. (b) Liu, C.-S.; Hwang, T.-L. *Adv. Inorg. Chem*. **1985**, *29*, 1.
(361) (a) Gehrhus, B.; Hitchcock, P. B.; Lappert, M. F.; Heinicke, J.; Boese, R.; Bläser, D. *J. Organomet. Chem*. **1996**, *521*, 211. (b) Yamashita, H.; Reddy, N. P.; Tanaka, M. *Macromolecules* **1993**, *26*, 2143. (c) Suginome, M.; Iwanami, T.; Matsumoto, A.; Ito, Y. *Tetrahedron: Asymmetry* **1997**, *8*, 859. (d) Yamashita, H.; Tanaka, M. *Chem. Lett.* **1992**, 1547. (e) Yamashita, H.; Catellani, M.; Tanaka, M. *Chem. Lett.* **1991**, 241.
(362) Klinkhammer, K. W.; Schwarz, W. *Angew. Chem.* **1995**, *107*, 1448; *Angew. Chem., Int. Ed. Engl.* **1995**, *34*, 1334.
(363) Arif, M. A.; Cowley, A. H.; Elkins, T. M. *J. Organomet. Chem.* **1987**, *325*, C11.
(364) (a) Davidson, P. J.; Harris, D. H.; Lappert, M. F. *J. Chem. Soc., Dalton Trans.* **1976**, 2268. (b) Goldberg, D. E.; Hitchcock, P. B.; Lappert, M. F.; Thomas, K. M.; Thorne, A. J.; Fjeldberg, T.; Haaland, A.; Schilling, B. E. R. *Ibid.* **1986**, 2387. (c) Onozawa, S.-Y.; Hatanaka, Y.; Choi, N.; Tanaka, M. *Organometallics* **1997**, *16*, 5389.
(365) Weidenbruch, M.; Kilian, H.; Peters, K.; von Schnering, H. G.; Marsmann, H. *Chem. Ber.* **1995**, *128*, 983.
(366) Jonas, V.; Frenking, G.; Reetz, M. T. *J. Comput. Chem.* **1992**, *13*, 919.
(367) Frenking, G.; Antes, I.; Boehme, M.; Dapprich, S.; Ehlers, A. W.; Jonas, V.; Neuhaus, A.; Otto, M.; Stegmann, R.; Veldkamp, A.; Vyboishchikov, S. F. In *Reviews in Computational Chemistry*, Lipkowitz, K. B., Boyd, D. B., Eds.; VCH: New York, 1996; Vol. 8, pp 63−144.
(368) Couty, M.; Hall, M. B. *J. Comput. Chem.* **1996**, *17*, 1359.
(369) Hay P. J.; Wadt, W. R. *J. Chem. Phys.* **1985**, *82*, 299.
(370) The latest version is Gaussian 98: Frisch, M. J.; Trucks, G. W.; Schlegel, H. B.; Scuseria, G. E.; Robb, M. A.; Cheeseman, J. R.; Zakrzewski, V. G.; Montgomery, J. A.; Stratmann, R. E.; Burant, J. C.; Dapprich. S.; Milliam, J. M.; Daniels, A. D.; Kudin, K. N.; Strain, M. C.; Farkas, O.; Tomasi, J.; Barone, V.; Cossi, M.; Cammi, R.; Mennucci, B.; Pomelli, C.; Adamo, C.; Clifford, S.; Ochterski, J.; Petersson, G. A.; Ayala, P. Y.; Cui, Q.; Morokuma, K.; Malick, D. K.; Rabuck, A. D.; Raghavachari, K.; Foresman, J. B.; Cioslowski, J.; Ortiz, J. V.; Stefanov, B. B.; Liu, G.; Liashenko, A.; Piskorz, P.; Komaromi, I.; Gomberts, R.; Martin, R. L.; Fox, D. J.; Keith, T. A.; Al-Laham, M. A.; Peng, C. Y.; Nanayakkara, A.; Gonzalez, C.; Challacombe, M.; Gill, P. M. W.; Johnson, B. G.; Chen, W.; Wong, M. W.; Andres, J. L.; Head-Gordon, M.; Replogle, E. S.; Pople, J. A. Gaussian Inc., Pittsburgh, PA, 1998.
(371) Ehlers, A. W.; Böhme, M.; Dapprich, S.; Gobbi, A.; Höllwarth, A.; Jonas, V.; Köhler, K. F.; Stegmann, R.; Veldkamp, A.; Frenking, G. *Chem. Phys. Lett.,* **1993**, *208*, 111.
(372) Dargel, T. K.; Hertwig, R. H.; Koch, W.; Horn, H. *J. Chem. Phys.* **1998**, *108*, 3876.
(373) Torrent, M.; Gili, P.; Duran, M.; Solà, M. *J. Chem. Phys.* **1996**, *104*, 9499.
(374) Cizek, J. *J. Chem. Phys.* **1966**, *45*, 4256.
(375) (a) Pople, J. A.; Krishnan, R.; Schlegel, H. B.; Binkley, J. S. *Int. J. Quantum Chem.* **1978**, *14*, 545. (b) Barlett, R. J.; Purvis, G. D. *Int. J. Quantum Chem.* **1978**, *14*, 561. (c) Purvis, G. D.; Barlett, R. J. *J. Chem. Phys.* **1982**, *76*, 1910. (d) Purvis, G. D.; Barlett, R. J. *J. Chem. Phys.* **1987**, *86*, 7041. (e) Raghavachari, K.; Trucks, G. W.; Pople, J. A.; Head-Gordon, M. *Chem. Phys. Lett.* **1989**, *157*, 479. (f) Barlett, R. J.; Watts, J. D.; Kucharski, S. A.; Noga, J. *Chem. Phys. Lett.* **1990**, *165*, 513.
(376) Pyykkö, P. *Chem. Rev.* **1988**, *88*, 563.
(377) (a) Antes, I.; Frenking, G. *Organometallics* **1995**, *14*, 4263. (b) Bauschlicher, C. W.; Langhoff, S. R.; Partridge, H.; Barnes, L. A. *J. Chem. Phys.* **1989**, *91*, 2399. (c) Barnes, L. A.; Rosi, M.; Bauschlicher, C. W. *J. Chem. Phys.* **1990**, *93*, 609.
(378) Cundari, T. R.; Benson, M. T.; Lutz, M. L.; Sommerer, S. O. In *Reviews in Computational Chemistry*; Lipkowitz, K. B., Boyd, D. B., Eds.; VCH: New York, 1996; Vol. 8, pp 145−202.
(379) (a) Kutzelnigg, W. *Z. Phys. D* **1990**, *15*, 27. (b) Balasubramanian, K. In *Encyclopedia of Computational Chemistry*; Schleyer, P. v. R., Allinger, N. L., Kollmann, P. A., Clark, T., Schaefer, H. F., III, Gasteiger, J., Eds.; Wiley: Chichester, 1998; Vol. IV, p 2471. (c) Schwerdtferger, P.; Seth, M. In *Encyclopedia of Computational Chemistry*; Schleyer, P. v. R., Allinger, N. L., Kollmann, P. A., Clark, T., Schaefer, H. F., III, Gasteiger, J., Eds.; Wiley: Chichester, 1998; Vol. IV, p 2481. (d) Hess, B. In *Encyclopedia of Computational Chemistry*; Schleyer, P. v. R., Allinger, N. L., Kollmann, P. A., Clark, T., Schaefer, H. F., III, Gasteiger, J., Eds.; Wiley: Chichester, 1998; Vol. IV, p 2499.
(380) (a) Becke, A. D. *Phys. Rev. A* **1988**, *38*, 3098. (b) Perdew, J. P. *Phys. Rev. B* **1986**, *33*, 8822; *34*, 7406E.
(381) (a) Becke, A. D. *J. Chem. Phys.* **1993**, *98*, 5648. (b) Lee, C.; Yang, W.; Parr, R. G. *Phys. Rev. B* **1988**, *37*, 785. (c) Stevens, P. J.; Devlin, F. J.; Chablowski, C. F.; Frisch, M. J. *J. Phys. Chem.* **1994**, *98*, 11623.
(382) Becke, A. D. *J. Chem. Phys.* **1997**, *107*, 8554.
(383) Hamprecht, F. A.; Cohen, A. J.; Tozer, D. J.; Handy, N. C. *J. Chem. Phys.* **1998**, *109*, 6264.
(384) Becke, A. D. *J. Chem. Phys.* **1998**, *109*, 2092.
(385) Becke, A. D. *J. Comput. Chem.* **1999**, *20*, 63.
(386) (a) Chang, Ch.; Pelissier, M.; Durand, Ph. *Phys. Scr.* **1986**, *34*, 394. (b) Heully, J.-L.; Lindgren, I.; Lindroth, E.; Lundquist, S.; Martensson-Pendril, A.-M. *J. Phys. B* **1986**, *19*, 2799. (c) Van Lenthe, E.; Baerends, E. J.; Snijders, J. G. *J. Chem. Phys.* **1993**, *99*, 4597. (d) Van Lenthe, E.; Snijders, J. G.; Baerends, E. J. *J. Chem. Phys.* **1996**, *105*, 6505.
(387) Rappe, A. K.; Casewit, C. J. *Molecular Mechanics Across Chemistry*; University Science Books: Sausalito, California, 1997.
(388) Morokuma, K., manuscript in preparation.
(389) Hoffmann, R.; Woodward, R. B. *Acc. Chem. Res.* **1968**, *1*, 17.
(390) (a) Roos, B. O. *Int. J. Quantum Chem.* **1980**, *14*, 175. (b) Siegbahn, P. E. M.; Almlöf, J.; Heiberg, A.; Roos, B. O. *J. Chem. Phys.* **1981**, *74*, 2384.
(391) Siegbahn, P. E. M. *Int. J. Quantum Chem.* **1983**, *23*, 1869.
(392) Szabo, A.; Ostlund, N. S. *Modern Quantum Chemistry. Introduction to Advanced Electronic Structure Theory*; Macmillan Publishing: New York, 1982.
(393) (a) Pople, J. A.; Santry, D. P.; Segal, G. A. *J. Chem. Phys.* **1965**, *43*, S129. (b) Pople, J. A.; Segal, G. A. *J. Chem. Phys.* **1965**, *43*, S136. (c) Pople, J. A.; Segal, G. A. *J. Chem. Phys.* **1966**, *44*, 3289.
(394) (a) Parr, R. G.; Yang, W. *Density-Functional Theory of Atoms and Molecules*; Oxford University: New York, 1989. (b) Ziegler, T. *Chem. Rev.* **1991**, *91*, 651. (c) Kryachko, E. S.; Ludeña, E. V. *Energy Density Functional Theory of Many-Electron Systems*; Kluwer: Dordrecht, The Netherlands, 1990.
(395) (a) Szasz, L. *Pseudopotential Theory of Atoms and Molecules*; Wiley: New York, 1985. (b) Krauss, M.; Stevens, W. J. *Annu. Rev. Phys. Chem.* **1984**, *35*, 357. (c) Gordon, M. S.; Cundari, T. R. *Coord. Chem. Rev.* **1996**, *147*, 87 and references therein.
(396) Hoffmann, R. *J. Chem. Phys.* **1963**, *39*, 1397.
(397) Hehre, W. J.; Radom, L.; Schleyer, P. v. R.; Pople, J. A. *Ab Initio Molecular Orbital Theory*; Wiley: New York, 1986.
(398) Slater, J. C. *Adv. Quantum Chem.* **1972**, *6*, 1.
(399) (a) Jones, R. O.; Gunnarsson, O. *Rev. Mod. Phys.* **1989**, *61*, 689. (b) Gunnarsson, O.; Jones, R. O. *Phys. Rev. B* **1985**, *31*, 7588.
(400) (a) Ahlrichs, R.; Scharf, P.; Ehrhardt, C. *J. Chem. Phys.* **1985**, *82*, 890. (b) Chong, D. P.; Langhoff, S. R. *J. Chem. Phys.* **1986**, *84*, 5606.
(401) (a) Eade, R. H. A.; Robb, M. A. *Chem. Phys. Lett.* **1981**, *83*, 362. (b) Schlegel, H. B.; Robb, M. A. *Chem. Phys. Lett.* **1982**, *93*, 43.
(402) (a) Møller, C.; Plesset, M. S. *Phys. Rev.* **1934**, *46*, 618. (b) Binkley, J. S.; Pople, J. A. *Int. J. Quantum Chem.* **1975**, *9*, 229. (c) Krishnan, R.; Frisch, J. A.; Pople, J. A. *J. Chem. Phys.* **1980**, *72*, 4244.
(403) Ziesche, P.; Kurth, S.; Perdew, J. P. *Comput. Mater. Sci.* **1998**, *11*, 122.
(404) Pople, J. A.; Head-Gordon, M.; Raghavachari, K. *J. Chem. Phys.* **1987**, *87*, 5968.
(405) (a) Maseras, F.; Morokuma, K. *J. Comput. Chem.* **1995**, *18*, 463. (b) Gao, J. *Acc. Chem. Res.* **1996**, *29*, 298. (c) Bersuker, I. B., manuscript in preparation. (d) Woo, T. K.; Cavallo, L.; Ziegler, T. *Theor. Chem. Acc.* **1998**, *100*, 307.

CR980452I